TriDurLE

National Center for Transportation Infrastructure Durability & Life-Extension

Project ID: 2020-MST-02

Exploring the Feasibility of Innovative Integration of Phase Change Materials for Thermo-Adaptive Asphalt Pavements

Jenny Liu

James A. Heidman Professor

Yizhuang David Wang

Research Associate

Farshad Saberi K

Graduate Research Assistant

Department of Civil, Architectural and Environmental Engineering

Missouri University of Science and Technology

Rolla, MO, 65409

for

National University Transportation Center TriDurLE
Department of Civil & Environmental Engineering
405 Spokane Street PO Box 642910
Washington State University Pullman, WA 99164-2910

09/04/2022

Disclaimer

The contents of this report reflect the views of the authors, who are responsible for the facts and the accuracy of the information presented. This document is disseminated under the sponsorship of the Department of Transportation, University Transportation Centers Program, in the interest of information exchange. The U.S. Government assumes no liability for the contents or use thereof.

Table of Contents

List of Figures

List of Tables

Executive Summary

Many types of distresses on the road can be attributed to the dramatic temperature changes and the extreme high and low temperatures in the pavement. For example, sudden temperature drop can cause transverse thermal cracking, and the high temperature in summer can accelerate the formation of permanent deformation on wheelpath. Incorporating phase change materials (PCMs) into asphalt pavement is an effective method to regulate the extreme temperature changes. A PCM melts and solidifies at a certain temperature and is capable of storing and releasing large amounts of energy during the phase transition processes. Moreover, pavements with PCM in cities can also mitigate the urban heat island effects.

In this research study, the feasibility and the performance of PCM-incorporated asphalt are evaluated at different scales. At the binder scale, the selected PCM (polyethylene glycol or PEG) was directly mixed with Gilsonite-modified binder. The Superpave performance grading tests were conducted to determine the optimum contents of the modifiers. The thermal behaviors of the modified binder were fully evaluated using the thermogravimetric analysis and the differential scanning calorimetry (DSC) analysis, and the thermal conductivity and the volumetric heat capacity were also measured. In addition to the Superpave performance tests, rheological evaluation such as the linear amplitude sweep (LAS) test and the multiple stress creep and recovery test were performed to access the binders' resistance to cracking and rutting, respectively. The testing results indicate that with the proper dosage of Gilsonite and PEG, the rutting resistance of the binder can be improved without sacrificing its low-temperature performance. With the addition of the PCM, the binder was tested to have high volumetric heat capacity, which indicates PCM can reduce the rate and the magnitude of the temperature changes in pavements.

To incorporate PCM into asphalt mixtures, the researchers in this study evaluated the feasibility of using porous filler as the carrier for PCM. The investigation was conducted at the asphalt mastic scale. Two different carrier materials (diatomite and expanded perlite) and four types of phase change materials were used in the study. The candidate filler, PCM, and the corresponding proper blending ratios were determined based on the results of the Scanning Electron Microscopy image analysis, the filter paper test, and the temperature sweep test. The thermal and rheological behaviors of the mastics with PCMs were further evaluated with different filler replacement ratios. The thermal analysis through the DSC test, thermal conductivity and volumetric heat capacity test, and the real-time temperature performance test were performed on the asphalt mastics. Rheological tests including the complex shear modulus test, the beam bending rheometer (BBR) test, and the LAS test were also conducted. The modified mastics were found to have high heat capacity with the latent heat storage ability. The rheological analyses showed that with the addition of PEG, while low-temperature performance of the asphalt mastics was improved, the performance at intermediate and high performance was not adversely affected by the PCM.

In summary, the study has shown that it is feasible to incorporate PCM into asphalt for both asphalt binders and mastic. The performance was not adversely affected by the addition of PCM, and the modified materials have exhibited great potential to regulate the temperature changes in pavements.

Chapter 1. Introduction

1.1. Problem Statement

It is expected that the market size of the asphalt manufacturing industry increases 0.3% and reach to $27.2 billion in 2022[1]. This enormous budget can prove the importance of developing asphalt pavements with enough durability. Fig. 1 presents the distribution of the different types of the crack in asphalt pavement based on a field survey (Tan et al. 2017). As shown, the rutting and transverse cracks that happened at high and low temperatures can lead to 25.9 and 40% of pavement damages, respectively. These percentages highlight the importance of addressing thermal damages in asphalt pavements. In this respect, the use of additives to improve the performance of hot mixes continues to generate worldwide interest and attention, and various asphalt binder modifiers have been used to enhance the properties of asphalt binders. The efforts resulted in many types of additives that can improve the performance of asphalt pavement, such as styrene-butadiene-styrene (SBS), ethylene-vinyl-acetate (EVA), styrene-butadiene rubber (SBR), carbon black, bio-oil, etc.

Rutting distress happens in flexible pavements by the accumulation of small permanent deformations in any of the pavement layers or the subgrade (Gheni 2020, Pourhassan et al. 2022). The temperature of asphalt pavement is one of the major factors in developing rutting resistance. In this way, at high temperatures, the asphalt binder between aggregate shows viscous behavior so that causes a decrease in the friction between the mineral aggregate which leads aggregate to lose their interlock and friction and move next to each other. Finally, since the shear resistance is not enough against the repeated traffic loads, the tracks of the vehicles' wheels appear on the surface road, which reduces the pavement serviceability and may cause a safety hazard. Therefore, the stiffness of asphalt at high temperature plays an important role in the resistance against rutting. In general, it looks essential to prevent plastic flow by controlling the asphalt temperature (Saberi et al. 2017).

Other primary thermal distress in asphalt pavement is low thermal cracking which is one of the most typical transverse cracking types. Low thermal cracking occurs by abrupt temperature decrease and at extremely low temperature when the binder is very stiff to easily crack since the thermal stress exceeds the tensile strength of the binder in asphalt pavement. This type of distress can quickly cause dysfunctional pavement. When the stiff binder between aggregate starts to crack the water can penetrate between aggregate and develop the fracture in the surface pavement. Water can also infiltrate the pavement and reduce the loading and structural capacity of the pavement (Anderson et al. 2001).

Regarding the ability to regulate extreme temperature changes of PCMs, it also can be considered as a material to improve the thermal distresses in asphalt pavements at high and low temperatures. A PCM melts and solidifies at a certain temperature and is capable of storing and releasing large amounts of energy during the phase transition processes. Since asphalt is temperature sensitive, it is hypothesized that proper incorporation of PCMs into AC can regulate the temperature in the pavement, and thus mitigate thermal damages. The potential merits of PCMs in asphalt pavements are sketched in Fig. 2. If an AC incorporates a PCM, whose phase transition temperature (T_{tr}) is somewhat lower than the threshold of high temperature damage (at or above which asphalt softens, leading to rutting), the PCM would melt and absorb heat when the material temperature reaches T_{tr} during a heating process, keeping a constant material temperature. When the heat storage capacity of the PCM is saturated, the material temperature would increase and then decrease following the environmental temperature variations, resulting in a reduced maximum temperature. In the case of long heating/high temperature duration, the maximum temperature in a PCM incorporated asphalt will be the same as a reference case. However, the appearance of maximum

[1] https://www.ibisworld.com/industry-statistics/market-size/asphalt-manufacturing-united-states/

temperature will be delayed, and thus the duration in which material is subjected to a temperature higher than the damage threshold will be shortened. In an opposite scenario, a low T_{tr} (somewhat higher than the threshold of low temperature damage facilitating low temperature cracking) PCM, incorporated in AC, tends to result in a higher minimum temperature during a cooling process. It can also delay the appearance of minimum temperature and shorten the duration in which material is subjected to a temperature lower than the low temperature damage threshold. In general, geographic areas where high-temperature and low-temperature impact asphalt pavements periodically, the high-T_{tr} and low-T_{tr} PCMs can be combined to mitigate both high-temperature and low-temperature damages. It has also been proposed to achieve the same purpose using one PCM of a T_{tr} slightly higher than 0℃ (e.g., 5.8℃). No matter using one or multiple types of PCMs, the magnitude of temperature variation tends to be reduced, and the heating/cooling rates can be reduced. These effects are able to reduce the stress levels induced by temperature changes, thus mitigate thermal fatigue.

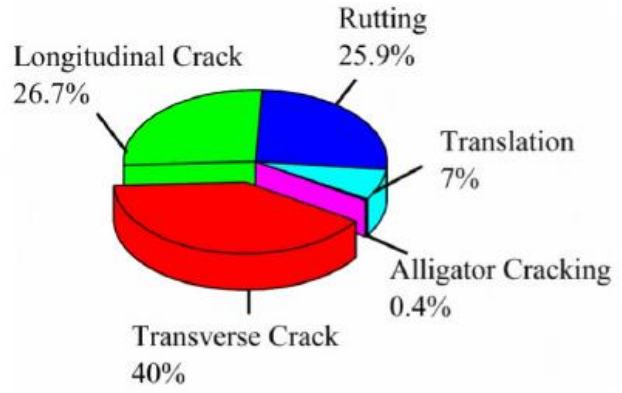

Fig. 1 Distribution of cracks in asphalt pavements (Tan et al. 2017).

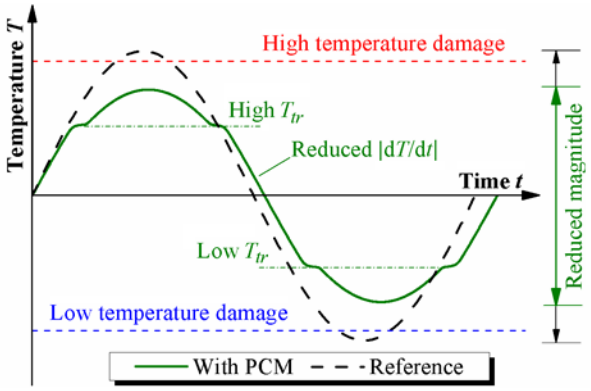

Fig. 2 Potential merits of PCMs in pavements.

In addition, the intrinsic feature of asphalt pavement with black surface and very low solar reflectance index (SRI) equals to 0.04 to 0.06 makes it as a high potential material to absorb solar radiation resulting in high temperature of asphalt pavement; and subsequently, it leads to many social and urban issues and environmental phenomenon of urban heat island (UHI) effect (Du et al. 2019). Urban heat island develops when the temperature of an urban area is higher in comparison to the temperatures of

surrounding suburban and rural areas (Santamouris 2013). This phenomenon leads to the increasing usage of air-conditionings and power consumption in urban areas, and elevates the environmental pollution, especially in summer. Some studies estimate that the cooling energy consumption becomes double due to the UHI. Therefore, balancing the temperature of asphalt pavement has been considered as an essential action in asphalt industry. Researchers were developed different technologies to mitigate the urban heat island in cities such as cool coating, porous asphalt pavement, solar energy collecting pavement, etc. (Du et al. 2019).

Recently, phase change materials (PCMs) could attract many attentions to address all above problems, including asphalt distresses and environmental issues, in asphalt industry. Additional benefits of PCMs in asphalt pavement also include mitigations of urban heat island effect and permafrost thawing, since the PCMs can store large amounts of heat thus delay the heating processes in specific temperature ranges.

1.2. Objectives

The main goal of this research was to assess the feasibility of developing a thermo-adaptive asphalt pavement with high sustainability. In this study, the PCMs as latent heat storage materials were integrated into asphalt materials on the binder and mastic levels. Several testing methods were used to address the thermal properties of binder and mastic. Also, to verify the performance of asphalt binder and asphalt mastic, several rheology tests were used to address the low and high temperature performance of materials. Following the main goal, the below objectives were sought in the current research:

- To evaluate different types of PCMs and selecting the appropriate one to meet the requirements for asphalt application,
- To apply and evaluate two different integration methods, including direct mixing method and using carrier material to incorporate in asphalt binder and asphalt mastic, respectively,
- To investigate the high and low temperature performance of asphalt materials after incorporating PCMs,
- To investigate the feasibility of developing a cooler asphalt pavement to mitigate the temperature variant in asphalt pavement.

1.3. Organization of the Report

After an introduction of the study in Chapter 1, a thorough literature review about the history, mechanism, and the state-of-the-art applications are presented in Chapter 2. Chapter 3 presents the study of the performance and feasibility of the PCM-modified bituminous materials at the binder scale, and the investigation of the PCM-incorporated asphalt at the mastic scale is presented in Chapter 4. The findings, conclusion, and future study are presented in Chapter 5.

Chapter 2. Literature Review

2.1. Phase Change Material Definition

Phase Change Materials (PCMs) are known as novel and capable materials which can absorb and release a large amount of energy in the form of latent heat (ΔH) during the phase transition and act as a balancer in modifying the changing temperature of temperature-sensitive materials. For the first time, PCM was studied by Sharma and Sagara (Sharma and Sagara 2005); however, it did not attract much attention. In the late 1970s, during the energy crises and high cost of fossil fuels, it was considered again as a precursor to using as a heating system in buildings. Nowadays, to reduce the emission of greenhouse gases, it has been considered greatly as a cleaner production to prepare efficient air conditioning in the buildings and diminish fuel consumption. In addition, PCM has also been utilized in many commercial projects for thermal storage, including solar water heater, space heating, space cooling, greenhouse heating, solar cooking, battery industries, space crafts, and so forth. Latent heat fusion is an endothermic process that absorbs heating energy. By applying heat to the system, the PCM starts to absorb energy so that its temperature will be increased. In the melting point temperature, it begins to melt by absorbing more heating energy, but the temperature of the system will stay constant. If the temperature of the system increases and it passes the maximum wide range of PCM, after a delay, the temperature will be increased in the system. Thus, it is necessary to select the appropriate type of PCM to be compatible with the system temperature changes. The amount of heating energy that the system can absorb without increasing its temperature is latent heat storage. Fig. 3 describes the simplified process of absorbing heat and the latent heat storage concept. Also, Fig. 4 presents a schematic of the PCM performance in absorbing and releasing heat energy.

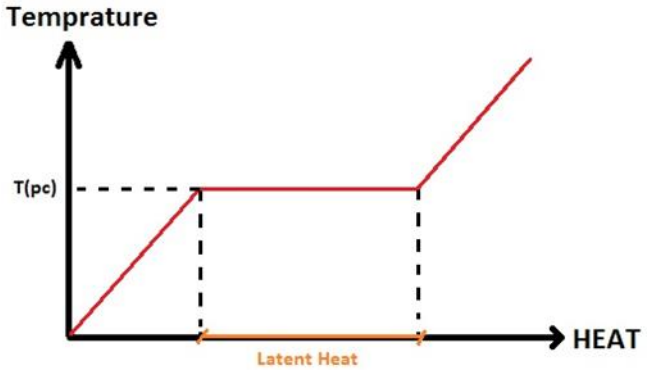

Fig. 3 The simplified process of Latent Heat Storage (LHS).

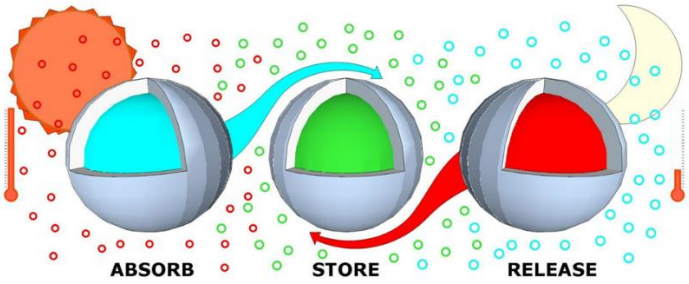

Fig. 4 Schematic of the PCM performance in absorbing and releasing the heat energy.

According to Fig. 3, two main features of latent heat storage can be summarized: 1) PCM can absorb a large amount of energy and keep the temperature constant; 2), it creates a delay in temperature increase in the system. Fig. 5 presents the effects of PCM on system temperature changes.

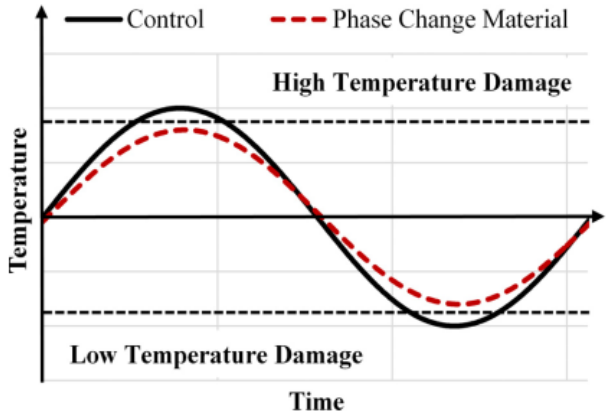

Fig. 5 Theory of employing PCMs in asphalt pavements (Manning et al. 2015).

After investigation of PCM in cementitious material and conducting many research studies, some initial research showed the potential of this material in asphalt concrete. However, these studies did not mention the influence of this material on the mechanical properties and service life of the asphalt pavement. In this regard, this report presents a review of the literature to investigate the different types of PCMs, their physical and chemical characteristics, incorporations methods in asphalt materials, and their potential to mitigate thermal damages, including rutting and low thermal cracking, in asphalt pavements.

2.2. PCM Classification

PCMs can be categorized into different classes, as shown in Fig. 6. In terms of chemical composition, they can be classified into three groups, including inorganic PCM, organic PCM, and eutectics (composite of inorganic and organic PCMs) (Fig. 7). In terms of the range of phase change temperature, they can be categorized into three groups: high phase temperature, mid-phase temperature, and low phase temperature. In terms of the form of phase changes during absorbing heating energy, they can be grouped into four types: solid-solid, solid-liquid, solid-gas, and liquid-gas phase transitions (Guan et al. 2011).

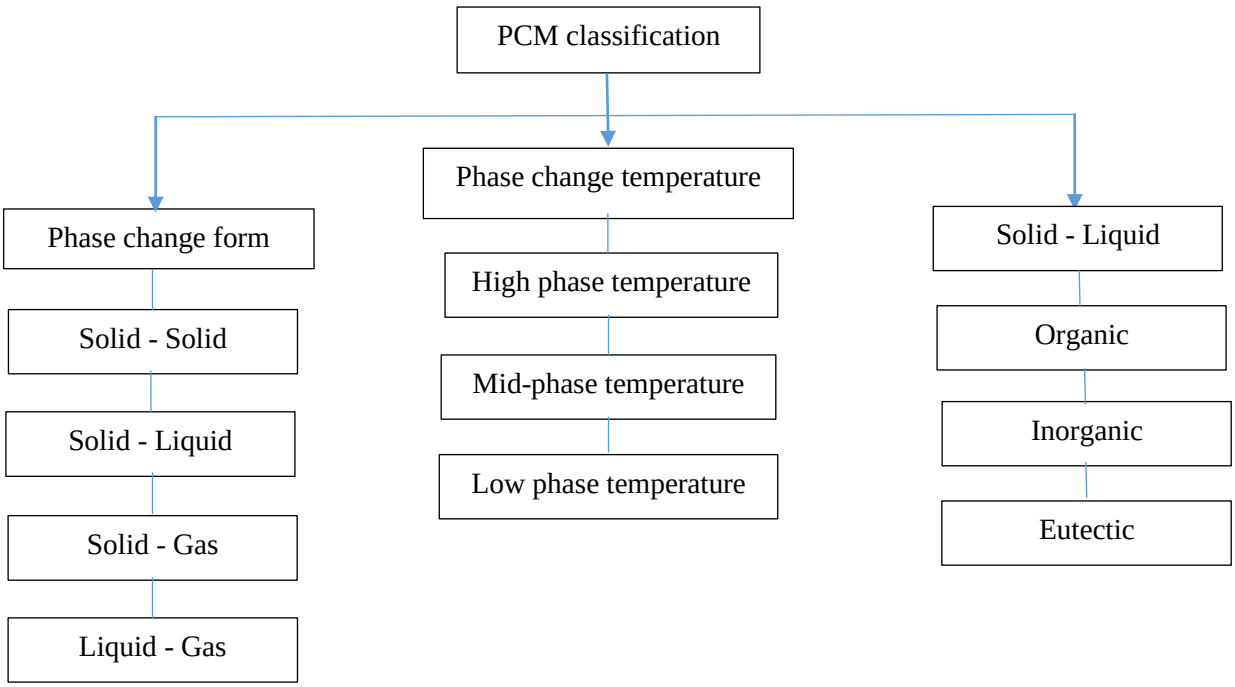

Fig. 6 PCM classification based on different terms.

Solid-gas and liquid-gas transition have high latent heat storage and they can release high amount of energy; however, they are associated with large volume changes which results in containment problems. Solid-gas and liquid-gas PCMs have some specific utilities in thermal storage systems (Sharma and Sagara 2005).

Solid-solid PCMs have some advantages which includes no leakage of melted PCM during phase change process, no additional storage container for encapsulation, terminating the reactivity of PCM with the outside of environment, easily preparing in desired dimensions (Alkan et al., 2012). However, they present less latent heat compared to the other groups.

Solid-liquid PCMs can be classified in three main groups organic, inorganic and eutectics. Their properties are elaborated in Table 1.

Table 1. Properties of Different Types of Solid-liquid PCMs

Classification	Advantages	Disadvantages
Organic PCMs	Availability in a large temperature range	Low thermal conductivity (around 0.2 W/m K)
	High heat of fusion	Relatively large volume change
	No supercooling	Flammability
	Chemically stable and recyclable	
	Good compatibility with other materials	
Inorganic PCMs	High heat of fusion	Supercooling
	High thermal conductivity (around 0.5 W/m K)	Corrosion
	Low volume change	
	Availability in low cost	
Eutectics	Sharp melting temperature	Lack of currently available test data of thermo-physical properties
	High volumetric thermal storage density	

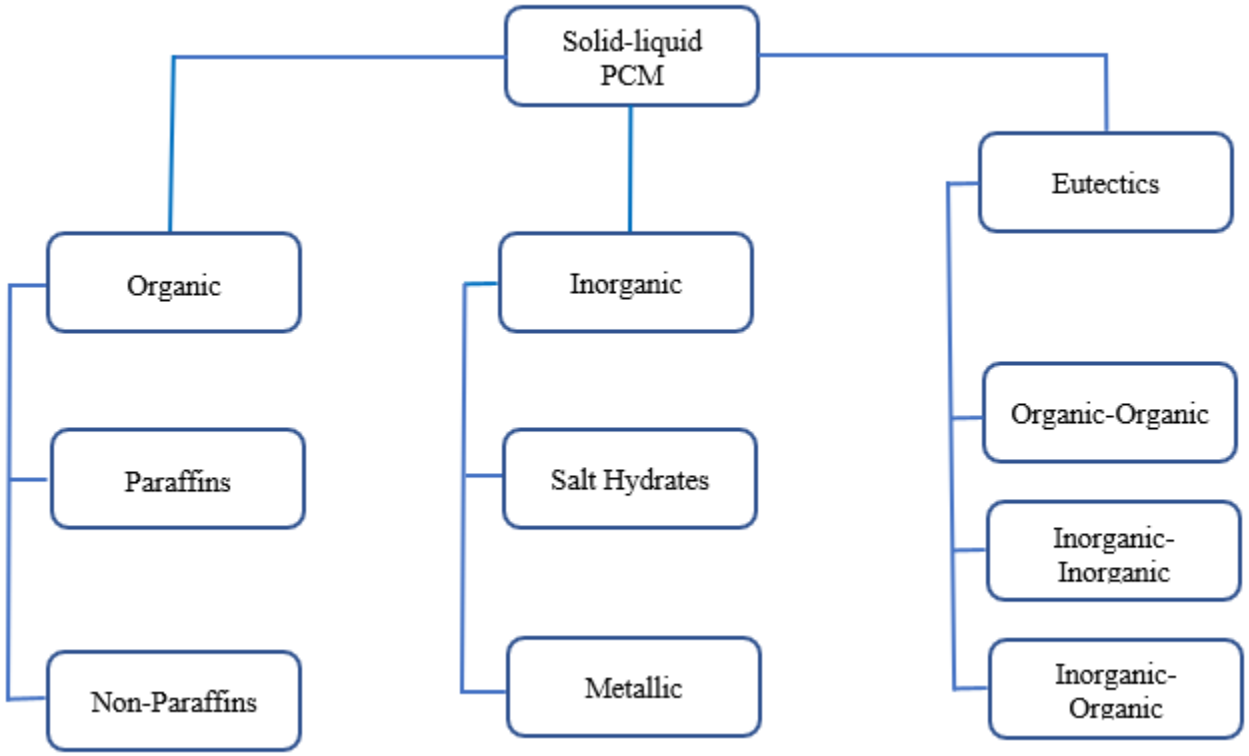

Fig. 7 Solid-liquid phase change materials classification.

Since there are different types of PCM with different chemical, physical and thermal properties, it is important to select the suitable type of PCM for each project. In this respect, there are some criteria that should be considered in selecting an appropriate PCM including properties such as thermos-physical, kinetics, and chemical properties, which are elaborated in Table 2.

Table 2. The Important Criteria in The Selection of a Suitable PCM (Sharma and Sagara 2005)

Thermo-physical properties
Melting temperature should be corresponding to the system requirement
High latent heat of fusion
High specific heat
High thermal conductivity
Small volume changes
Kinetic properties
High nucleation rate to prevent from supper cooling in the liquid state
High rate of crystal growth for rapid recovery
Chemical properties
Chemical stability
Complete reversible freezing and melting cycle
No degradation after a great number of freezing and melting cycles
Non-corrosiveness to the construction materials

The most common utilizations of PCM include (Ryms et al. 2017):

- Construction: To improve the energy efficiency in the floor and wall heating;
- Transportation: To use in containers for transforming thermos-sensitive materials such as blood, body organs, drugs, groceries, etc.;
- Electronics industry: To use in the heat sink to prevent circuit over-heating;
- Textiles: To use in special clothes such as sports clothes, firefighter clothes, astronaut clothes, etc.

2.3. Common PCMs Used in Asphalt Materials

2.3.1. Paraffins

One of the most common groups of organic PCMs is paraffin waxes which are a family of hydrocarbons with similar properties. Their chemical composition is known as the molecular formula of $CH_3\_(CH2)_n\_CH_3$. Paraffin waxes have enough potential to absorb, store, and release a large amount of energy during phase transmission between solid and liquid. Also, they can manifest a wide range of melting temperature and latent heat of fusion which can put them in the group of PCMs with a wide variety of applications. In general, longer hydrocarbon chain can yield a higher melting point and higher latent heat fusion (Sarier and Onder 2012). Table 3 presents paraffin waxes along with their thermal properties. Also, Table 4 indicates the advantages and disadvantages of paraffin waxes.

Table 3. Paraffin Waxes and Their Thermal Properties (Sarier and Onder 2012)

Paraffin wax	Molecular formula	Molar mass ($g \cdot mol^{-1}$)	Melting temperature (°C)	Crystallization temperature (°C)	ΔH_{fus} ($kJ \cdot kg^{-1}$)
n-Dodecane	$CH_3(CH_2)_{10}CH_3$	170.3	-10	-16	216
n-Tridecane	$CH_3(CH_2)_{11}CH_3$	184.4	-5	-9	160
n-Tetradecane	$CH_3(CH_2)_{12}CH_3$	198.0	5-6	0	227
n-Pentadecane	$CH_3(CH_2)_{13}CH_3$	212.0	10	5	205
n-Hexadecane	$CH_3(CH_2)_{14}CH_3$	226.0	18-19	17	237
n-Heptadecane	$CH_3(CH_2)_{15}CH_3$	240.0	22	22	171
n-Octadecane	$CH_3(CH_2)_{16}CH_3$	254.0	28	25	242
n-Nonadecane	$CH_3(CH_2)_{17}CH_3$	268.0	32-33	27	222
n-Eicosane	$CH_3(CH_2)_{18}CH_3$	282.0	36-37	31	247
n-Heneicosane	$CH_3(CH2)_{19}CH_3$	296.0	39-41	32	201
n-Docosane	$CH_3(CH2)_{20}CH_3$	310.0	42-45	43	157
n-Tricosane	$CH_3(CH_2)_{21}CH_3$	324.0	48.9	51	142
n-Tetracosane	$CH_3(CH_2)_{22}CH_3$	338.0	50-51	48-49	160
n-Pentacosane	$CH_3(CH_2)_{23}CH_3$	352.0	54	47	164
n-Hexacosane	$CH_3(CH_2)_{24}CH_3$	366.0	56	53-54	255
n-Heptacosane	$CH_3(CH_2)_{25}CH_3$	380.0	59	53	159
n-Octacosane	$CH_3(CH_2)_{26}CH_3$	394.0	61	54	202

Table 4. The Advantages and Disadvantages of Paraffin Waxes as Latent Heat Storage Materials (Sharma and Sagara 2005)

Advantages	Disadvantages
- No tendency to segregate - Chemically stable - Stable properties after high heat cycling - High heat of fusion - No tendency to supercooling - Safe and non-reactive - Compatible with all metal containers	- Oxidation happens when exposed to oxygen (needs close container) - Low thermal conductivity (using additives like expanded graphite or metallic fillers) -High volume changes in phase transmissions from solid to liquid - flammable

2.3.2. Fatty Acids

Fatty acids have almost the same characteristics as paraffins, and their chemical formula is defined as $CH_3(CH_2)_{2n}COOH$. Compared to paraffins, they have sharper phase transformation. Table 5 presents the phase change thermal properties of the fatty acids with the different number of C atoms. Also, Table 6 summarizes the advantages and disadvantages of fatty acids. As mentioned in Table 6, one major disadvantage is its high leakage potential. To prevent leakage, researchers have suggested two methods: first, encapsulating fatty acids by polymer pellets, and second, readily immersing porous materials such as expanded perlite into fatty acid (Wei et al. 2014). Also, fatty acids can be used to produce eutectic mixtures. In fact, some researchers use this technique to improve the thermal storage capacity of the final mix or even modify the phase transition temperature. Fatty acid ester is a new material that can be prepared by esterification reactions of fatty acids with alcohols. The melting temperature and heat capacity of the fatty acid esters is in a range from 20 ˚C to 40 ˚C and 180 kJ kg^{-1} to 200 kJ kg^{-1}, respectively (Sari and Biçer 2012).

Table 5. Thermal Properties of Common Fatty Acids (Sarier and Onder 2012)

Fatty acid	Molecular formula	Melting temperature (℃)	ΔH_{fus} ($kJ \cdot kg^{-1}$)
Butyric acid	$CH_3(CH_2)_2COOH$	-5.6	126
Caproic acid	$CH_3(CH_2)_4COOH$	-3	131
Caprylic acid	$CH_3(CH_2)_6COOH$	16-17	148-149
Capric acid	$CH_3(CH_2)_8COOH$	30-32	153-163
Lauric acid	$CH_3(CH_2)_{10}COOH$	41-44	178-183
Tridecylic acid	$CH_3(CH_2)_{11}COOH$	41.4	154
Myristic acid	$CH_3(CH_2)_{12}COOH$	49-58	167-205
Pentadecanoic acid	$CH_3(CH_2)_{13}COOH$	52-53	178
Palmitic acid	$CH_3(CH_2)_{14}COOH$	61-64	186-212
Margaric acid	$CH_3(CH_2)_{15}COOH$	60	172.2
Stearic acid	$CH_3(CH_2)_{16}COOH$	65-70	196-253
Nonadecylic acid	$CH_3(CH_2)_{17}COOH$	67	192
Arachidic acid	$CH_3(CH_2)_{18}COOH$	N.a.	N.a.
Heneicosylic acid	$CH_3(CH_2)_{19}COOH$	73-74	193
Tricosylic acid	$CH_3(CH_2)_{21}COOH$	79	212

Table 6. Advantages and Disadvantages of Fatty Acids as Latent Heat Storage Materials (Sharma and Sagara 2005, Sarier and Onder 2012, Wei et al. 2014)

Advantages	Disadvantages
- Thermally stable - Chemically stable - Stable properties after high heat cycling - High energy storage - Proper melting temperature range for several heat storage applications - Good option to make eutectic mixtures - Non flammability - No or less subcooling - Easy impregnation into composite structures	- Corrosive - Undesirable odor - High sublimation rate - High leakage potential - Low thermal conductivity

2.3.3. Poly-Ethylene Glycols (PEGs)

Poly-ethylene glycols (PEGs) with the chemical formula of HO_CH_2_(CH2_O_CH_2_) n_CH_2_OH have both features of water solubility and organic solubility. The melting temperature and latent heat fusion of the PEGs increase by growing their average molar mass ($g.mol^{-1}$). For instance, PEG 400 has a melting point and latent heat fusion equal to 3.2 ℃ and 91.4 kJ kg^{-1}, respectively, but these values for PEG 20,000 equal to 68.7 ℃ and 187.8 $kJ.kg^{-1}$. Table 7 presents different types of PEGs with a wide range of average molar mass. Table 8 presents the advantages and disadvantages of PEGs.

Table 7. Thermal Properties of PEGs with Different Molecular Weights (Sarier and Onder 2012).

Average molar mass (g mol^{-1})	Melting temperature (◦C)	ΔH_{fus} (kJ kg^{-1})	Crystallization temperature (◦C)	ΔH_{cryst} (kJ kg^{-1})
400	3.2	91.4	-24	85-86
600	22.2	108.4	-7	116
1000	32.0	149.5	28	140
1500	46.5	176.3	39-40	169
2000	51.0	181.4	35	168
3400	56.6	174.01	29	159
4000	59.7	189.7	22	167
6000	64.8	189.0	33	161
10,000	66.0	189.6	38	167
20,000	68.7	187.8	38	161

Table 8. The Advantages and Disadvantages of PEGs as Latent Heat Storage Materials (Sarier and Onder 2012, He et al. 2018)

Advantages	Disadvantages
- High heat of fusion - Low and moderate melting temperature intervals - Low vapor pressure when melted - Chemically stable - Thermally stable - Non-toxic - Non-corrosive - Inexpensive	- Low thermal conductivity - Poor absorptive performance in solar energy applications

2.4. PCM Incorporation Methods

Based on the literature, different types of incorporation methods have been considered to modify asphalt materials. The methods include: macro encapsulation method, micro encapsulation method, direct incorporation method, shape-stabilized PCM. A review of these methods and their applications in asphalt materials is summarized hereunder.

2.4.1. Macro Encapsulation Method

Macro encapsulation method is highly applicable, especially in concrete materials, and ideal in concrete buildings as latent heat storage system. In this method, the lightweight aggregate (LWA) which is porous aggregate acts as the supporting or carrier material. Examples of aggregate carriers are expanded to clay, expanded perlite, expanded shale (Fig. 8). One of the two macro encapsulation methods is impregnation. It can be performed in three simple steps. First, the LWA needs to be dried in the oven to lose the moisture; then, the vacuum pump evacuates air from the pores in the LWA, and simultaneously the melt PCM is added to the LWA so that air is substituted with PCM in the pores. In the end, the lightweight aggregate filled with PCM is ready to mix with the normal aggregate in order to use in concrete or asphalt mixtures. Instead of using a vacuum pump, it is possible to immerged LWA into liquid PCM, and PCM can be gradually absorbed by the porous structure and capillary effect of the LWA. This method is known as the

immersion method. Sakulich and Bentz employed two different types of LWA, including expanded clay and porous pumice, as supporting materials to absorb PCM. To this purpose, they immerged both types of LWA in the liquid PCM for two time periods, 1 day and 7 days. According to their reports, a longer immersion time results in a more PCM impregnated in the LWA. Also, a less viscous PCM led to more PCM impregnation (Sakulich and Bentz 2012). To compare between the impregnation method and the immersion method, Zhang et al. investigated both methods by checking the maximum water that can be absorbed by expanded clay in each technique. They reported that expanded clay aggregate could absorb water equals to 11.0% and 72.5% through immersion and impregnation methods, respectively (Zhang et al. 2004, Roshan et al. 2022). The finding indicates the high efficiency of the impregnation method. The immersion method is less efficient duo to the presence of the air in the porous structure of the LWA in the immersion method.

The main problem of the macro encapsulation method is the high possibility of leaking PCM from supporting material after multiple thermal cycling; also, the thermal properties of PCM may be declined. Also, the level of absorption of PCM is challenging to control and maximize. There are some critical factors that can affect the absorption ratio such as porous aggregate structure, duration of immersion, the viscosity of PCM, the surface area of immersion, liquid pressure and temperature of the materials (Hawes et al., 1992).

Fig. 8 Aggregate carriers for PCM: a) expanded clay, b) expanded shale, c) expanded perlite (Tang et al. 2018).

Kakar et al. used two types of lightweight aggregate (expanded burnt clay and foam glass) and liquid tetradecane as the carrier material and phase change material, respectively. To prevent leakage, they coated LWA by epoxy glue. Afterward, ordinary Portland cement (OPC) was used to cover the glue on the surface of particles; then, they left particles for about 10 hours to dry. Then, the particles were covered with a second layer of epoxy and left for 10 h to dry (Fig. 9). The CT-scan results confirmed that the internal structure of foam glass included well established interconnected voids in comparison to expanded burnt clay. This structure resulted in high capacity of foam glass to absorb PCM compared to expanded clay (Kakar et al. 2020).

Diatomite can also be considered as carrier material to absorb phase change materials. Fig. 10 describes a schematic of impregnation diatomite by PEG (Karaman et al. 2011). Jin et al. investigated two different kinds of PCMs, polyethylene glycol (PEG) and ethylene glycol distearate (EGD) and used ceramsite (CS) as the carrier material. Then, the CPCM was encapsulated by an epoxy as shown in Fig. 11 (Jin et al. 2018).

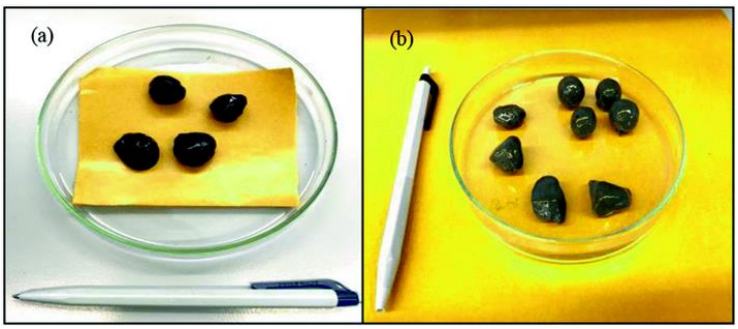

Fig. 9 Impregnated PCM particles coated with epoxy resin and ordinary cement (Kakar et al. 2020).

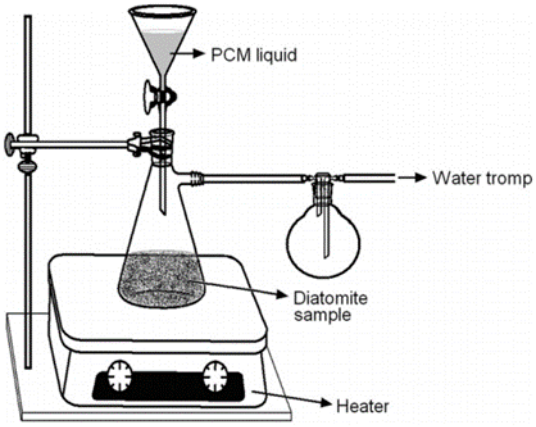

Fig. 10 Schematic of vacuum impregnation system (Karaman et al. 2011).

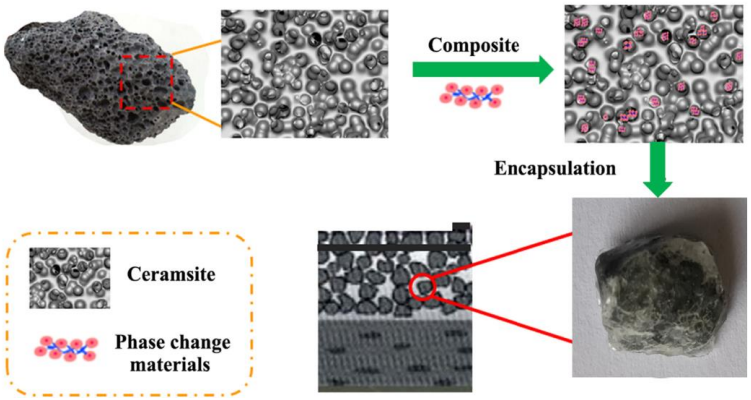

Fig. 11 Schematic view for the preparation of encapsulated CPCM (Jin et al. 2018).

2.4.2. Micro Encapsulation Method

In this method, PCM is enclosed and encapsulated with a microscopic container and a membrane layer (such as polymer) which works like a shell (Hawes et al. 1992). This method can contribute some advantages to the system. The shell material around the PCM can protect PCM from oxygen, water, and light. Other benefits include: prevents the leakage of PCM; a high ratio of surface area to the volume which increases the thermal conductivity; enough potential to withstand against volume changes during

phase transition. However, there are also some key disadvantages to this method. The composite PCM resulted from this method may have poor stability that causes short life service; thus, the shell should be stable enough against environmental factors such as freezing and thawing phenomenon. Another disadvantage is the cost. It is more expensive to complete the encapsulation compared to other forementioned methods (Ren et al. 2014, Tang et al. 2018). As mentioned, the stability of carrier material is important and the thermal properties of carrier material can play an essential role in the thermal properties of the whole system; thus, it should be determined accurately based on parameters such as particle diameter, thickness of shell, thermal capacity and conductivity, durability, and so forth. The purpose of using microcapsules is to prevent PCM dispersion in the structure, decline evaporation and reaction of PCMs with the outside environment, prepare an increased heat-transfer area and a constant volume, and finally cause an easy application (Sarier and Onder 2007).

2.4.3. Direct Incorporation Method (Melt Blending Method)

The direct incorporation method is simple and suitable for applying PCM in asphalt materials. In this method, PCM is directly added to asphalt binder and mixed; therefore, PCM can be considered as a modifier in asphalt binder. The process is to separately melt PCM and supporting material at high temperature; then, those can be mixed together. The disadvantage of this method is the high possibility of separation which can cause leaking in the latent heat storage system; however, this method is highly cost-effective since it does not require any encapsulation of PCM (Ren et al. 2014). It is worth mentioning that this method has been widely used for modifying asphalt binders with additives such as bio-oil. As mentioned, the stability and compatibility of the mixture is important. The stability of the PCM-modified binder is attributed to material properties such as modulus, viscosity, density of the two materials (Liang et al. 2019), mixing temperature, and shear speed of mixer.

2.4.4. Sol-Gel Method

Another effective method to prepare composite phase change material is the sol-gel method. This method involves a precursor, a solvent, and a catalyst material. To form silica shell, the hydrolysis reaction needs to be rapid, which can occur under a complicated process (Zhang et al. 2010). Ma et al. utilized different types of carriers and encapsulation materials to prepare composite shape-stabilized phase change energy storage material. The results showed that the PCM absorption of silica was greater than the PCM absorption of activated carbon (Ma et al. 2011). Chen et al. also utilized sol-gel method to prepare a system of PCM, carrier and shell material. In this regard, paraffin was used as the core material, and SiO_2 prepared with methyl triethoxysilane (MTES) acted as the shell material (Chen et al. 2013). Li et al. used Tetraethyl silicate (TEOS), Ethanol (C_2H_5OH), Hydrochloric acid as the precursor, solvent, and catalyst materials. They mixed different portions of the aforementioned materials into a pH value of 2. To make a reaction in the mixture, the flask was kept in a water bath at 60 °C for 90 min, which formed the silicon dioxide sol. Then, the silicon dioxide sol was dried in the oven, and silicon dioxide gel was obtained. After that, paraffin as the PCM in the presence of the distilled water was added to the silicon dioxide gel to produce the Composite Phase Change Material (CPCM) (Li et al. 2012). Ma et al. developed a shape-stabilized PCM with a mixture of the PCM and different percentages of carrier material, carbon and silica. They used Tetradecane as PCM which is usually used in cold climate pavement to prevent low temperature distresses, thermal cracking. As membrane material, they utilized Ethyl Cellulose (EC) to cover the PCM material to obtain CPCM. Also, two different carrier materials, carbon and silica, were used to absorb PCM. To increase the heat storage capacity, dispersing agent was employed, and it decreased the clusterization of the shape-stability PCM particles. Based on their observation, CPCM with silica carrier without dispersing agent had a smother surface compared to CPCM with active carbon carrier without

dispersing agent. They believed the regular shape of activated carbon led to lower cohesiveness between the activated carbon and the thin EC membrane that provided weak force between the activated carbon and membrane molecules. Based on the testing results, they continued their test just on silica carrier and made two different CPCM with silica carrier in different dosages of EC membrane and dispersing agent, i.e., 5%, 10%, and 15%. Based on DSC test and the calculated enthalpy, they found the maximum enthalpy of samples which were 10% EC – 10% dispersing agent and 10% EC – 15% dispersing agent (Ma et al. 2013).

2.5. Civil engineering applications of PCM

PCMs have numerous potential applications in the construction industry. They can be utilized in different sections of buildings such as roof, floor, walls, and so forth. The main idea of using PCMs in buildings is to mitigate energy consumption, especially regarding the rapid economic growth worldwide. Therefore, the energy systems of buildings can take the advantage of high latent heat storage of PCMs in a narrow temperature interval. Also, PCMs have recently attracted many attentions in modifying asphalt mixtures against thermal distress such as rutting, thermal cracking, and thermal fatigue cracking. In the following sections, a review of PCM applications in the concrete industry is very shortly reviewed. Then, the asphalt industry as another potential application of PCM was considered, and the scientific effort in this area is reviewed.

2.5.1. PCM in Cementitious Materials

Phase change material in concrete has been considered as a novel technology to reduce energy usage and keep the temperature of interior spaces at the comfortable range. The other benefits of using PCM in buildings are to reduce the cost of fossil fuels and mitigate environmental concerns, especially in winter when energy consumption accelerates. Fig. 12 presents a schematic application and the mechanism of PCM in the walls of buildings. In this respect, one major factor to select the suitable type of PCM in building applications is the melting point of the PCM which should be between 18 ˚C and 28 ˚C, the human comfort temperature range (Zhang et al. 2007). Fig. 13 manifests a comparison among indoor, outdoor, and comfort zone temperatures.

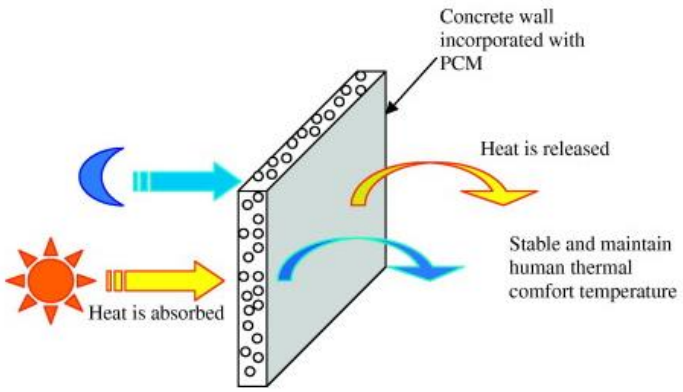

Fig. 12 A schematic of PCM performance in buildings.

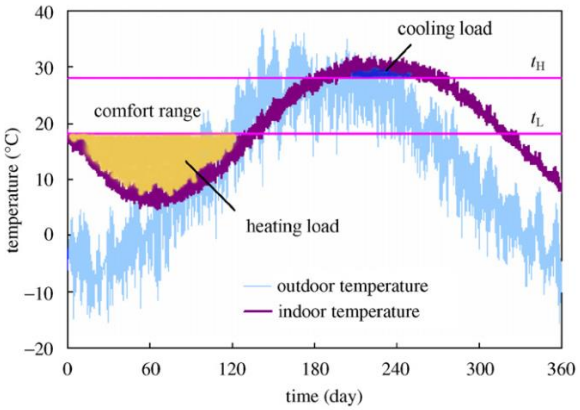

Fig. 13 Indoor, outdoor, and comfort zone temperatures and heating/cooling loads (Zhang et al. 2006).

2.5.2. PCM in Asphalt Materials

2.5.2.1. Penetration, Softening Point, Ductility, and Viscosity

As mentioned, there are different methods to incorporate PCM in asphalt materials. One of them is the direct incorporation method. The direct incorporation of PCMs in asphalt can enhance the saturated content of asphalt and reduce the consistency of asphalt, resulting in higher penetration and lower ductility (Jin et al. 2017). Bian et al. employed three different types of organic phase change materials, including palmitic acid, PEG4000, and myristic acid, with different concentrations 0, 10, 20, and 30%, in asphalt binder by direct incorporation method. Palmitic acid could increase the penetration of modified asphalt binder, but PEG4000 and myristic acid did not change the penetration significantly. Also, testing results indicated a considerable decrease in softening point of asphalt binder for palmitic modified binder, but there was not a noticeable change in softening point for PEG4000 and myristic acid modified binders. Finally, the ductility of modified binders was decreased. The reduction in ductility for palmitic and myristic acids was more significant in comparison to the PEG4000 modified binder (Bian et al. 2012). In another research study, the potential application of polyurethane solid-solid phase change material (PUSSPCM) as a polymer modifier in asphalt binder. The penetration, softening point, and ductility of the modified binder were investigated. It is worth mentioning that the direct incorporation method was used to mix asphalt binder and PCM in different dosages of 0, 3, 5, and 7%. Softening point and penetration were approximately in the same range compared to control asphalt binder. However, ductility was significantly reduced by adding PCM so that for the sample with 7% PCM the maximum reduction was observed. The viscosity of asphalt binder at high temperature is significant for the workability of asphalt mixture. The results showed adding more PCM results in more viscosity. It is worth mentioning that by increasing the temperature the difference between the viscosities of samples (modified and neat binders) reduced, and eventually, their viscosity was in the same range at 175 ℃ (Wei et al. 2019). Dissanayaka and Senadheera used a polymer-encapsulated micro phase change material (MPCM) containing paraffin wax to modify asphalt binder. MPCM was a white powder with a PCM inner core (paraffin) encapsulated in a polymer shell. The Brookfield rotational viscosity test showed increasing the amount of MPCM in asphalt binder can still keep the viscosity to less than 3 Pa·s which is desirable, respecting SHRP criteria (Dissanayaka and Senadheera 2018). Kakar et al. employed microencapsulated PCM with Tetradecane and the melting point of 6 ℃. According to their observations, adding more microencapsulated PCM increases the penetration and decreases the softening point of modified binder; thus, leading to a softer binder (Kakar et al. 2019).

2.5.2.2. Rheological Properties

Multi-Stress Creep Recovery, MSCR, test (AASHTO TP 70) is a recently developed test protocol to evaluate the rutting performance of asphalt binders. MSCR test findings showed adding MPCM and Evotherm to asphalt binder can decrease rutting susceptibility as the Jnr values at 0.1 kPa and 3.2 kPa decreased in comparison to the neat binder (Dissanayaka and Senadheera 2018). Wei et al. utilized polyurethane solid-solid phase change material (PUSSPCM) with low phase change temperature in asphalt binder with the direct incorporation method. They used different concentrations of PCM, including 0, 3, 5, and 7%. Rutting parameter ($G^*/\sin\delta$) was used to evaluate the performance of modified asphalt binder against rutting. The results showed polyurethane solid-solid PCM has a low improvement effect on the high-temperature performance (rutting) of asphalt binder. Also, the bending beam rheometer test could result in two values, creep stiffness and m-value, to predict the low-temperature performance (thermal cracking) of asphalt binder. The results indicated a reduction in creep stiffness of asphalt binder, especially at very low temperature (-24℃). However, the m-value, which defines the stress relaxation in the asphalt binder, was adversely decreased for all samples in comparison to the control sample (Wei et al. 2019). Polyethylene glycol was another type of PCM evaluated at different dosages in asphalt binder with the direct incorporation method. The results showed that the addition of PEG decreased the complex shear modulus (G^*) of asphalt at different frequencies at low temperature (40℃) and increased the complex shear modulus in the range of low frequencies at high temperature (80℃). It was also found that that the addition of PEG decreased the phase angle (δ), regardless of test temperature and frequency. Also, the MSCR test showed that adding PEG reduced J_{nr} at the loading level of 0.1 kPa; however, it increased J_{nr} when the loading level is 3.2 or 12.8 kPa (Du et al. 2019). In addition, the influence of expanded graphite/polyethylene glycol composite phase change material (EP-CPCM) with the melting point of 46.9 ℃ on the rheological performance of base binder and SBS modified binder was evaluated. EG/PEG functioning as fillers led to a decrease of phase angle and an increase of complex modulus and rutting performance. In addition, EG/PEG increased the value of the fatigue parameter $G^*\cdot\sin\delta$ which indicated a deterioration of the fatigue resistance at intermediate temperature. Finally, at low temperatures, the creep rate (m) of modified binders decreased while the creep stiffness increased, which was detrimental to the prevention of the low temperature cracking (Zhang et al. 2019). Kakar et al. employed microencapsulated PCM with Tetradecane and the melting point of 6℃ in two different dosages, 1% and 3%. The temperature sweep test indicated adding PCM decreased the complex modulus at different temperatures for binder 10/20; however, it increased the complex modulus for binders 70/100 and 160/220 (Kakar et al. 2019). Du et al. used the direct incorporation method to employ PEG at different percentages of 1%, 5%, 10% and 20% by weight of asphalt binder. A frequency sweep test at 60℃ showed adding PEG decreased the complex modulus and increased the phase angle which meant PED reduced the stiffness and limited the elastic component of the behaviors of the modified binders. In addition, temperature sweep tests indicated that the complex modulus and rutting factor of PEG modified binders were decreased by increasing the temperature compared to the control binder. Also, MSCR results at 60℃ indicated that J_{nr} decreases at the low stress of 0.1 kPa by adding PEG which explains the improving effect against deformation. However, at higher stress levels (3.2 and 12.8 kPa) adding PEG led to higher J_{nr} or lower resistance against permanent deformation. Also, it was noticed that at 25℃ with the increase of PEG content, the uniaxial compressive strength and split strength of asphalt mixtures were reduced, which led to lower shear strength (Du et al. 2019).

2.5.2.3. Modified Asphalt Mixture

Chen et al. employed two types of PCMs PCM-L and PCM-Z with different phase change temperatures and latent heat storage equal to 45 °C, 110 J/g and 50 °C, 100 J/g, respectively. Both types of PCMs were

organic acids, and expanded graphite was used as supporting material with capillary and surface tension forces to prevent PCM from leaking. The results of the indirect tensile strength tests at different temperatures (10, 25, and 50 ℃) showed that the tensile strength of both PCM-modified mixtures was lower than the control sample. The researchers believed that the supporting material of PCMs provides a lubricant function in the mix. Also, a decrease happened in the rutting resistance of modified asphalt samples, and more permanent deformation was observed in PCM-modified mixtures. A three-point bending test was conducted to determine the low-temperature cracking resistance of asphalt mixtures with PCMs. It was observed that PCM-Z manifested the best performance against low-temperature cracking in comparison to the control and PCM-L samples (Chen et al. 2012). Yinfei et al. used the impregnation method to fabricate CPCM consisting of polyethylene glycol and fly ash ceramsite with three different particle size ranges. Also, some CPCMs were coated with cement paste and cures for 24 h (Fig. 14). The results showed fly ash with smaller particle size had higher PEG absorption and higher heat enthalpy. No visible leakage was observed in the CPCMs coated with cement paste after 1 hour at 160 ℃. Moreover, the uniaxial compressive test and split test at the temperature of 25 ℃ on modified asphalt mixtures exhibited a lower mechanical strength. It is worth mentioning that the composite PCM with a smaller particle size had lower impact on the overall strength of the asphalt mixture (Yinfei et al. 2020).

Fig. 14 Impregnated LWA coated with cement paste (Yinfei et al. 2020).

Li et al. used a high-temperature epoxy resin adhesive to microencapsulate n-tetradecane/tetradecanol and melamine-urea-formaldehyde as the core and wall materials, respectively. Then, the PCM microcapsules were used to replace part of the coarse aggregate. Based on their findings, the immersion stability of asphalt mixtures decreased as the content of the reinforced PCM microcapsules increased. Also, the residual stability of the immersion Marshall sample decreased insignificantly. PCM microcapsules had a slight decrease in the freeze-thaw splitting strength of asphalt samples. The bending beam rheometer test at low temperature suggested that adding microencapsulated PCM decreased the stiffness of asphalt mixtures (Li et al. 2018). Chen et al. evaluated modified asphalt with a paraffin/expanded graphite shape-stabled phase change material with a phase change temperature range of 40 °C – 50 °C. Paraffin wax and expanded graphite were utilized as PCM and supporting (to prevent from PCM leaking) materials in mixtures, respectively. They used an apparatus to simulate solar radiation (by a 300W metal halide lamp and temperature sensors). Based on their observations, in the heating process, the temperature increasing rate of the modified asphalt concrete was lower than that of the control asphalt sample, but in the cooling process, the temperature decreasing rate of the modified asphalt sample was higher than that of the control sample. The temperature of the sample with PCM is about 2℃ lower than the control sample on average (Chen et al. 2011). Ryms et al. impregnated lightweight aggregate

(size 4-8 mm) with ceresin (MP: 43 – 78 ℃); then, they used it in the asphalt mixture by two methods. In the first method, the modified asphalt sample was 60 mm thick; in the second method, a cover of asphalt with the thickness of 30 mm was added to the modified asphalt sample. Rutting results showed that the asphalt mixture with PCM had lower rutting resistance at 60 ℃ (Fig. 15) although adding the second layer improved the rutting resistance of asphalt sample (Fig. 16) (Ryms et al. 2017).

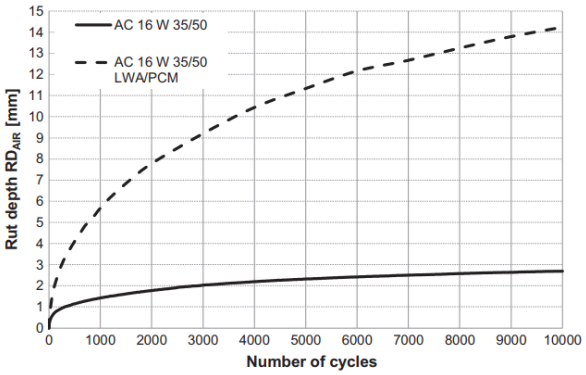

Fig. 15 Rut depth of LWA modified asphalt mixture compared to control sample (Ryms et al. 2017).

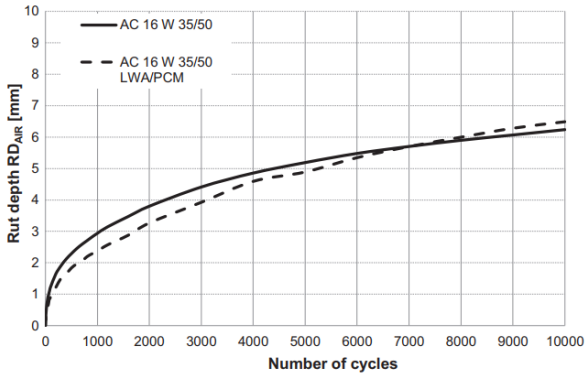

Fig. 16 Rut depth of LWA modified asphalt mixture (with a cover of 30 mm asphalt layer) compared to control sample (Ryms et al. 2017).

2.5.2.4. Thermal Stability

As mentioned, one of the important criteria in selecting appropriate PCM as thermal energy storage in asphalt applications is the thermal stability of PCM. TGA (thermogravimetric analysis), DSC (differential scanning calorimetry), FTIR (Fourier-transform infrared spectroscopy), and SEM (scanning electron microscope) have been used to evaluate the thermal stability of phase change materials. Sari and Kaygusuz assessed the thermal stability of palmitic acid; they reported good thermal stability and no supercooling phenomenon. Also, they found the melting point and latent heat capacity as 58 – 64 C and 190–220 kJ/kg, respectively (Sari and Kaygusuz 2002). Wei et al. fabricated micro-encapsulated CPCM by encapsulating tetradecane with melamine formaldehyde (MF) resin for asphalt applications. The proper performance of MF as encapsulation materials prevented leaking and improved the thermal stability in asphalt material (Wei et al. 2019). He et al. employed the sol-gel incorporation method to develop SSPCM as shape-stabilized phase change material. TGA curve showed the good thermal stability of the composition of

PEG and SiO_2 which indicated that PEG was dispersed into the carrier of SiO_2, forming a stable core-shell structure. In addition, they did not report any leakage after repeating heating and cooling cycles (Wei et al. 2019). Zhou et al. used LWA (lightweight aggregate) as porous material and employed the impregnation method to produce macro encapsulation PCM. Polyester resin was used to coat LWA. Also, to prevent agglomeration of LWA coated with resin, they used granite powder. Granite powder was used to increase the roughness of the surface, the interlock with a potential matrix during hardening, and aggregate-paste bond strength. They measured the melting temperature and latent heat storage capacity of PCM before and after thermal cycling. According to their investigation, the melting temperature changed only 0.7 °C while the enthalpy changed by 12.56 kJ/kg, which indicates good thermal stability of PCM (Zhou et al. 2018). Fig. 17 presents the macro encapsulated PCMs prepared by them.

Fig. 17 Impregnated LWA coated with polyester resin and granite powder (Zhou et al. 2018).

Mix blending method has also been used to mix asphalt binder and lauric acid (PCM) which is a type of fatty acids. After 100 heating and freezing cycles, the thermo-physical properties of modified asphalt exhibited a very slight change of the phase change temperature of modified asphalt; besides, no leakage was observed after 100 cycles. Finally, thermogravimetric analysis was performed to evaluate the thermal reliability and stability of mixtures. Overly, the results showed good thermal stability of modified samples (Kong et al. 2017). Wei et al. prepared capric acid/expanded perlite (CA/EP) and capric-stearic acid/expanded perlite (CA-SA/EP) composites by the macro encapsulation method. To find the thermal stability of the samples, they heated the samples at different temperatures, i.e., 50 °C, 70 °C, and 90 °C. They evaluated the leakage of the PCMs at the aforementioned temperatures. Based on their observations, the optimum mass ratio of fatty acids was 50%, without any leakage; so, the composite with 50% fatty acid could be considered as a form-stable PCM. Also, the DSC curve, after 500, 800, and 1000 thermal cycles, indicated slight changes in the phase change temperature and latent heat. In general, the composite PCMs with 50% fatty acids manifest excellent thermal reliability, as confirmed by the variations in their phase change temperatures and latent heat storage potentials (Wei et al. 2014). In another research, paraffin was used as the core material, and SiO_2 prepared with methyl triethoxysilane (MTES) acted as the shell material, using a sol-gel method. TGA results proved that microcapsules had good thermal stability due to the synergistic effect between the paraffin and SiO_2 shell (Chen et al. 2013). He et al. employed the method of shape-stabilized phase change materials to incorporate PCM in the asphalt concrete. They used polyethylene glycol 2000 (PEG2000) and silica sol (SiO_2) as the PCM and supporting material, respectively, and mixed them using the sol-gel method in the mixtures. Since the asphalt samples need to resist against high temperature during asphalt production; therefore, the thermal stability was evaluated. In this regard, the shape-stabilized PCM were kept in oven at 200 °C for 60 min, but no mass loss was observed (He et al. 2013). Karaman et al. fabricated composite phase change material by

incorporating polyethylene glycol (PEG 1000) into the pores of the diatomite using the vacuum impregnation method. The TG curves before and after 1000 thermal cycling number indicated good thermal stability of the composite PCM (Kamran et al. 2013). Sari et al. evaluated CPCM consisting of lauric acid (LA, 98% pure) within expanded perlite (EP). During the impregnation, the PCMs were simultaneously heated at a constant temperature above the melting temperature of LA. To assess the thermal stability, DSC test was performed after 1000 thermal cycling to compare with the original CPCM. The results showed that the phase transition temperatures had a little drop after 1000 thermal cycling. After repeated 1000 thermal cycling, the latent heat value of melting changed by -1.2% as the latent heat value of freezing changed by -4.1%. The FT-IR spectra test showed that the shape and frequency values of all peaks did not change after thermal cycling, which indicated the chemical structure of the composite was not affected by repeated melting/freezing cycling. Finally, SEM images of CPCMs were similar after thermal cycling. This finding meant that no degradation in the structure of composite occurs after thermal cycling. Therefore, it can be concluded that the LA/EP composite was chemically and structurally stable after 1000 thermal cycling (Sari et al. 2009). Jin et al. encapsulated the composition of PCM and ceramsite (with particle size between 4.75 mm and 9.5 mm) by epoxy. After 100 thermal cycling the latent heat of the microencapsulated PCMs decreased which can related to the evaporations of the PCMs in the pores of the CS. They could also investigate the leakage of the PCMs by placing the samples in oven at 80℃ for 1 h using filter paper. It was observed that the encapsulation decreases the leakage of PCMs although there still was leakage (Jin et al. 2018).

2.6. Summary

In this chapter, a review of the recent research works was presented to illustrate new findings of employing phase change materials in cementitious and asphalt materials. Various types of thermal distresses, including rutting, low-temperature cracking, and thermal fatigue cracking (block cracking), in asphalt pavements were defined, and the factors and mechanisms that lead to the thermal distresses were elaborated. In addition, phase change materials (PCMs) were defined, and their performance as latent heat storage materials in storing and releasing heat energy were discussed. Moreover, the different classification of PCMs and the advantages and disadvantages of PCMs which were commonly used in construction materials, concrete and asphalt, were mentioned. Finally, civil engineering applications and the incorporation methods of employing PCMs in asphalt materials and basic binder testing, rheology properties, thermal stability, and asphalt mixture were stated.

Chapter 3. Improving Rheological and Thermal Performance of Gilsonite-Modified Binder with Phase Change Materials

3.1. Introduction

Phase-change materials (PCMs) have been used in civil infrastructures to regulate the temperature changes and improve the thermal behaviors of construction materials. In this study, Gilsonite and a polyethylene glycol (PEG) which is a latent heat storage PCM with a low melting point (Rowe et al. 2014) were used as asphalt binder modifiers to improve the binder performance under a large range of temperatures. In the previous study, Gilsonite was found to be able to improve the binder rutting resistance while compromising the low-temperature cracking resistance (Liu and Li 2008). The objective of this study is to identify the allowable Gilsonite content without compromising the binder low-temperature performance with the incorporation of PCM. A series of rheological tests were conducted to evaluate the behaviors of the Gilsonite-PEG-modified binder at high, low, and intermediate temperatures. Thermal tests were performed to assess the impact of the additives on the thermal properties of the binders.

Gilsonite is a naturally occurring glossy black asphaltic and known as asphalt binder modifier for its good affinity with asphalt and superior bonding. As a natural lake asphalt, Gilsonite can be quickly dissolved in the binder and coat aggregate particles during the mixing process providing additional bonding strength between different components. In a previous research study, the researchers have found that using Gilsonite-modified binders can improve stripping resistance of pavements and reduce the shoving and rutting susceptibility (Liu and Li 2008). Kok et al. confirmed that as the dosage of Gilsonite increased, the value of the rutting parameter ($G^*/\sin\delta$) increased, indicating the rutting resistance was improved. The findings have been confirmed by other researchers using testing methods such as the multiple-stress creep- recovery (MSCR) test (Ameri et al. 2011 2012 2018, Ren et al. 2018, Mirzaiyan et al. 2019). However, it has also been reported that incorporating Gilsonite may adversely affect the fatigue and low-temperature performance of pavements as it changes the oil-to-asphaltene content (Aflaki and Tabatabaee 2009, Ameri et al. 2012, Roshan et al. 2014, Quintana et al. 2016, S. Ren et al. 2018, Sehhat and Mahdianikhotbesara 2021). The addition of Gilsonite can also increase the mixing and compaction temperatures as the Gilsonite increases the binder viscosity; thus, leading to greater energy consumption (Aflaki and Tabatabaee 2009, Kök et al. 2011).

3.2. Materials and Specimen Preparation

3.2.1. Materials

An Alaskan PG 52-28 binder was selected as the base binder in this study. A U.S. manufactured Gilsonite was used as the binder modifier for improving the high-temperature performance. It was in powder form before mixed with the base binder. A PEG with an average molar mass of 400 $g \cdot mol^{-1}$, or PEG 400, was added to ensure the binder's low-temperature performance. It is worth mentioning that PEG 400 is a safe and non-toxic material with different applications such as medicines used in eye drops to treat dry eyes (Fig. 18). In this regard, the PEG with a low melting point (4 ℃) is selected in this study. The testing results from the preliminary study suggested that when over 5% of PEG was mixed with binder, segregation between PEG and binder started to occur. Therefore, to avoid segregation, the dosage of PEG 400 was limited at 5%. Table 9 presents the physical and thermal properties of PEG 400. To determine the optimum dosage of the modifiers, Gilsonite was added at different concentration levels, i.e., 0%, 3%, 6%, 9%, and 12%, by weight. Table 10 presents the physical properties of Gilsonite. The process to determine the dosage of Gilsonite is illustrated in the following section.

Fig. 18 Eye drops containing polyethylene glycol 400.

Table 9. Basic Characteristics of Polyethylene glycol

Physical properties	**Values or characteristics**
Molecular weight ($g.mol^{-1}$)	400
Physical state	Liquid
Flash point (℃)	235
Specific gravity	1.128
Viscosity (mPa·s at 20℃)	110-125
Solubility	Soluble in water
Melting Point (℃)	4

Table 10. Gilsonite Specification and Properties

Physical properties	**Measured values**
Penetration	0
Softening point (℃)	160-185
Flash point (℃)	316
Specific gravity	1.06
Ash	≤1.0%
Decomposition temperature (℃)	287.8

3.2.2. Preparation of PEG and Gilsonite-modified Asphalt Binders

The mixing temperature to blend the base binder and the additives was determined to be 185℃ based on the softening point of Gilsonite. The neat binder was first heated to the target temperature in a heating mantle. The Gilsonite powder was added gradually to the binder to ensure a uniform dispersion. The mixture was stirred for 30 minutes using a high shear mixer at 2000 rpm. PEG 400 was added afterwards

and mixed for another 30 minutes at 4000 rpm. To limit the evaporation and decomposition of PEG, the heating temperature was decreased to 150 ℃ before the addition of PEG. Different dosages of Gilsonite were used in this study, and the samples were designated based on the percentages of the modifiers. For example, P5G6 indicated the binder contained with 5% PEG and 6% Gilsonite by weight. **Error! Reference source not found.** presents the designations of the modified binders, types of modifiers, and the percentages used in this research.

Table 11. Modified Binders with Different Dosages of Gilsonite and PEG

Designation	Polyethylene glycol (%)	Gilsonite (%)
Neat binder	0	0
G3	0	3
P5G3	5	3
G6	0	6
P5G6	5	6
G9	0	9
P5G9	5	9
G12	0	12
P5G12	5	12

3.3. Research Methods

In this study, the performance of the modified asphalt binders was evaluated through rheological tests at different temperatures targeting different types of distresses. The tests included dynamic shear modulus test, the bending beam rheometer (BBR) test, the multiple stress creep recovery (MSCR) test, and the linear amplitude sweep (LAS) test. The binders with different dosages of modifiers were graded based on the Superpave performance grading system, and the testing results were analyzed by the performance models and parameters such as ΔT_c, the Glover-Rowe (G-R) parameter, and the ViscoElastic Continuum Damage (VECD) model. Thermal tests and analyses were conducted following the rheological tests to evaluate the impact of the PCM on asphalt binder thermal behaviors. The thermal conductivity, heat capacity, and glass transition temperatures of the modified binders were measured, the decomposition temperature was evaluated using thermogravimetric analysis (TGA) methods. The testing methods and the corresponding evaluation parameters in this study are summarized in Table 12.

Table 12. Summary of Binder Tests

Test	Purpose	Parameter	Specification
Rotational viscometer test	Mixing and compaction temperature	η	AASHTO T 316
Bending beam rheometer	Low temperature performance	*S*, *m-value*, ΔT_c	AASHTO T 313
Dynamic shear rheometer (DSR) test	High temperature performance grade	$G^*/\sin\delta$	AASHTO M 320
Multiple Stress Creep Recovery (MSCR) test	High temperature performance	J_{nr} and *R*	AASHTO T 350
Glover-Rowe (G-R) parameter analysis	Cracking potential	*G-R*	Not Applicable
Linear amplitude sweep (LAS) test	Fatigue resistance	C-S curve, N_f	AASHTO T 391
Thermal conductivity and heat capacity test	Thermal conductivity and heat capacity test	*k*, *c*	Not Applicable
Thermogravimetric Analysis (TGA)	Degradation temperature	*T*	Not Applicable
Differential Scanning Calorimetry (DSC) Test	Glass transition temperature	T_g	Not Applicable

3.3.1. Tests for Binder Viscosity and Workability

The viscosity of the binders was measured using the rotational viscometer (RV) at 125, 135, 145, and 155 ˚C. The RV test was conducted to evaluate the pumpability, mixability, and workability of the binder. The test was also used to determine the mixing and compaction temperatures for different binders.

3.3.2. Low-Temperature Tests for Cracking Susceptibility Evaluation

The BBR test was used to determine the low-temperature performance grades (PGs) of the binders. The tests were conducted at -12, -18, and -24 ˚C after the Rolling Thin-Film Oven (RTFO) and Pressure Aging Vessel (PAV) aging conditioning. In addition to using the low performance grade, the cracking resistance of the modified binders at low temperatures were also evaluated using the ΔTc parameter. The parameter was obtained by calculating the difference between the critical temperatures for creep stiffness ($T_{c,S}$) and relaxation rate ($T_{c,m}$). The critical temperatures were determined using Equations (1) and (2).

$$T_{c,S} = T_1 + \left(\frac{(T_1 - T_2) \times (\log 300 - \log S_1)}{\log S_1 - \log S_2}\right) - 10 \quad (1)$$

$$T_{c,m} = T_1 + \left(\frac{(T_1 - T_2) \times (0.300 - m_1)}{m_1 - m_2}\right) - 10 \quad (2)$$

where, S_1 is the creep stiffness at T_1 in MPa, S_2 is the creep stiffness at T_2 in MPa, m_1 is the creep rate at T_1, T_1 is the temperature (˚C) at which S and m pass the criteria (S≤300 MPa and m≥0.300), and T_2 is the temperature (˚C) at which S and m no longer meet the criteria (S>300 MPa or m<0.300). The ΔT_c value was then calculated using Equation (3).

$$\Delta T_c = T_{c,S} - T_{c.m} \quad (3)$$

3.3.3. High-Temperature Tests for Rutting Resistance Evaluation

In terms of rutting resistance, the binders were evaluated using the Superpave rutting factor ($G^*/\sin\delta$) and the MSCR test. Both tests were conducted on a dynamic shear rheometer (DSR). The rutting factor, $G^*/\sin\delta$, was obtained from the dynamic shear modulus tests at 10 rad/s conducted in the linear viscoelastic range on binder specimens at different aging levels, i.e., unaged, aging conditioned using the RTFO, and aging conditioned using the PAV after the RTFO conditioning. For the unaged and RTFO-aged specimens, the temperature sweep shear modulus test started at 40℃ and 46℃, respectively, and the testing temperature increased with a 6℃ increment according to AASHTO M 320. Two replicates were tested at each aging condition.

The MSCR test was conducted on the specimens after the RTFO aging conditioning as per AASHTO T 350. The test was performed by applying creep stresses with two magnitudes, i.e., 0.1 and 3.2 kPa at 52 and 58 ℃. Two parameters were obtained from the MSCR test, i.e., the non-recoverable creep compliance, Jnr, and the percent recovery, R. The recovery percent at creep stress levels of 0.1 and 3.2 kPa ($R_{0.1}$ and $R_{3.2}$) were calculated using Equations (4) and (5), respectively.

$$R_{0.1} = \frac{\sum_{N=11}^{20} [\in_{r(0.1,N)}]}{10} \quad (4)$$

$$R_{3.2} = \frac{\sum_{N=1}^{10} [\in_{r(3.2,N)}]}{10} \quad (5)$$

Where N is the cycle number at each stress level and $\in_r$ is the percent recovery at 0.1 kPa and 3.2 kPa. The non-recoverable compliance was calculated by the Equations (6) and (7), and the percent difference in non-recoverable creep compliance could then be expressed as Equation (8).

$$J_{nr_{0.1}} = \frac{\sum_{N=11}^{20} [J_{nr(0.1,N)}]}{10} \quad (6)$$

$$J_{nr_{3.2}} = \frac{\sum_{N=1}^{10} [J_{nr(3.2,N)}]}{10} \quad (7)$$

$$J_{nr_{diff}} = \frac{[J_{nr_{3.2}} - J_{nr_{0.1}}] \times 100}{J_{nr_{0.1}}} \quad (8)$$

3.3.4. Intermediate-Temperature Tests for Cracking Resistance Evaluation

In this study, the cracking potentials of the asphalt binders were assessed using the Glover-Rowe parameter and the fatigue performance predicted using the LAS tests and the ViscoElastic Continuum Damage (VECD) model.

The G-R parameter was calculated using the dynamic shear modulus data at 0.005 rad/s and 15℃. The parameter was developed as a rheological index to evaluate the fatigue cracking resistance of asphalt binders at low temperatures (Rowe et al. 2014, Moreno-Navarro et al. 2018). The parameter was defined as presented in Equation (9):

$$G\text{-}R = \frac{G^* \cos^2 \delta}{\sin \delta} \quad (9)$$

Where G* is the complex shear modulus and δ is the phase angle at the corresponding temperature and loading frequency. The thresholds for the damage onset and the significant cracking were 180 kPa and 450 kPa, respectively.

The LAS test was conducted to evaluate the binder fatigue resistance and predict its fatigue life under repeated loads as per AASHTO T 391. The test was performed using the DSR with 8 mm-diameter plates at 16 ℃ on specimens after the RTFO and PAV aging conditioning. Prior to the LAS test, a frequency sweep test at frequencies from 0.2 to 30 Hz with constant strain level of 0.1% was performed to obtain the undamaged material properties within the linear viscoelastic range. The LAS test was then conducted at a frequency of 10 Hz with increasing shear strain from zero to 30% over 3100 cycles of loading. The VECD model was used to analyze the testing results. According to the LAS testing protocol, the definition of failure was 35% reduction in modulus, or, in other words, when the material integrity, C, defined by Equation 10, decreased from the value of 1 to 0.65.

$$C(t) = \frac{\left|G^*\right|(t)}{\left|G^*\right|_{initial}} \quad (10)$$

where $|G^*|(t)$ is the complex modulus at time t, and $|G^*|_{initial}$ is the undamaged and initial value of $|G^*|$. The number of cycles to failure can be calculated by Equation 11.

$$N_f = A(\gamma_{\max})^B \quad (11)$$

where N_f is fatigue life, γ_{max} is the maximum shear strain for the pavement structure, and A and B are the model coefficients.

3.3.5 Thermal Behavior Evaluation

In addition to enhancing the binder low-temperature performance, another merit of using PCM is to improve materials' thermal behavior. PCM can absorb extensive amount of heat at temperatures close to their melting point and, thus, mitigate the temperature changes within the asphalt mixtures. In this study, two important thermal properties of the asphalt binders, i.e., the thermal conductivity and volumetric heat capacity were first measured using the Thermal Constants Analyzer (TPS 500S, Hot Disk, Sweden). The specimens were prepared as pellets and tested at room temperature of 21±1 ℃.

In addition, the thermogravimetric analysis (TGA) was performed to evaluate the thermal stability of the binders. In this test, the decomposition temperature was analyzed using the TGA and Differential Thermal Analysis (DTG) curves. During the test, binders with a mass of around 10 mg were heated from room temperature to 800 ℃ under nitrogen atmosphere flow. The heating rate was set at 10 ℃/min.

To complete a full evaluation of the thermal properties of the modified binder, the researchers also used a Differential Scanning Calorimetry (DSC) to measure the glass transition temperature. The glass transition was defined as a reversible change of material from the viscoelastic state to the glassy or brittle state (Wang et al 2017), and during the transition, the molecular motions were immobilized. Below the glass transition temperature, asphalt binder exhibited glassy and brittle behaviors, and at temperatures above the glass transition temperature, viscoelasticity dominated the material behaviors (Baldino et al. 2012). In this study, the DSC scan was conducted from -60℃ to 100℃ at a heating rate of 2℃/min under nitrogen atmosphere flow.

3.4. Testing results

3.4.1. Binder Performance Evaluations

3.4.1.1. Low-Temperature Performance of the Gilsonite-PCM-modified binders

While the dosage of PEG was fixed at 5% to prevent segregation, the low-temperature performance of the binders with different Gilsonite contents were evaluated using the BBR creep stiffness tests. Fig. 19 illustrates the creep stiffness and the m-values for the neat and modified binders. The critical temperatures for creep stiffness, S, and creep rate, m, were determined at threshold values at 300 MPa, and 0.3, respectively, as indicated by the red lines. Table 13 summarizes the critical temperatures and the low performance grades of the binders with different concentration levels of modifiers. As the Gilsonite content increased, the critical temperature increased, which indicates the adverse effects of Gilsonite on the low-temperature performance of asphalt binders. At the same Gilsonite concentration level, the critical temperature decreased by 2.4℃ in average with the addition of 5% PEG. As a result, the low PG of the G6 binder with PEG (P5G6) was restored from -22 to -28. Based on BBR testing results, the maximum Gilsonite level was determined to be 6%, and in the remaining investigation, the binders with up to 6% Gilsonite were tested.

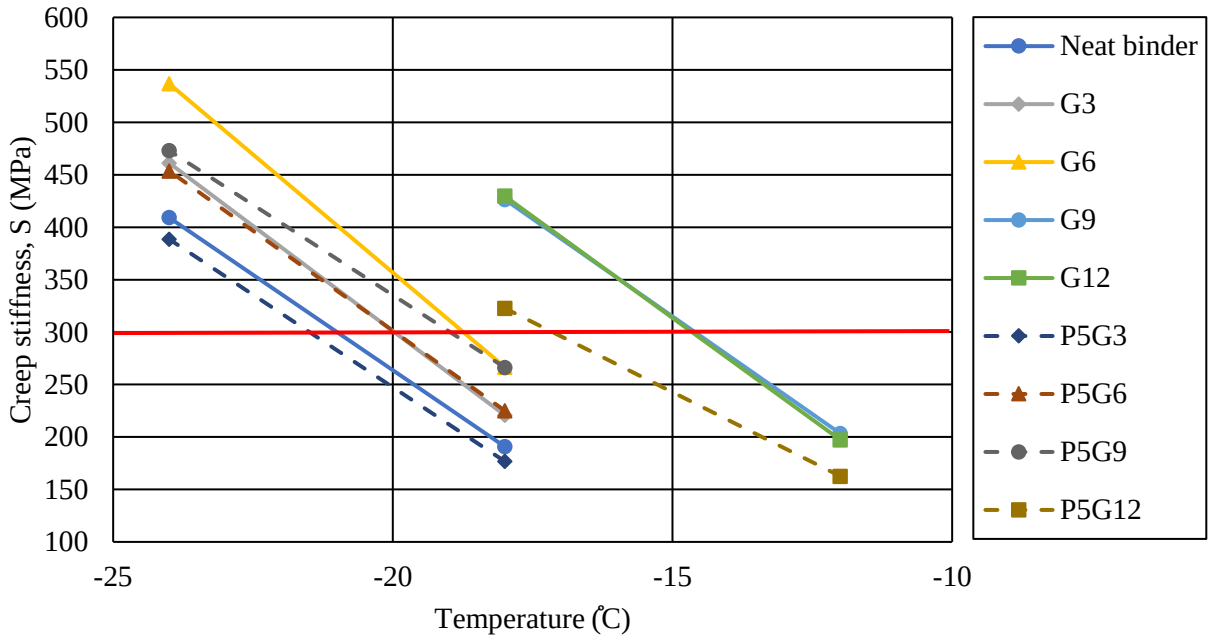

(a)

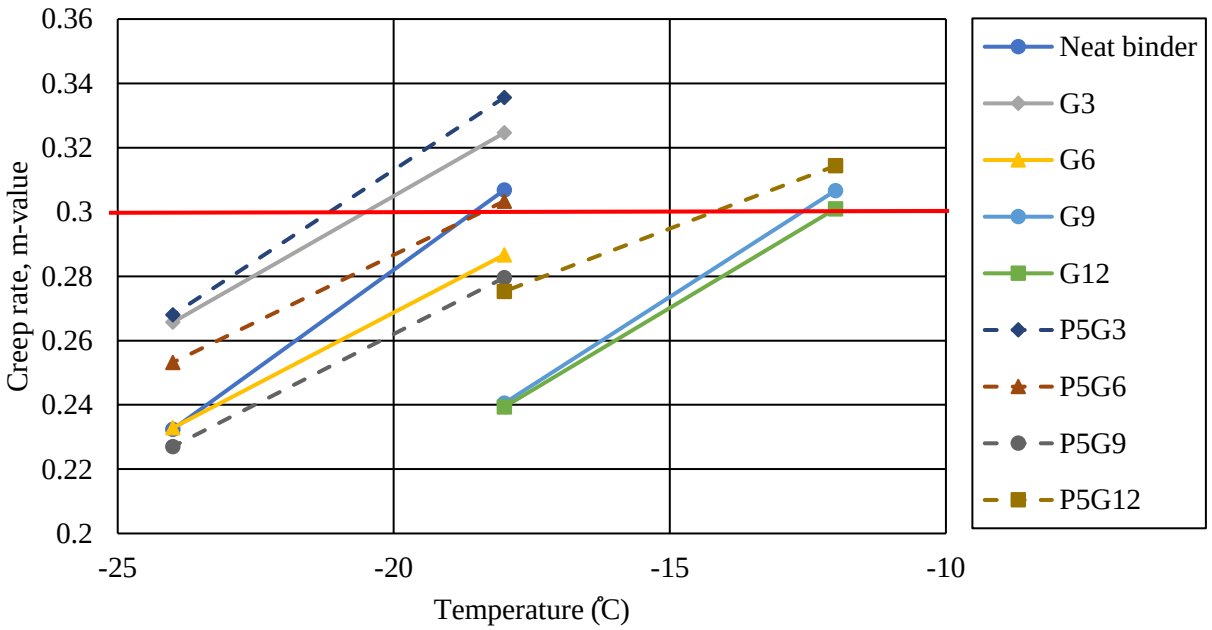

(b)

Fig. 19 Low-temperature performance of neat and modified binders, (a) creep stiffness value, and (b) m-value.

Table 13. Binder Codes, Composition, and Low-temperature Performance Grade of Binders

Binder	**Critical temperature by creep stiffness (°C)**	**Critical temperature by m-value (°C)**	**S or m-value controlled**	**Low PG**	**ΔT_c**
Neat binder	-21.0	-18.5	m-value controlled	-28	-2.5
G3	-20.0	-18.3	m-value controlled	-28	-1.7
G6	-18.7	-16.5	m-value controlled	-22	-2.2
G9	-14.6	-12.6	m-value controlled	-22	-2
G12	-14.6	-12.1	m-value controlled	-22	-2.5
P5G3	-21.5	-21.0	m-value controlled	-28	-0.5
P5G6	-19.9	-18.3	m-value controlled	-28	-1.6
P5G9	-19.0	-15.7	m-value controlled	-22	-3.3
P5G12	-17.8	-14.2	m-value controlled	-22	-3.61

The low temperature cracking resistance was further evaluated using the ΔTc parameter. The parameter indicates the difference between the critical temperatures of creep stiffness and relaxation rate obtained from the BBR tests. If $\Delta T_c > 0$, the binder is stiffness-controlled or S-controlled; if $\Delta T_c < 0$, the binder is m value-controlled. An S-controlled binder or binder with higher ΔT_c values is usually more desirable. Table 13 presents the ΔT_c values of binders with different PEG and Gilsonite contents. It can be observed that the binders with PEG exhibited higher ΔT_c values than the ones with the same Gilsonite concentration levels. The results showed that the addition of PEG improves the low temperature cracking resistance.

3.4.1.2. Evaluation of Binder Workability

After the performance evaluation, the workability of the modified binders was assessed using the rotational viscometer. Fig. 20 presents the dynamic shear viscosity curves at different temperatures for different binders. The testing results indicate that the Gilsonite increased the viscosity of the binder and the addition of the PEG had moderated the viscosity of the binder at all temperatures. The binder viscosities are related to their workability. A low viscosity at the mixing and compaction temperature ranges can provide sufficient workability and potentially decrease the mixing and compaction temperature, which can lower the energy consumption and limit the greenhouse gas emissions (Sun et al. 2016). The viscosity at the reference temperature of 135 ̊C was used as an index of the binder workability. Fig. 21 presents the viscosities of the binders at 135 ̊C. It can be observed that the binder with the Gilsonite (G3 and G6) had high viscosity at 135 ̊C and adding PEG to the Gilsonite-modified binders decreased the binder viscosity and improved the workability. According to ASTM D6373, all the binders including G6 exhibited sufficient workability since their viscosities at 135 ̊C were lower than 3 Pa·s. Fig. 22 present the binder mixing and compaction temperatures based on the RV test results. The results indicate that the addition of 6% Gilsonite increased the mixing and compaction temperatures by 10 °C compared with the neat binder; however, the mixing and compaction temperatures of the modified binders remained in the acceptable range.

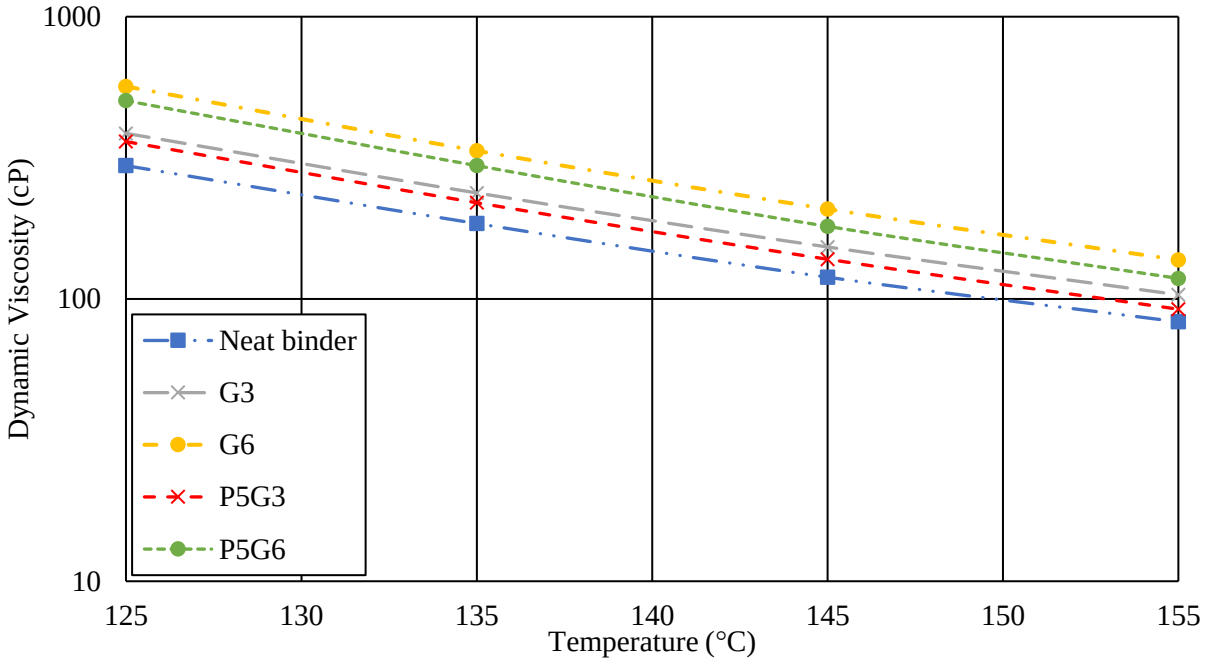

Fig. 20 Dynamic shear viscosity at different temperatures.

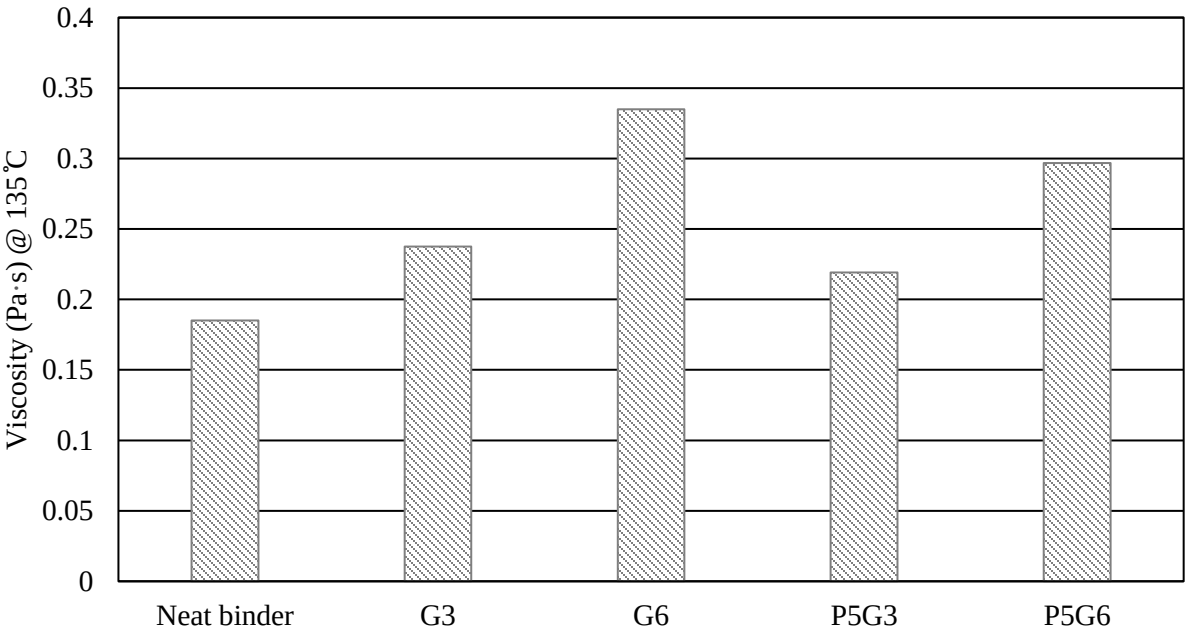

Fig. 21 The viscosity of samples at 135 ℃.

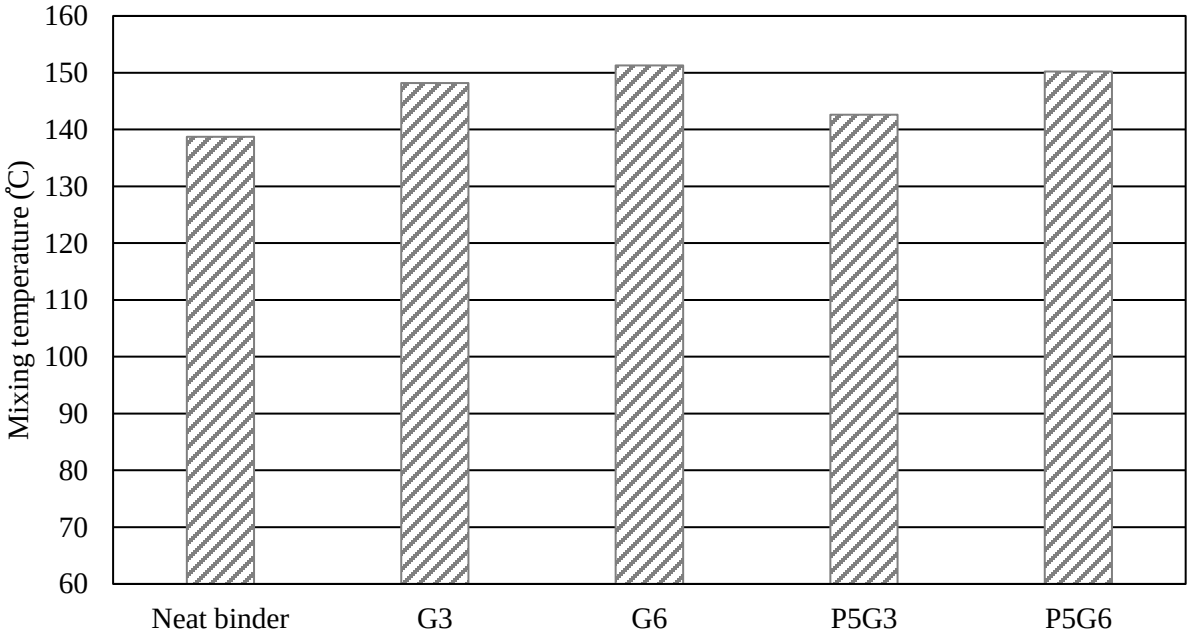

(a)

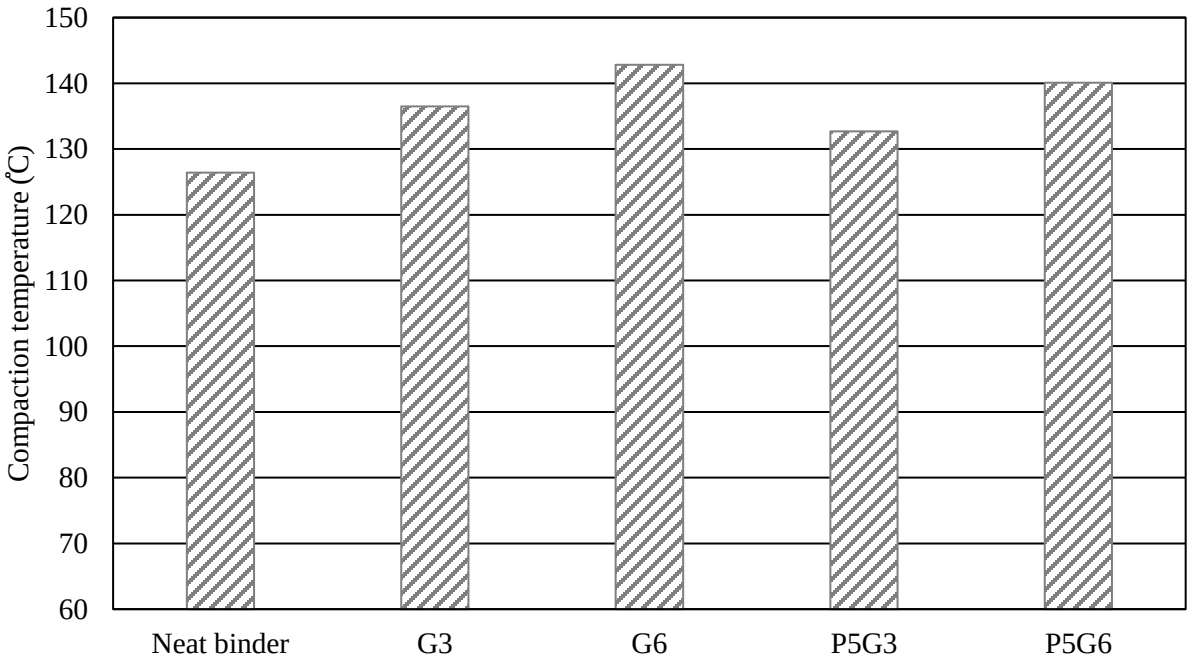

(b)

Fig. 22 (a) Average mixing temperature, (b) Average compaction temperature.

3.4.1.3. High-Temperature Performance of the Binders

The high PG of the modified binders were tested through the dynamic shear modulus tests using a DSR. Fig. 23 presents the complex shear modulus curves of specimens at various temperatures tested at 10 Hz. It can be observed that as the concentration level of Gilsonite increased, the shear modulus increased, and the addition of PEG also decreased the shear modulus at each temperature.

According to the Superpave PG grading specification AASHTO M 320, the rutting factor ($G^*/\sin\delta$) reflects the rutting resistance of the asphalt binder. A higher $G^*/\sin\delta$ value indicates greater rutting resistance. In Fig. 24, the G3 and G6 binders exhibited higher $G^*/\sin\delta$ values than the neat binder. The addition of PEG decreased the $G^*/\sin\delta$ values at each Gilsonite concentration level. According to Superpave specification, the rutting factor should be at least 1.00 kPa before RTFO aging and 2.2 kPa after RTFO short-term aging conditioning. The critical temperatures to pass the rutting criteria and the high PGs of the binders are presented in Table 14. The testing results indicated that the addition of 6% Gilsonite (G6) increased the high PG by two levels from PG 52 to 64. The addition of the 5% PEG balanced the performance at the high and low temperatures and lowered the high PG by one grade at each Gilsonite concentration level. Moreover, though the G6 binder is one level higher than that of the P5G6 binder, the critical temperatures for the unaged and the RTFO aged binder are only 2℃ and 2.4℃ lower than those of the G6 binder, respectively, and they are higher than those of the neat binder by 8.2℃ and 7.4℃, respectively. With the addition of PEG and Gilsonite, the P5G6 binder is almost qualified to be PG 64-28. The intermediate critical temperatures determined by the cracking factor $G^*\cdot\sin\delta$ are also presented in Table 14 for the purpose of performance grading.

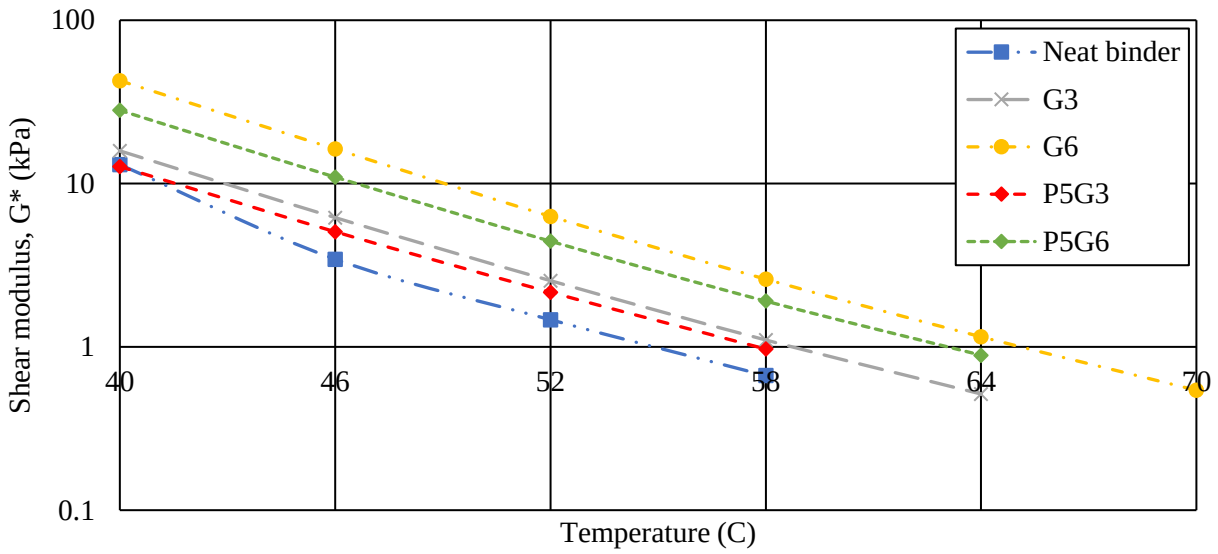

Fig. 23 Complex shear modulus of binders at different temperatures.

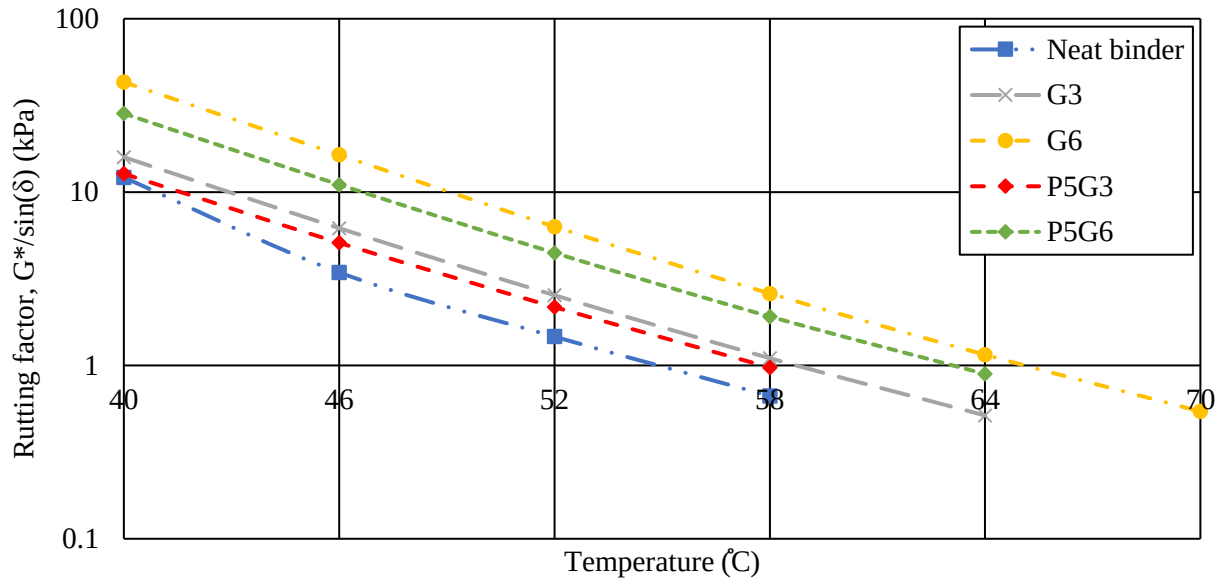

(a)

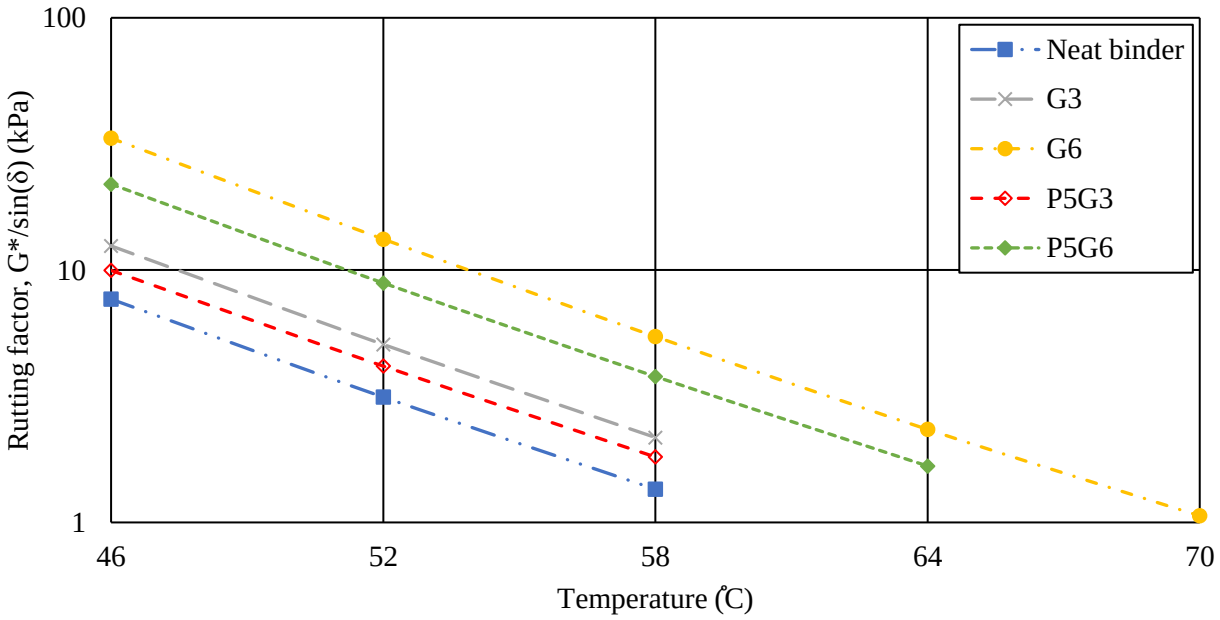

(b)

Fig. 24 Rutting factor of binders at different temperatures, (a) Unaged binder, (b) RTFO-aged binder.

Table 14. Critical Temperatures at Different Aging Conditions and Superpave Performance Grade (PG)

Binder	Critical temperature (℃)			Superpave performance grade (PG)
	Unaged binder ($G^*/\sin\delta$)	RTFO aged binder ($G^*/\sin\delta$)	RTFO+PAV aged binder ($G^*\cdot\sin\delta$)	
Neat binder	54.9	54.6	15.8	52-28
G3	58.8	57.9	18.2	52-28
G6	65.1	64.4	21.0	64-22
P5G3	57.8	56.6	16.0	52-28
P5G6	63.1	62.0	19.0	58-28

3.4.1.4. Multiple Stress Creep Recovery (MSCR) Test

In addition to the Superpave rutting factor, the rutting performance of the binders were evaluated beyond the linear viscoelastic range using the MSCR test on a DSR. The test was performed at 52 and 58 ℃ on specimens after RTFO aging conditioning. Table 15 and Fig. 25 present the average non-recoverable creep compliance (J_{nr}) at the stress levels of 0.1 and 3.2 kPa at 52 and 58 ℃. Gilsonite-modified binders exhibited lower Jnr values, which indicated a good performance of Gilsonite against rutting. This trend could be observed from tests at both stress levels and both temperatures. Introducing PEG to Gilsonite modified binder slightly increased the J_{nr} values. Comparing the testing results from binders with different Gilsonite concentration levels, it can be observed that the Jnr values were dominated by the content of Gilsonite. The modified binder P5G6 exhibited lower J_{nr} at different temperatures than the G3 binder and the neat binder.

Recovery values (R) is another indicator of the rutting resistance of the binders. A higher R value indicates more elastic recovery after loading. According to Table 15, while the elastic recovery of the neat binder at 3.2 kPa was found as zero, after adding 6% Gilsonite, the R value was increased to 6.34%. Table 15 and Fig. 26 also indicate that the R values of the P5G6 and G6 binder were significantly higher than binders with other Gilsonite concentration level. Unlike the trend in Jnr, the addition of 5% PEG slightly increased the R value at each Gilsonite concentration level. The MSCR testing standard requires the difference between the creep compliance at 3.2 kPa and 0.1 kPa to 75% and no binder exceeded the 75% limit.

In summary, both the rutting factor $G^*/\sin\delta$ and the MSCR test results indicated that the binders with 6% Gilsonite (i.e., G6 and P5G6) exhibited superior rutting resistance and the addition of PEG has a minor impact of the rutting susceptibility at each Gilsonite concentration level.

Table 15. R, J_{nr}, and $J_{nr,diff}$ of the Neat Binder and Modified Binders

Binder specimen	**Temperature (℃)**	J_{nr} **(kPa^{-1})**		**Recovery (%)**		$J_{nr,diff}$ **(%)**
		0.1 kPa	**3.2 kPa**	**0.1 kPa**	**3.2 kPa**	
Neat binder	52	2.72	3.09	2.96	0	13.59
	58	6.54	7.34	0.33	0	12.24
G3	52	1.68	1.86	4.42	0.49	10.70
	58	4.16	4.53	0.90	0	8.73
G6	52	0.57	0.63	11.57	5.43	10.88
	58	1.51	1.71	6.12	0.86	13.23
P5G3	52	1.95	2.43	4.81	1.02	24.21
	58	4.79	5.95	1.52	0	24.20
P5G6	52	0.78	0.94	13.52	6.34	21.50
	58	2.04	2.64	7.64	0.72	29.15

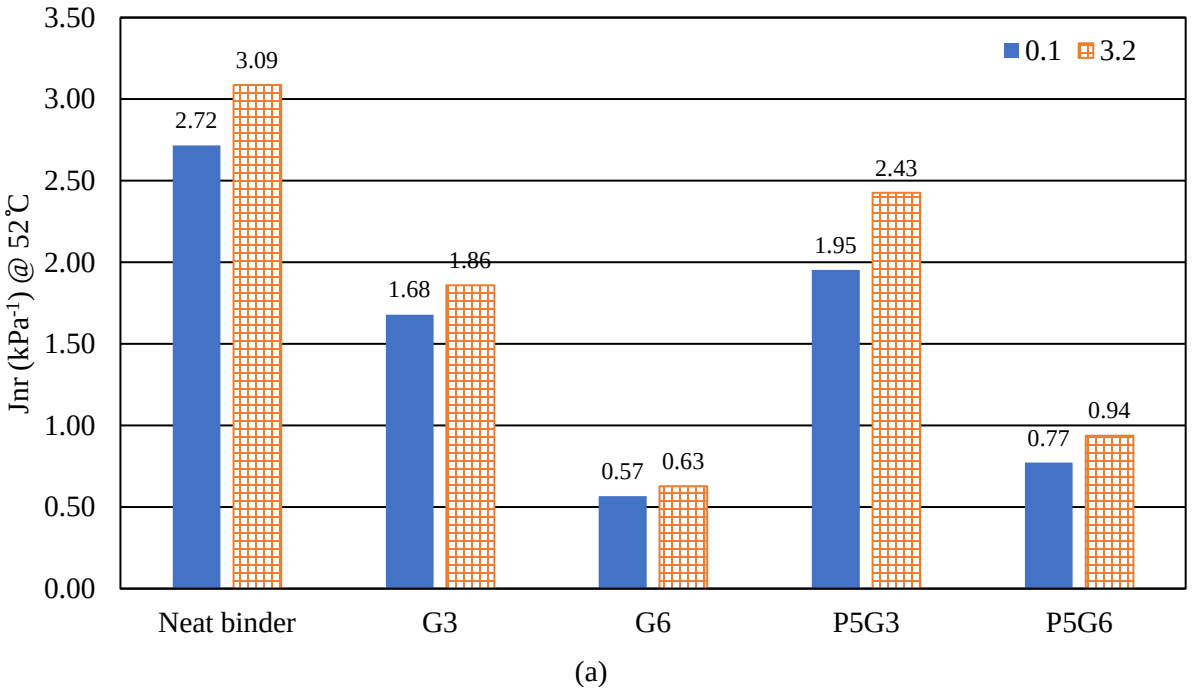

(a)

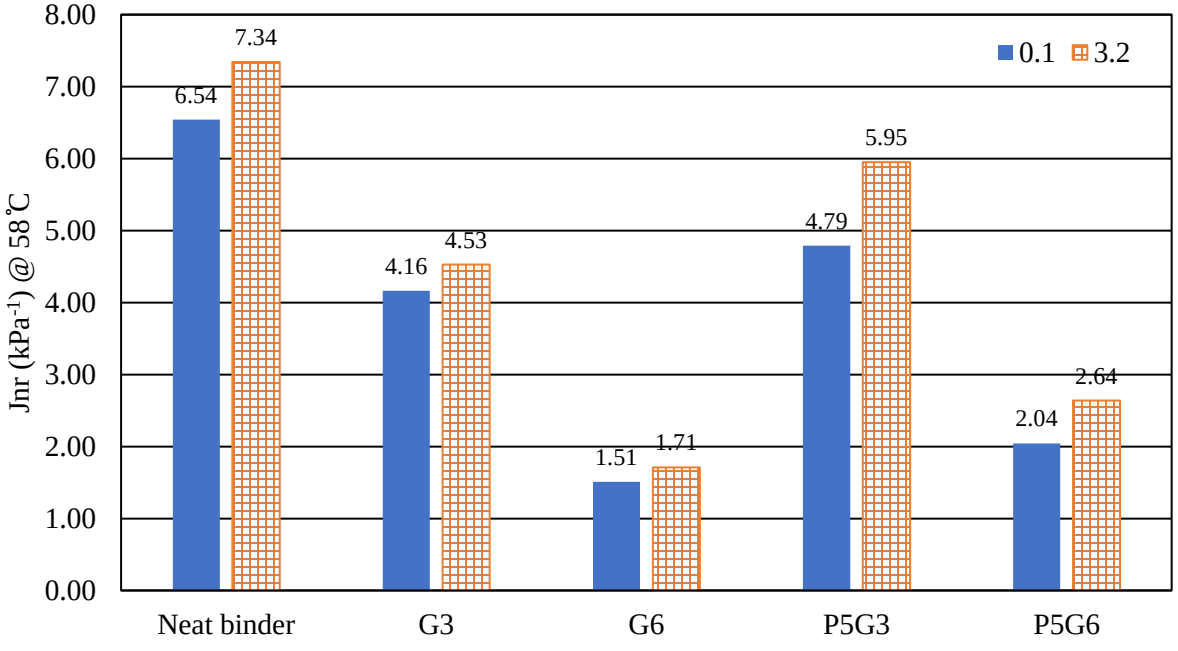

(b)

Fig. 25 Non-recoverable creep compliance at (a) 52 ℃, (b) 58 ℃.

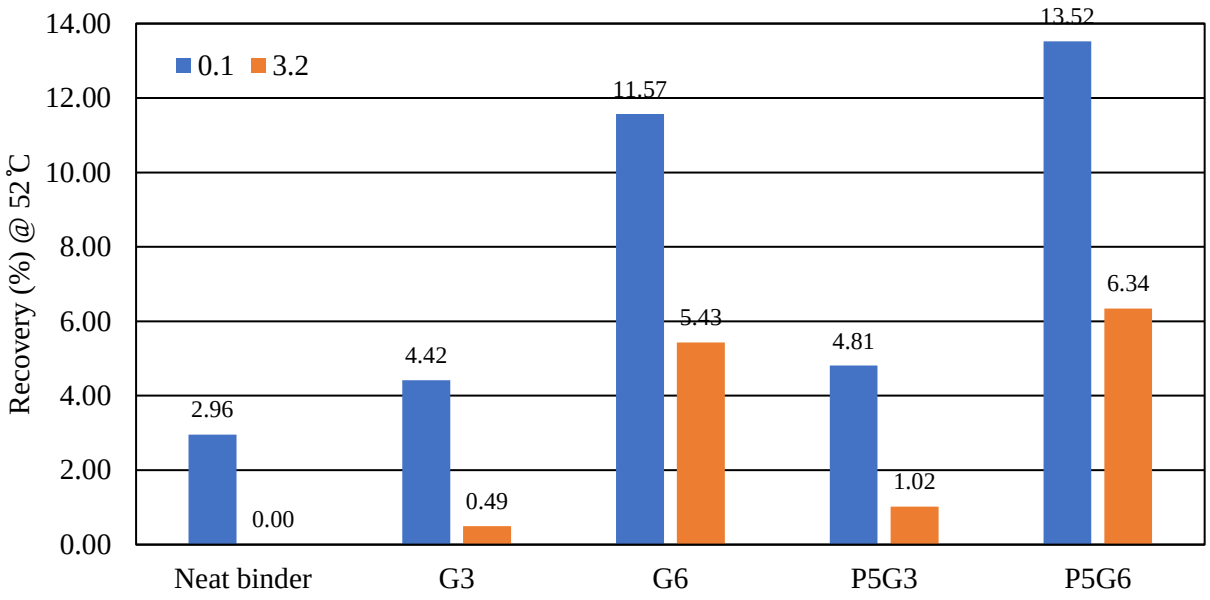

(a)

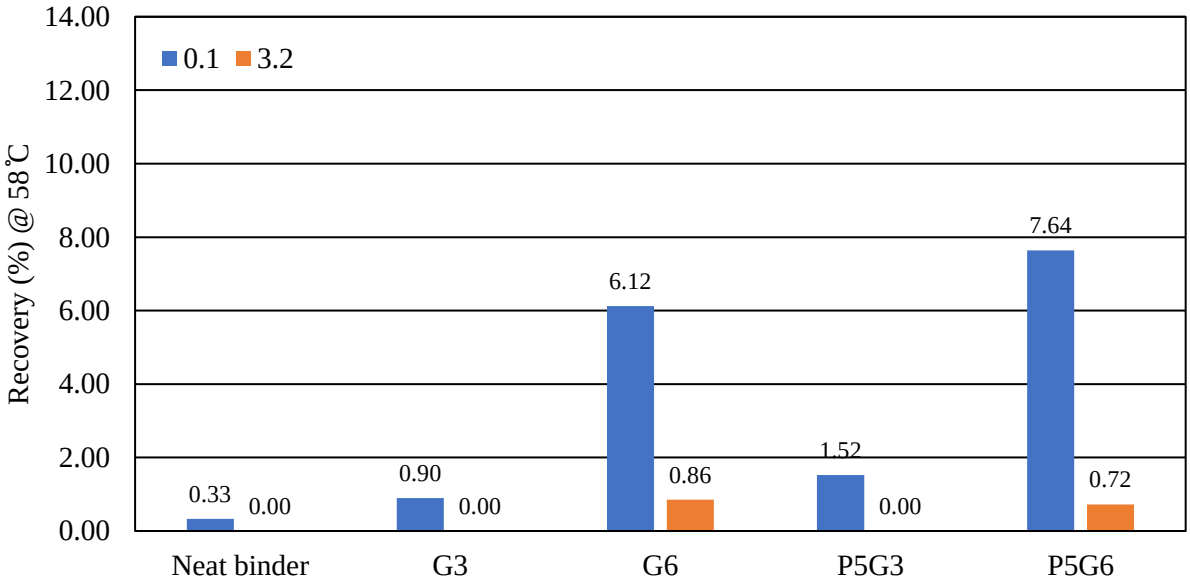

(b)

Fig. 26 Percent recovery at (a) 52 ℃, (b) 58 ℃.

3.4.1.5. Glover-Rowe Parameter

The Glover-Rowe (G-R) parameter was obtained from binder specimens after PAV aging conditioning to evaluate the binders' cracking resistance at intermediate temperatures. Fig. 27 presents the values of the G-R parameters of different binders in a Black diagram.

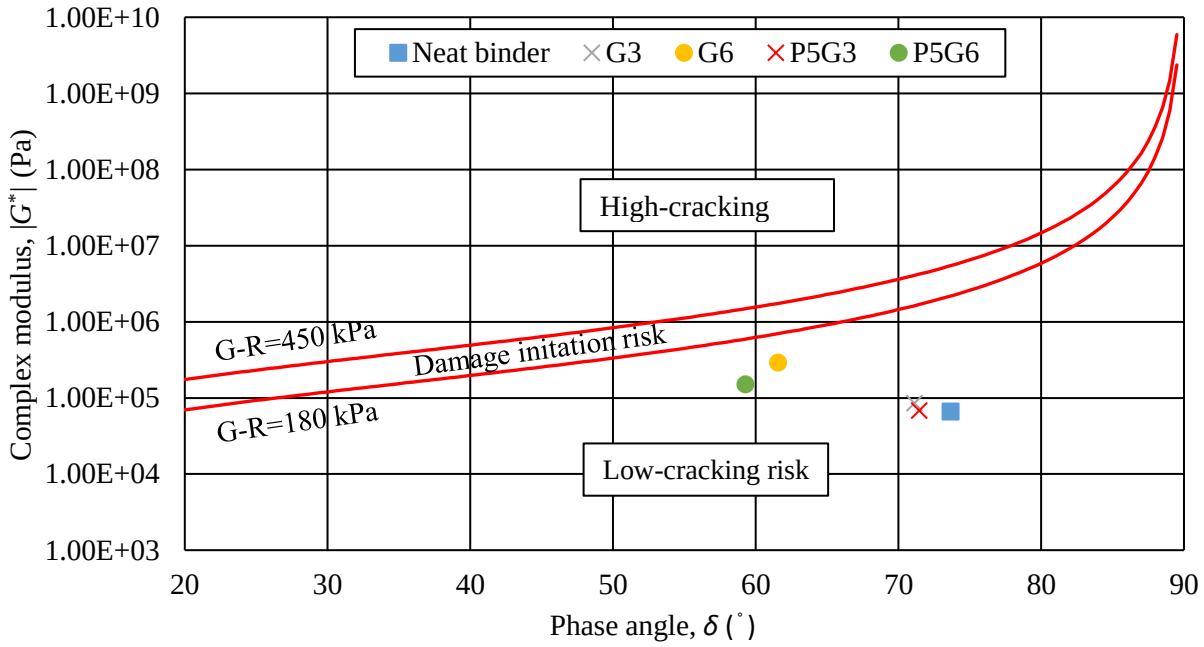

Fig. 27 Average values of the G-R parameter for the neat binder and modified binders.

The results presented in Fig. 27 indicates that all the binders can pass the limit of cracking resistance based on the G-R parameters. However, the binders with 6% Gilsonite had higher cracking potential than the ones with 3% or lower percentage of Gilsonite. The G-R parameter also showed the addition of PEG to Gilsonite-modified binders can decrease the risk of damage for 3% and 6% of Gilsonite to 23% and 38%, respectively.

3.4.1.6. Linear Amplitude Sweep (LAS) Test

In addition to using the G-R parameters obtained from tests within the linear viscoelastic range, the LAS tests were performed to further assess the fatigue cracking resistance of the binders at intermediate temperatures. A frequency sweep test, fingerprint, was first conducted before each LAS test to quantify the linear viscoelastic properties of the binders. The results are presented in Fig. 28. Similar to complex modulus showed in Fig. 23, the testing results indicates that the binders with higher Gilsonite content exhibited higher modulus and the addition of PEG can soften the binders at each Gilsonite concentration level. Following the fingerprint test, the LAS test was performed. The damage characteristic curve obtained from the LAS test analyzed is one important component of the VECD model. The curve describes the relationship between material integrity (C) and the increase of the damage intensity (S). A higher C-S curve represents a lower deterioration rate and indicates a potential superior cracking resistance of the asphalt binders. In some recent studies, the ranking of the C-S curves has been reported to have high correlations with the ranking of the material stiffness (Wang and Kim 2019, Wang et al. 2020). However, in this study, the testing results in Fig. 29 show that even though the G6 binder had the highest modulus,

it had the lowest C-S curve or the highest integrity deterioration rate. The addition of PEG yielded higher C-S curve at each Gilsonite concentration level, and the P5G3 binder had the highest C-S curve in this case.

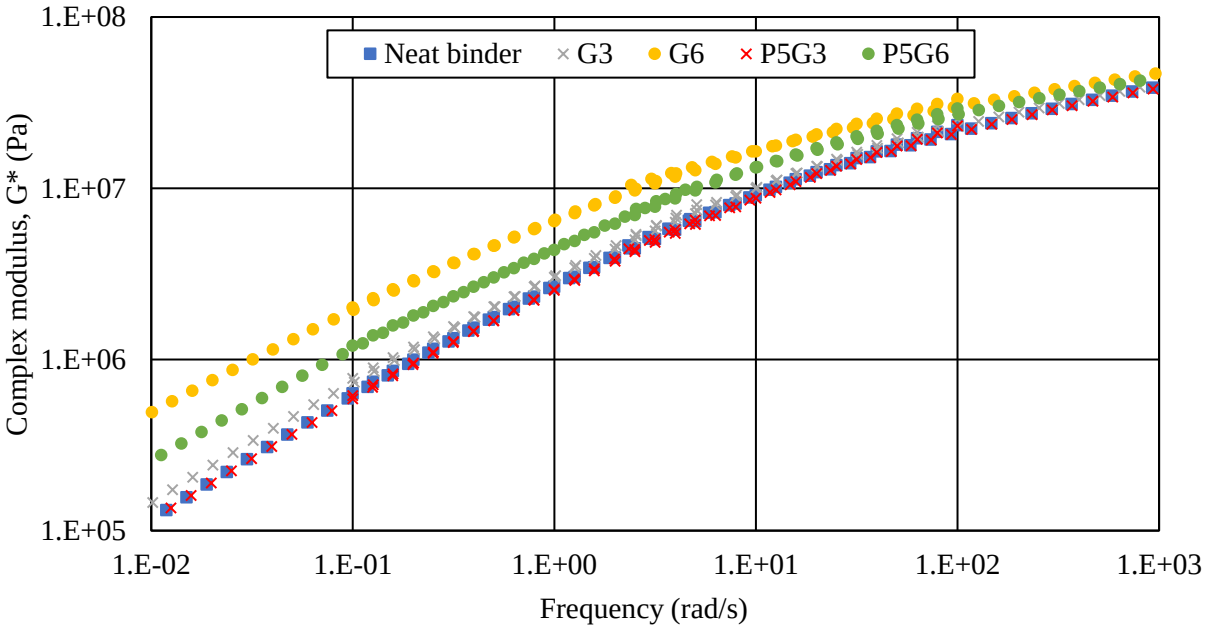

Fig. 28 Frequency sweep test of binders at 16 ℃.

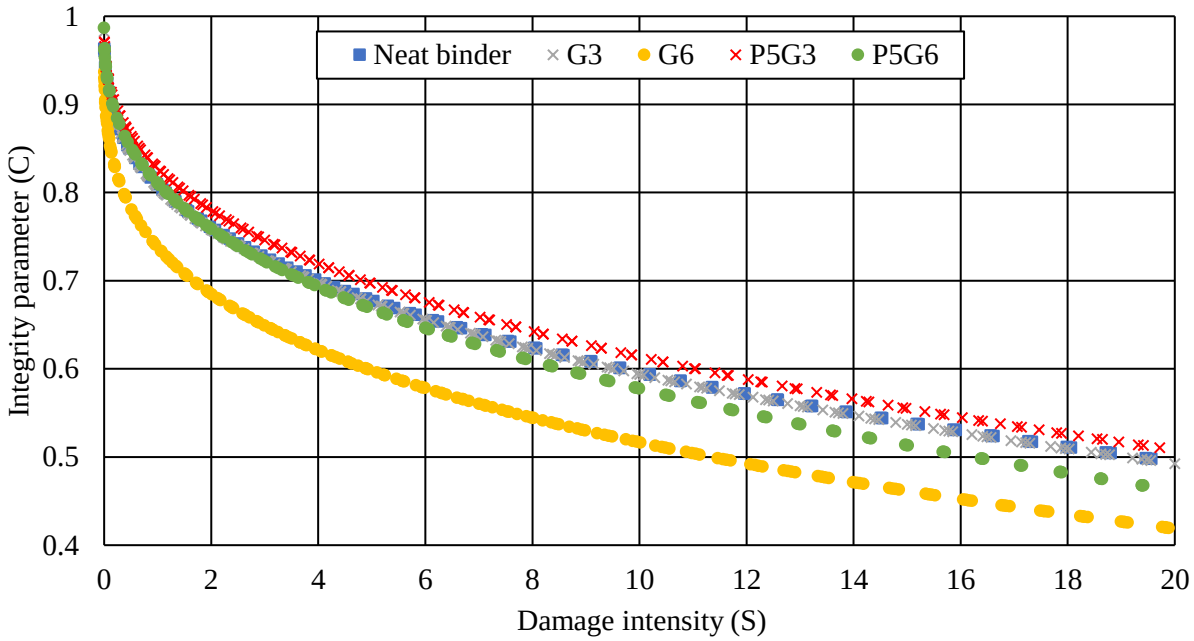

Fig. 29 Integrity parameter vs. damage intensity of binders.

Fig. 30 and Table 16 present the predicted numbers of cycles to failure for different binders at different strain levels. It can be observed that the binders with 6% Gilsonite yielded N_f vs. strain amplitude curves with high slopes, which means the fatigue lives of the G6 and P5G6 binders were greater than others at low strain amplitude levels and lower at high strain amplitudes. The addition of PEG increased the fatigue lives of the binders at each Gilsonite concentration levels. The trend can also be observed from Table 16. At high strain levels, the fatigue lives of binders with 3% Gilsonite were significantly higher than the binders with 6% Gilsonite. However, the ranges of strains and stresses on asphalt binders may vary because of the local strain concentration. While the LAS tests predicted the fatigue lives of the binders at different strain levels, a fatigue evaluation on the mixture level in the future study would provide more information about the cracking resistance of those binders.

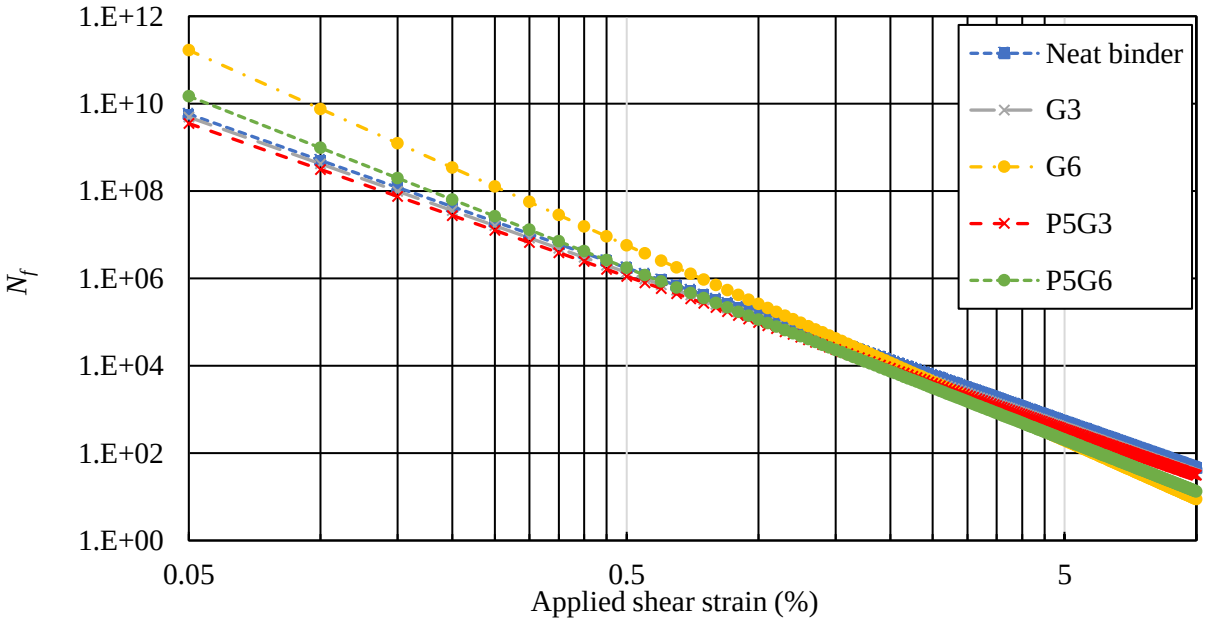

Fig. 30 Fatigue prediction model from the VECD model.

Table 16. Fatigue Parameters (A and B) and Fatigue Life at Different Strain Levels (1%, 2.5%, and 5.0%)

Binder specimen	**A**	**B**	N_f		
			Strain level (1.0%)	**Strain level (2.5%)**	**Strain level (5.0%)**
Neat binder	1.513E+05	-3.520	151,340	6,017	525
G3	1.161E+05	-3.556	116,054	4,464	380
G6	2.582E+05	-4.466	98,071	4,313	195
P5G3	9.807E+04	-3.500	258,192	3,970	351
P5G6	1.133E+05	-3.932	113,257	3,086	202

3.4.2. Thermal Analysis

3.4.2.1. Thermal Conductivity and Volumetric Heat Capacity

In addition to improving the binder's low-temperature performance, another merit of adding PEG is to improve the thermal behaviors of the modified binders. The thermal conductivity and the volumetric heat

capacity of the modified binders were measured in this study. A higher thermal conductivity leads to a quicker heat transfer through the asphalt pavement, which improves the thermoregulation of asphalt pavement and avoid the concentration of extreme temperature in the asphalt mixture (Pan et al. 2014). Fig. 31 presents the measured thermal conductivity of the neat binder and modified binders. A descending trend in thermal conductivity was observed with the increase of Gilsonite content, and the lowest thermal conductivity was observed in the sample P5G6. It also indicates that the addition of the PEG slightly decreases the thermal conductivity of Gilsonite-modified binders. The lowest thermal conductivity was observed in the sample P5G6.

Another related thermal characteristic of asphalt mixture is volumetric heat capacity. A high volumetric heat capacity means the material can observe more energy while changing temperatures. For paving materials, greater values of volumetric heat capacity can mitigate the pavement temperature swing in pavements caused by the ambient temperature changes. Fig. 32 presents the volumetric heat capacity of the neat and modified binders. The testing results indicate the volumetric heat capacity was raised after the addition of Gilsonite. Unlike the thermal conductivity results, the four Gilsonite-modified binders had similar values of the volumetric heat capacity. The P5G6 binder had the highest volumetric heat among all the tested binders, 19.1% higher than the neat binder.

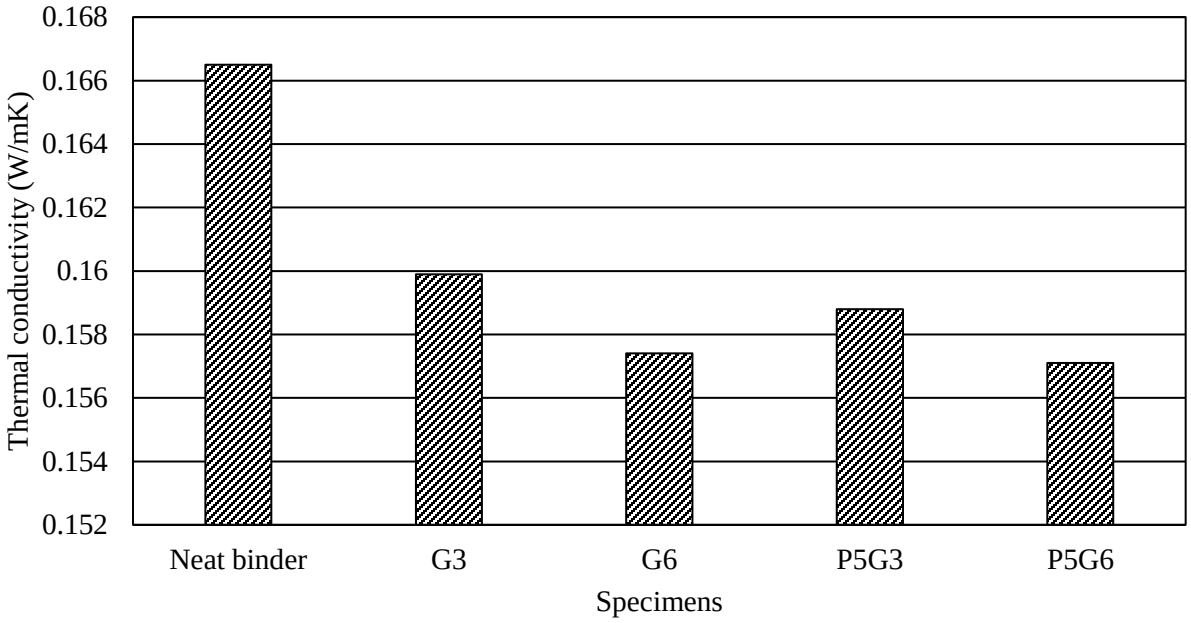

Fig. 31 Thermal conductivity of the neat binder and modified binders.

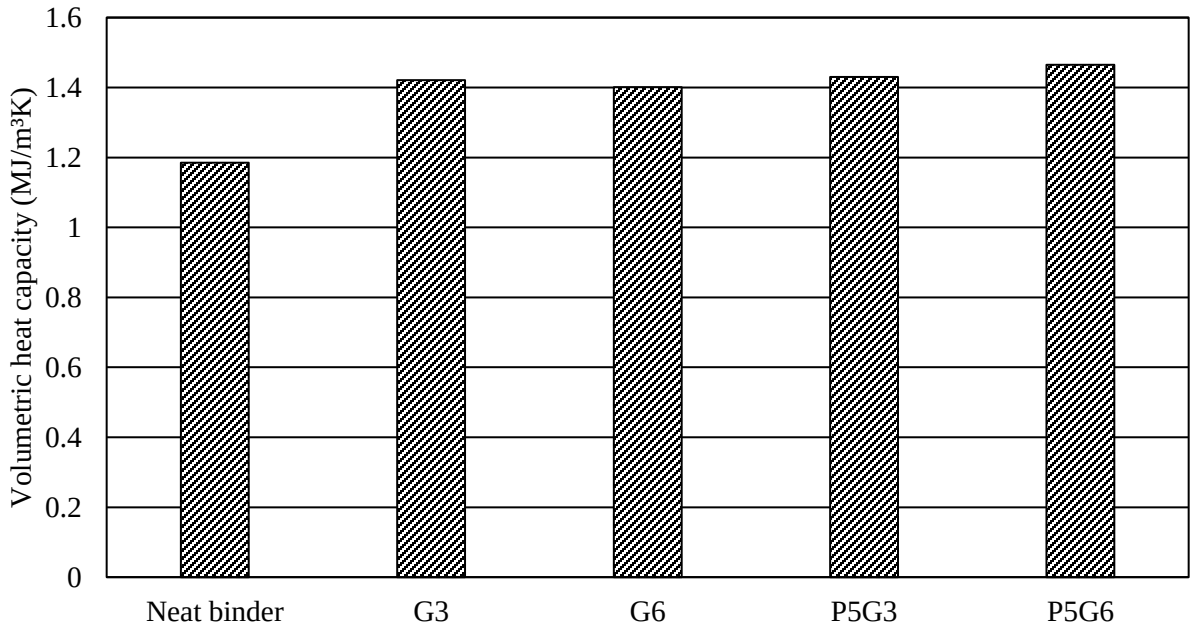

Fig. 32 Volumetric heat capacity of the neat binder and modified binders.

3.4.2.2. Thermo-Gravimetric Analysis (TGA)

TGA is an effective test to monitor the mass loss with temperature changes to determine the thermal stability of binders by increasing temperature. Fig. 33 presents the weight losses of the samples as functions of temperature changes during the TGA tests. It can be observed that all the binders remained thermally stable before 250℃. The neat binder first started to decompose as the temperature increased. At the same temperature, the neat binder had the most weight loss. The observation can be confirmed by the DTG curves presented in Fig. 34 which were obtained by calculating the first derivative of the weight loss over temperature. Furthermore, the single peak from the PEG-Gilsonite-modified binders suggested that relatively strong molecular bonds existed among the PEG, Gilsonite, and the neat binder, which led to the superior thermal stabilities of the modified binders.

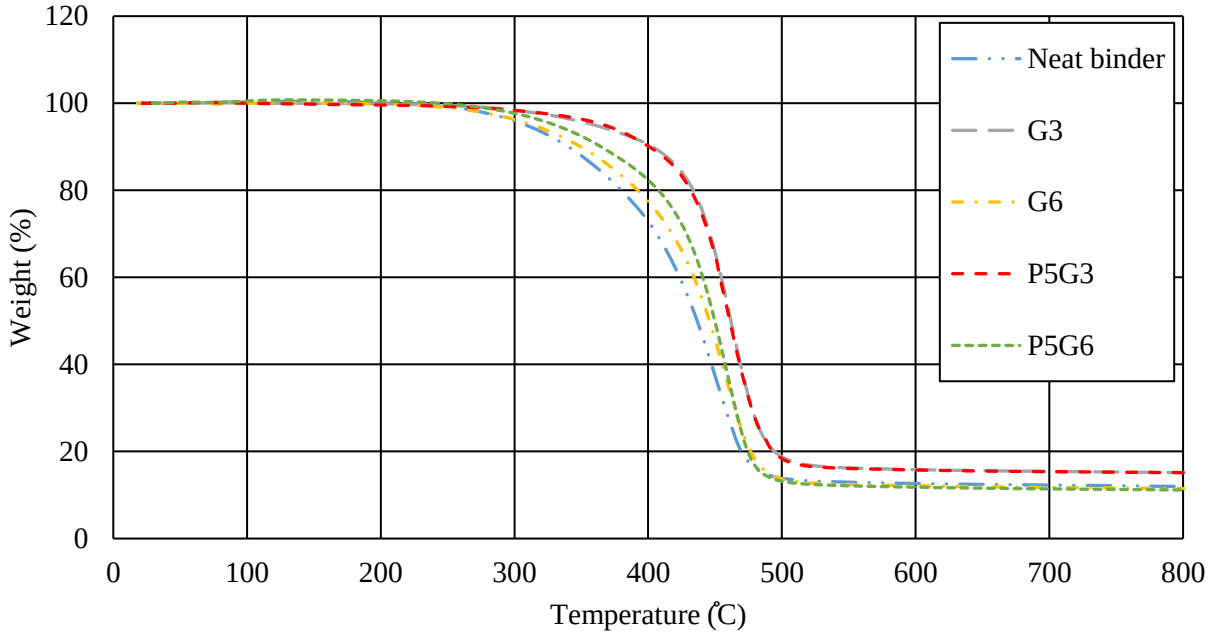

Fig. 33 TGA curves of the neat binder and modified binders.

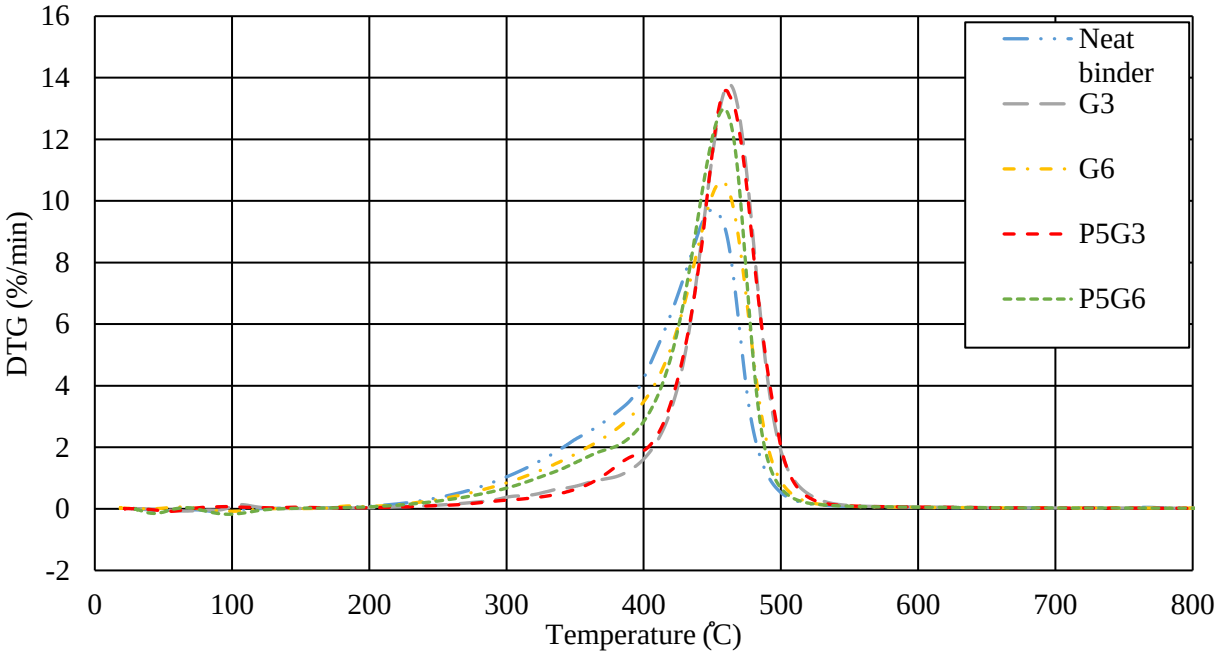

Fig. 34 DTG curves of the neat binder and modified binders.

3.4.2.3. Differential Scanning Calorimetry (DSC) Analysis

The heat flows of binders are presented in Fig. 35. It can be observed that as the temperatures changed from low to high, the heat flows increased and reached to peak values around -30℃ for all binders. The temperatures corresponding to the peaks of heat flows were the glass transition temperatures. The values of the glass transition temperatures for different binders are presented in Fig. 36. The testing results indicate that the addition of PEG was able to lower the binder glass transition temperature and allowed

the binder to remain viscoelastic and less brittle in a wider temperature range. As the dosage of Gilsonite increased, the glass transition temperatures increased. The introduction of PEG mitigated the impact of Gilsonite on the process of glass transitions. For example, with 6% Gilsonite, the transition temperature was raised from -28.7℃, the temperature of neat binder, to -24.9℃. With 5% PEG, the glass transition temperature was improved to -26.2℃. Based on molecular theory, there are two main factors affecting the glass transition temperatures, i.e., the force between the polymer molecules and the flexibility of molecule chains. It was believed that the addition of PEG increased the flexibility of the molecular chains; thus, lowered the glass transition temperatures and expanded the temperature range for the material to remain viscoelastic (Lei et al. 2015).

In summary, the performance test and thermal analysis results indicated that the G3 and P5G6 binders managed to increase the high PG of the original binder by one grade without increasing the low PG. The MSCR test results showed that even though the G3 and P5G6 binders had the same high PG, P5G6 had much lower non-recovery creep compliance and higher percentage recovery under the same loading scenarios; thus, having superior rutting resistance at high temperatures. With all the binders passed the cracking resistance requirements at intermediate temperatures, the Gilsonite-PEG-modified binders exhibited preferable thermal behaviors with higher heat compacity and higher thermal stability than the neat binder.

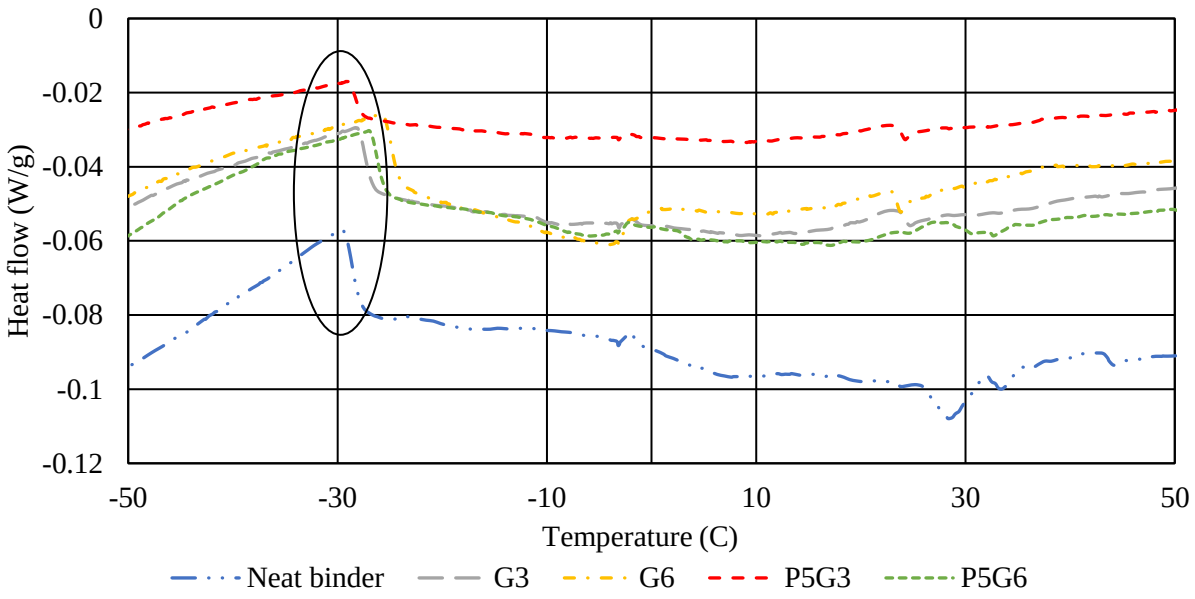

Fig. 35 DSC curves of the neat binder and modified binders.

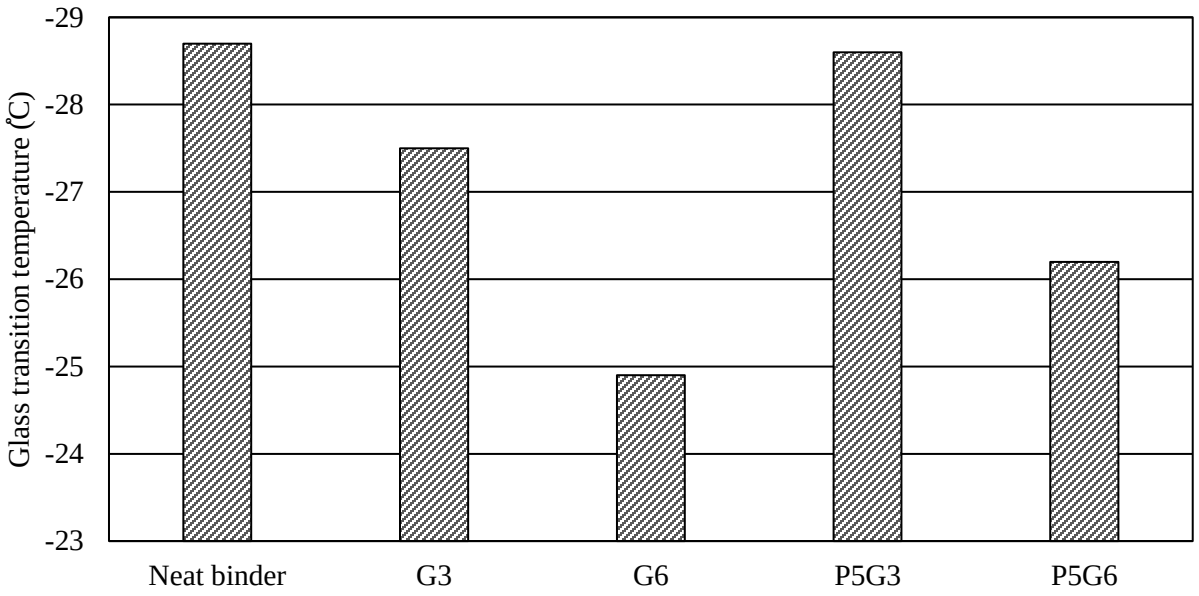

Fig. 36 Glass transition temperature of the neat binder and modified binders.

3.5. Summary

The objective of the study was to evaluate the impact of PCM on the Gilsonite-modified binder and assess the rheological and thermal behaviors of the modified binders. The findings are summarized in the following.

Gilsonite improves the high-temperature performance of asphalt binders and have adverse effects on their performance at low temperatures. With 5% PEG incorporated, binders with Gilsonite up to 6% was able to remain the same low PG as the neat binder. The Gilsonite-PEG-modified binder had one level higher in high PG and the same low PG as the neat binder. As for the continuous PG, the high PG of the P5G6 binder reached 63, nearly two level higher than the original binder.

The ΔT_c parameter was used to investigate the low-temperature performance of the binders. The results showed adding PEG to the Gilsonite-modified binder improves the low-temperature cracking resistance.

The MSCR test was performed at two creep stress levels of 0.1 and 3.2 kPa to evaluate the rutting resistance of the binders at high temperatures. The test results showed that the P5G6 binder had a low Jnr value and the higher percentage recovery among all the tested binders. The test results verified the findings from the Superpave PG tests and clearly showed that the P5G6 binder had superior rutting resistance and the addition of PEG had a minor impact of the rutting susceptibility at each Gilsonite concentration level.

The Glover-Rowe parameter and the LAS test were used to investigate the cracking susceptibility of binders. According to the evaluation using the Glover-Rowe parameter, all binders passed the limit for cracking resistance. However, both tests suggested that increasing the Gilsonite dosage increases the cracking susceptibility of the binders, and the usage of PEG mitigates the negative impacts of Gilsonite. The LAS test and the VECD analysis results indicated that the binders with 6% Gilsonite were stiffer and could yield longer fatigue life at low loading amplitudes and fewer numbers of cycles to failure with high loading amplitudes. Meanwhile, mixture tests were recommended for further fatigue cracking resistance evaluation.

Thermal analysis showed introducing PEG can slightly decrease the thermal conductivity and increase volumetric heat capacity of Gilsonite-modified binder. Increasing the heat capacity may help

thermoregulation of asphalt binder, which may result in a cool pavement system at high temperature.
The TGA test findings indicated that the interaction between PEG and Gilsonite could increase the thermal stability of the modified binder. The DTG curve of specimens containing PEG and Gilsonite showed a single-thermal decomposition which means the high molecular bonds between PEG, Gilsonite, and neat binder prevents the early evaporation of PEG.

Glass transition temperatures were measured for the modified and the original binders. Adding PEG to the specimens containing Gilsonite could move the glass transition temperature to a lower value. The findings indicated that PEG increased the viscoelastic region of binders at low temperatures.
For future studies, it is recommended that base binders with different PGs and sources be tested with the recommend dosages of PEG and Gilsonite to verify the findings from this study. The cost-benefit analysis will be conducted. Furthermore, performance tests and thermal behavior analyses can be performed on the corresponding asphalt mixtures in the future.

Chapter 4. Evaluation of Thermal and Rheological of Phase Change Material-incorporated Asphalt Mastic with Porous Fillers

4.1. Introduction

Phase change materials (PCMs) have been drawing much attention in civil engineering due to unique thermal behavior. They have been utilized in walls, ceilings, and floors of buildings functioning as a thermal regulator to avoid extreme temperature swings, which has yielded human comfort and reduced energy consumption and costs (Zhang et al. 2013). In recent years, pavement engineers have also been trying to incorporate PCM in asphalt pavements. It is believed that they can limit the temperature changes in asphalt pavements, increase the service life of pavements, and mitigate the heat island effects (Du et al. 2019). PCM is known as a novel and capable material which can absorb and release a large amount of energy in the form of latent heat (ΔH) during the phase transition and act as a balancer in modifying the temperature of temperature-sensitive materials. As heat is transferred into the system, PCM begins to melt and keep absorbing energy when the temperature reaches to a certain point (the so-called melting point temperature). During the phase transitioning stage, the system temperature can remain constant. The amount of heating energy that the system can absorb without increasing its temperature is defined as latent heat storage.

Different methods have been applied to incorporate PCMs in construction materials. For example, one popular approach is the macro encapsulation method where porous aggregate is used as carrier material for PCMs in asphalt and concrete cement mixtures (Zhang et al. 2004, Tang et al. 2018). However, engineers have been facing some critical challenges in using large porous aggregate in asphalt materials, for example the leakage of the PCM. One effective solution to reduce the risk of leaking is to use the coating method to coat the porous aggregate surface. Coating materials such as epoxy resins, polyester resins, granite powder and cement paste have been used (Jin et al. 2018, Zhou et al. 2018, Kakar et al. 2020, Yinfei et al. 2020). However, the coating method is complex, expensive, and hard to be applied in the asphalt plants. Another challenge of using porous aggregates is the associated structural problem. The light-weight porous aggregates usually have lower strength than regular coarse aggregates; thus, leading to cracking and rutting problems in pavement in their early service life. Therefore, it is necessary to develop a practical and cost-effective method to incorporate PCMs in asphalt mixtures.

In this research, the feasibility of using porous fillers as PCM carriers in asphalt mixtures was investigated in the scale of mastic. A few existing studies have reported the efficiency of using the composition of some PCMs and mineral fillers (CPCM) in asphalt pavement in terms of their thermal behaviors (Xu et al. 2015, Jin et al. 2017); however, the rheological behaviors and durability of the binders with CPCM have not been evaluated. In this study, the thermal and rheological behaviors of the asphalt mastic with CPCM were systematically tested. Two types of porous fillers and four types of PCMs were included as candidate materials. The types of PCMs and fillers and the blending ratios were first selected through a series of morphological and rheological tests. After the material design, the rheological tests including the complex shear modulus test, the beam bending rheometer (BBR) test, and the Linear Amplitude Sweep (LAS) test were conducted on asphalt mastic. The thermal analysis through the Differential Scanning Calorimetry (DSC) test, thermal conductivity and volumetric heat capacity test, and the real-time temperature performance test were also performed. Also, climate data was collected to model the temperature profile of pavement by using TEMPS (Temperature Estimate Model for Pavement Structures) program.

4.2. Research Methods

In this study, three tests were first performed to select the candidate CPCM combination and the optimum blending ratio. The tests include the SEM image analysis, the filter paper test to evaluate the risk of leakage, and the temperature sweep test on asphalt mastic to evaluate their rheological behaviors.

The SME image analysis was conducted mainly to investigate of the particle shape and the surface conditions of the porous fillers. The test was performed using a RAITH e-Line Plus Electron Beam Lithography SEM. Before the test, the sputter coating technique was applied, and the samples were coated with a thin gold film (Hung et al. 2021). Fillers with and without the incorporation of PCM were analyzed.

The filter paper test was conducted to evaluate the leakage ratio of each type of CPCM. The test was performed on filter papers with the diameter of 150 mm at the temperature of 80 °C. To prepare the test samples, a certain amount of CPCM specimens were dispersed on the filter paper. Then, the samples were kept in the oven at 80 °C for 30 minutes. The specimens were then retained at room temperature. The PCM leakage ratio was calculated based on the PCM absorption in the filter paper. Fig. 37 demonstrates the setup of the tests with different CPCMs ratios.

Fig. 37 Filter paper test: (a) DI:PEG, (b) DI:Lu, (c) DI:Pa-42, and (d) DI:Pa-58.

To characterize the rheological behaviors of CPCM mastics, the temperature sweep test was performed on the mastic samples with 50% filler replacement ratio. The mastics were tested using an 8 mm parallel plate geometry with a testing gap of 2 mm. To improve the adhesion of the parallel plates and mastic before trimming, the mastic between plates was preheated to 64ºC.

The testing temperature ranged from 20 °C to 45ºC which was below the melting point of the PCMs. At each temperature, loading frequencies ranging from 100 to 0.1 rad/s were applied on the testing sample. The mastercurve of the complex shear modulus were constructed with the reference temperature of 35°C. The candidate filler was expected to have high PCM absorption rate and low risk of leakage, and the mastic with the selected CPCM was expected to have similar rheological behaviors to the regular mastic.

After the candidate fillers, PCM, and the optimum blending ratio were selected, thermal analyses and rheological tests were conducted to further characterize the material behaviors. The thermal properties, such as the phase change temperature (T_m) or the melting point, specific heat capacity, and enthalpy (ΔH_m) can be obtained from the DSC curve. The PCM efficiency was also calculated using Equation (1)

$$\eta(\%) = \frac{\Delta H_{tm}}{\Delta H_{Tm}} \times 100 \quad (1)$$

where ΔH_{tm} is the testing enthalpy (J/g), and ΔH_{Tm} is the theoretical enthalpy (J/g). In addition, the thermal conductivity of the mastics was measured using the TPS 500S Hot Disk.

To assess the thermoregulation of asphalt mastics during heating process, a real-time temperature performance test was conducted. In the test, the mastics were placed in 8-oz cans and K-type thermocouples were installed in the center inside of mastics. A data logger was used to monitor and log the temperature of mastics during heating process. Water bathes were prepared with at two different temperatures, i.e., 10 ℃ and 58 ℃. The mastics were first retained in cool water bath for about one hour. The cans were then transferred to the hot water bath, and in the meantime the temperatures changes were monitored using the data logger. The temperature changes of the mastic samples were continued to be monitored for about 30 minutes as the temperature of the control mastic sample increased from the cool to the hot water bath temperature.

Rheological tests were performance on the mastics as well. Rutting performance was evaluated by Superpave rutting factor ($G^*/\sin\delta$). For Superpave rutting factor, the temperature sweep test was conducted at the temperature range of 52 – 82 ℃ with temperature increment of 6 ℃ on unaged specimens. Bending beam rheometer (BBR) test was performed at low temperatures of -6, -12, and -18 ℃ to determine the creep stiffness (S) and creep rate (m-value) on mastic specimens after RTFO and PAV conditioning according to AASHTO T 313. Lastly, the fatigue performance at intermediate temperatures investigated by linear amplitude sweep (LAS) test in compliance with AASHTO T 391. It was performed on mastics after RTFO and PAV conducting at 25 ℃ and fatigue performance was assessed by integrity parameter (C) and fatigue life before failure (N_f).

4.2.1. Determination of Candidate CPCMs and Optimum Blending Ratio

4.2.1.1. Scanning Electron Microscope (SEM) Image Analysis

The microstructure of carriers (DI and EP) as well as the CPCMs was investigated using this method. Fig. 38 (a) presents the cylindrical shape of diatomite with high dense porous structure and large specific surface area, which makes it a good candidate for the impregnation process. Fig. 38 (b) demonstrate the spherical shape and round edges of expanded perlite with a low number of pores on the surface. The observation indicated that the diatomite particles contained more pores on the surface compared to the expanded perlite. The compacted porous network of diatomite had the potential to be fully filled and saturated with PCMs.

The morphology of carriers after PCM (PEG) absorption was presented in Figs. 38 (c) and (d). It can be observed that, based on their particle surface conditions, PCM was able to be trapped inside the porous structure of diatomite more efficiently.

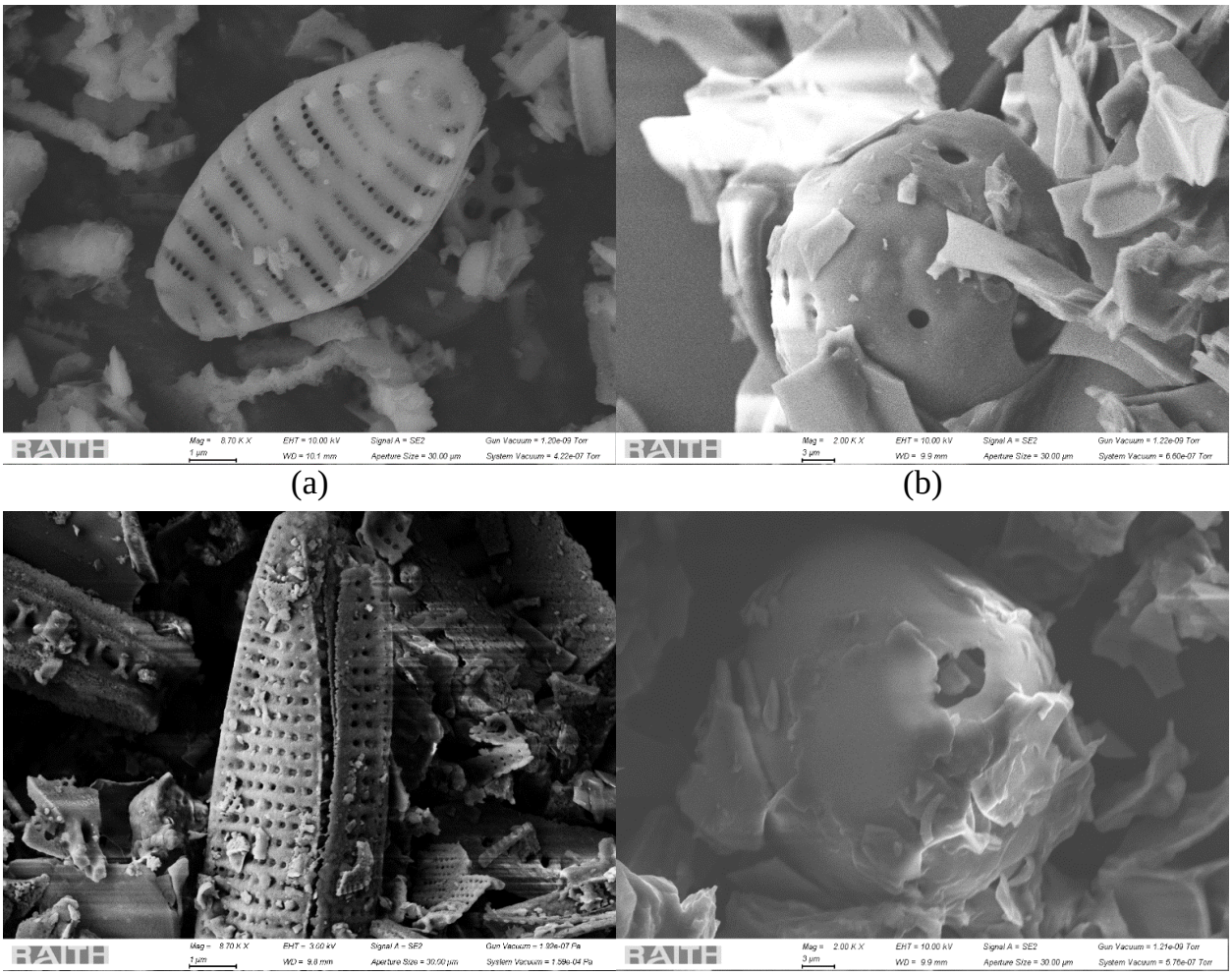

Fig. 38 SEM images of the (a) Diatomite, (b) Expanded perlite, (c) Diatomite/PEG, and (d) Expanded perlite/PEG.

4.2.2.2. Filter Paper Testing Results

To verify the SEM results, the filter paper test was performed to access the risk of PCM leakage and determine the optimum blending ratio. Fig. 39 presents the measured leaking ratios of the CPCMs with different blending ratios. It can be observed that CPCMs consisting of diatomite exhibited a lower leaking ratio in comparison to those made with expanded perlite regardless of the type of PCM. The testing results confirmed the SEM observation that diatomite was able to preserve more PCM compared to expanded perlite and act as a proper carrier for PCMs. Also, as found in Fig. 39, the leaking ratio of the CPCMs with diatomite was reduced by changing the ratio from 40:60 to 50:50, but no significant change in leakage percentage for lower PCM percentage. Therefore, the optimum ratio of DI:PCM was at 50:50. Likewise, the ratio for EP:PCM was limited to 60:40 based on the testing result.

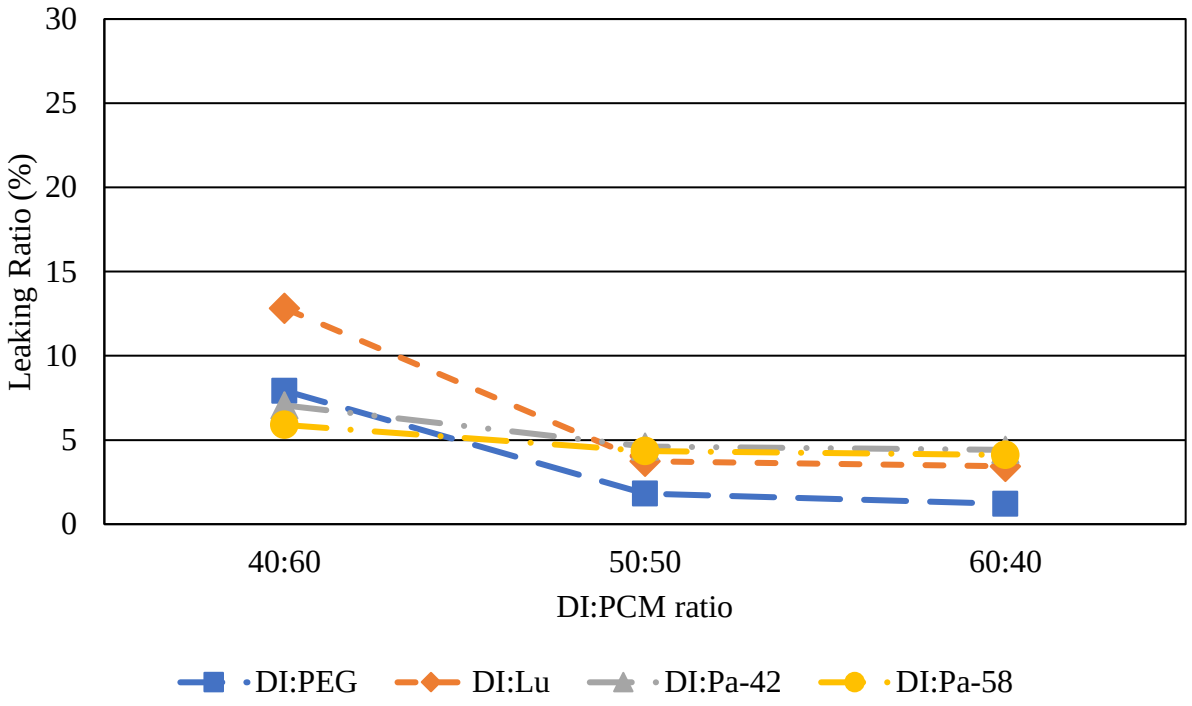

(a)

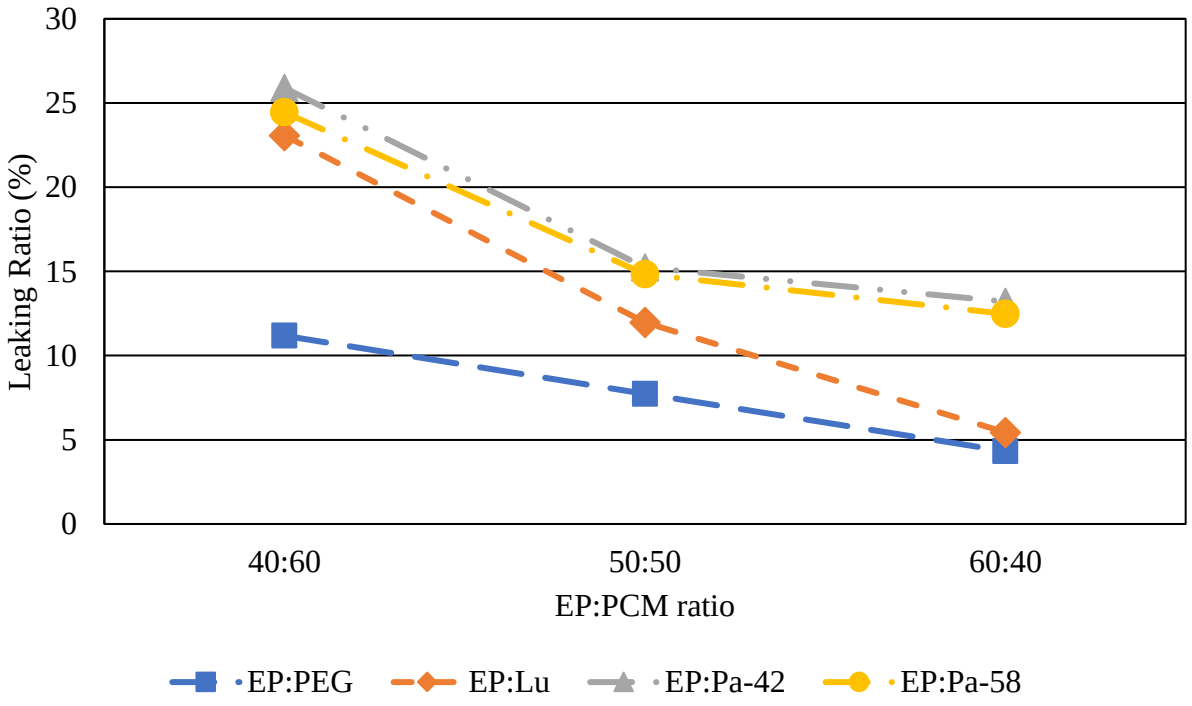

(b)

Fig. 39 Leaking ratio of PCM from carrier (a) DI:PCM and (b) EP:PCM.

4.2.2.3. Master Curve of Complex Shear Modulus

After the optimum blending ratio was determined using the filter paper tests, the dynamic shear modulus

of the mastics was measured and the mastercurve were constructed to ensure that the rheological properties were not adversely affected by the addition of the PCM. In the temperature sweep tests, the filler replacement ratio was fixed at 50%, which was a representative value assuming 50% of the fillers in the asphalt mixtures were replaced by the CPCM. Table 17 presents the component and the designation of different mastic samples.

Table 17. Mix Proportions of Mastics Prepared by CPCMs

Mastic Sample	CPCM	CPCM ratio (carrier : PCM) (by weight)	Filler replacement (%) by CPCM (by volume)	Designation
1	-	-	-	HL (control sample)
2	DI/PEG	50:50	50	DI-PEG_P50F50
3	DI/LU	50:50	50	DI-LU_P50F50
4	DI/Pa-42	50:50	50	DI-Pa(42)_P50F50
5	DI/Pa-58	50:50	50	DI-Pa(58)_P50F50
6	EP/PEG	60:40	50	EP-PEG_P40F50
7	EP/LU	60:40	50	EP-LU_P40F50
8	EP/Pa-42	60:40	50	EP-Pa(42)_P40F50
9	EP/Pa-58	60:40	50	EP-Pa(58)_P40F50

Fig. 40 presents the obtained complex shear modulus curve of the mastic samples. The mastics containing Pa-42 and Pa-58 became very soft during the test setup and could not be stably placed and tested between the Dynamic Shear Rheometer (DSR) parallel plates. The softening indicated that the paraffin had unexpected effects on the rheological behaviors of asphalt mastic. The complex modulus mastercurves of the mastics with PEG and LU are presented in Fig. 40. It can be observed that the DI-LU_P50F50 samples exhibited significantly low modulus than the other materials, and the shape of the mastercurve could not be fitted with the CAM model, which indicated this CPCM might have changed the rheological behaviors of the asphalt mastic and was not recommended to be used in further analysis. The mastic with EP-LU had similar modulus with the control sample, and the CPCMs containing PEG lowered the mastic modulus at high temperatures.

Given the testing results from the SEM analysis, the filter paper test, and the complex shear modulus tests, it can be concluded that compared to the expanded perlite, diatomite contained a higher porous structure and were able to preserve more PCM with lower risk for leaking. The combination of DI and PEG with blending ratio at 50:50 was recommended to be used for further analyses. In the following thermal and rheological tests, different filler replacement ratios, i.e., 50%, 75%, and 100% were also applied to complete the study.

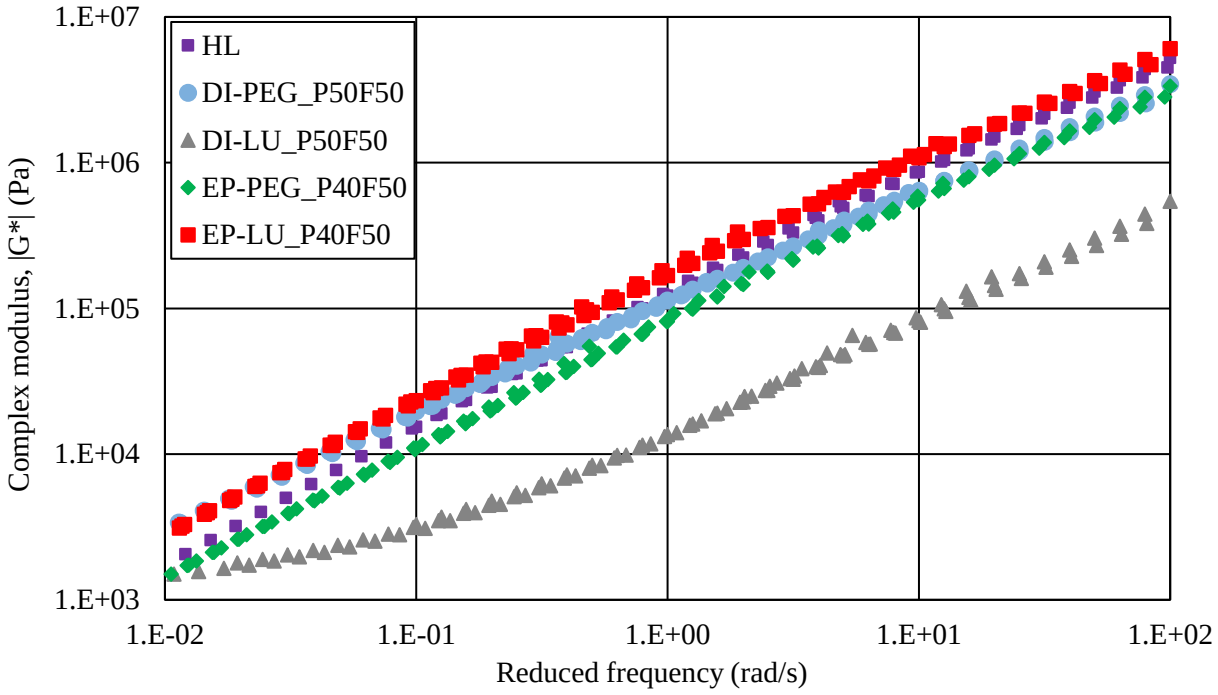

(a)

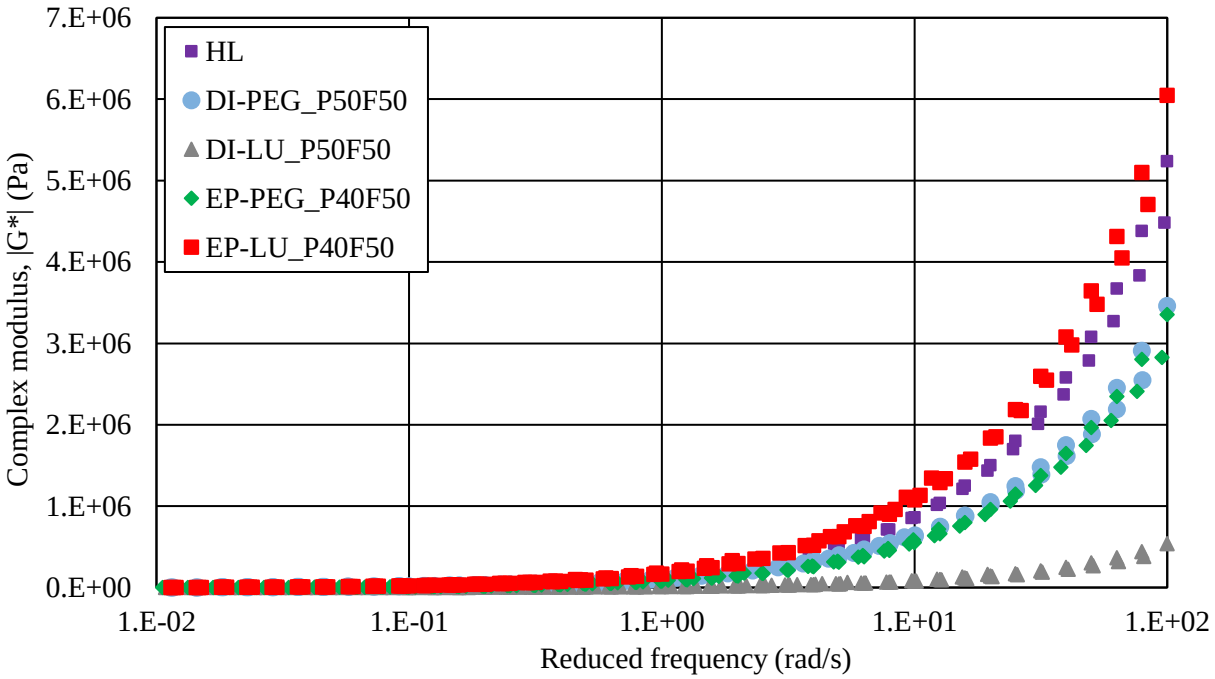

(b)

Fig. 40 Master curve of complex shear modulus (G*): (a) Logarithmic and (b) Semi-logarithmic.

4.3. Results of Thermal and Rheological Analyses

4.3.1. Thermal Stability by Thermal-Gravimetric Analysis (TGA)

The thermal stability of hydrated lime, diatomite, polyethylene glycol, and asphalt mastics were evaluated by using TGA technique. Fig. 41 shows the measured TGA curve of samples. As seen in Fig. 41 (a) the thermal stability of diatomite is significantly higher than hydrated lime and can present an excellent thermal stability (Jeong et al. 2013, Fu et al. 2015). The weight loss of diatomite was found 6.8% which is considerably lower than hydrated lime with weight loss of 27.5% at 800 ℃. A two-step thermal degradation occurred for hydrated lime. The first weight loss happened between 290 ℃ and 550 ℃ and indicates the dihydroxylation of $Ca(OH)_2$. The second weight loss happened between 550 ℃ and 800 ℃ which corresponds to the decomposition of $CaCO_3$ (Yang et al. 2016). The TGA curve of PEG could imply that the decomposition temperature of PEG started at 265 ℃ and ended at 510 ℃ (Karaman et al. 2011). As the mixing temperature of mastics weas selected as 160 ℃; therefore, it could be concluded that no PEG degradation happened during mixing. At 800 ℃, the weight loss of diatomite, polyethylene glycol, and diatomite-polyethylene glycol (CPCM) were found 6.8%, 98.5%, and 51.8%, respectively; therefore, it can be calculated that the PEG mass fraction absorbed by diatomite is 49.1%. Moreover, Fig. 41 (b) describes the TGA curves of control (HL) mastic and modified mastics. The weight loss of samples HL, DI-PEG_P50F50, DI-PEG_P50F75, and DI-PEG_P50F100 at 800 ℃ were found 61.5%, 67.4%, 71.0%, and 73.7%, respectively. The higher weight loss of modified mastics compared to control mastic can be attributed to the existing of PEG which increases the rate of weight loss in modified mastics. Totally, the TGA results could show good thermal stability of modified mastics with the wide degradation range between 265 ℃ and 800 ℃.

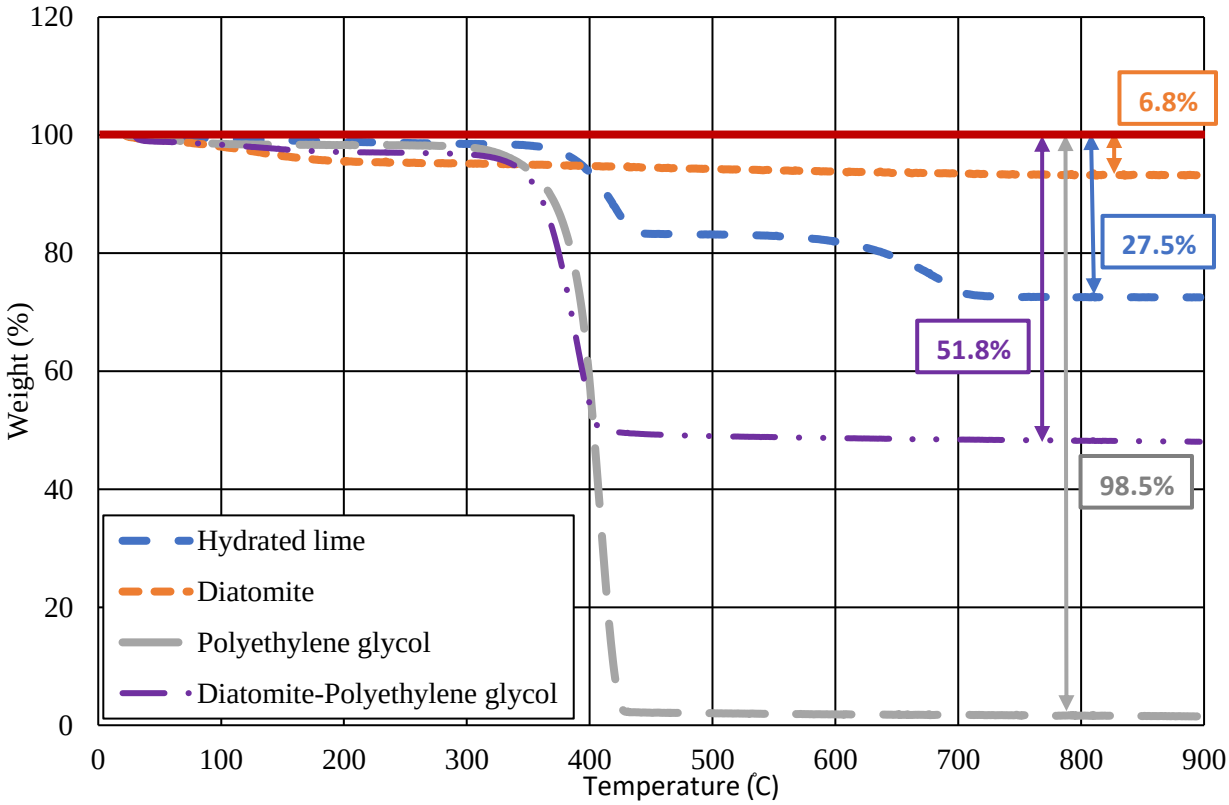
120
100
80
60
40
20
0
Weight (%)
0
100
200
300
400
500
600
700
800
900
Temperature (C)
6.8%
27.5%
51.8%
98.5%
Hydrated lime
Diatomite
Polyethylene glycol
Diatomite-Polyethylene glycol

(a)

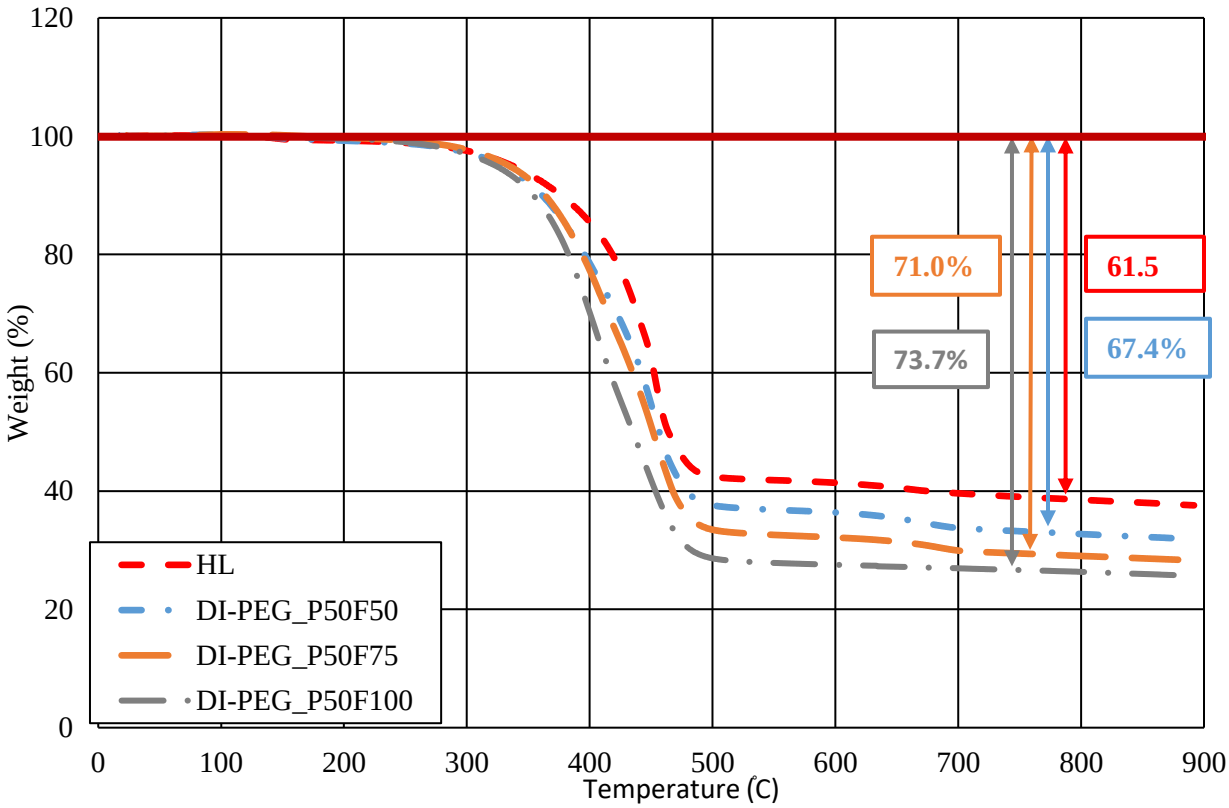
120
100
80
60
40
20
0
Weight (%)
0
100
200
300
400
500
600
700
800
900
Temperature (C)
71.0%
61.5
73.7%
67.4%
HL
DI-PEG_P50F50
DI-PEG_P50F75
DI-PEG_P50F100

(b)

Fig. 41 Thermo-gravimetric analysis of the samples (a) hydrated lime, diatomite, polyethylene glycol, and diatomite-polyethylene glycol; (b) control and modified mastics.

4.3.2. Differential Scanning Calorimetry Test Results

Thermal properties of pure PEG, CPCM, and modified mastics were tested by a DSC instrument to detect the melting point and enthalpy (latent heat storage). Fig. 42 presents the DSC curves of the tested PEG and the mastics. The melting point is calculated at the intercept temperature of the tangent line of the ascending part of the curve and the baseline, and the enthalpy is defined as the area under the curve at the phase transition region. In Fig. 42, it can be observed that the control mastic exhibited no apparent peak, which indicated that there was no endothermic process in control mastic as expected. The calculated melting point, enthalpy, and the efficiency of PCM in modified mastic are presented in Table 18. The temperature range of modified mastic was found between 39.7℃ to 40.0℃, almost equal to PEG (39.8℃) as expected. The testing enthalpy of modified mastic listed in Table 18 shows that the sample DI-PEG_P50F100 had the highest enthalpy, indicating the highest thermal storage among modified mastic as more fillers were replaced by the CPCM.

In terms of the efficiency of PCM, 87% efficiency was obtained for the modified mastic. The 13% loss could be attributed to the mass loss of PEG during mixing with binder at high temperatures. In the research conducted by Zhang et al., expanded graphite was used to preserve PCM, and 65.5 % to 71.0 % efficiency was reported (Zhang et al. 2019). Despite the slightly different testing conditions, the differences suggested that diatomite is a suitable PCM carrier due to its honeycomb microstructure.

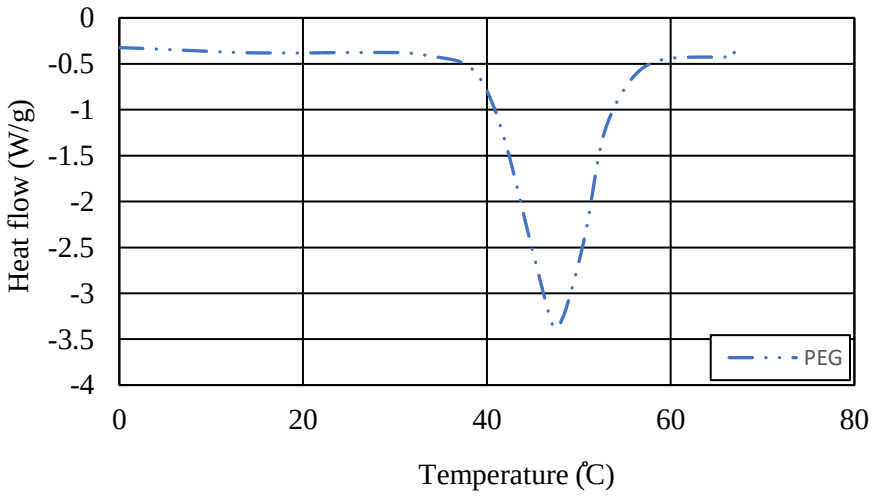

(a)

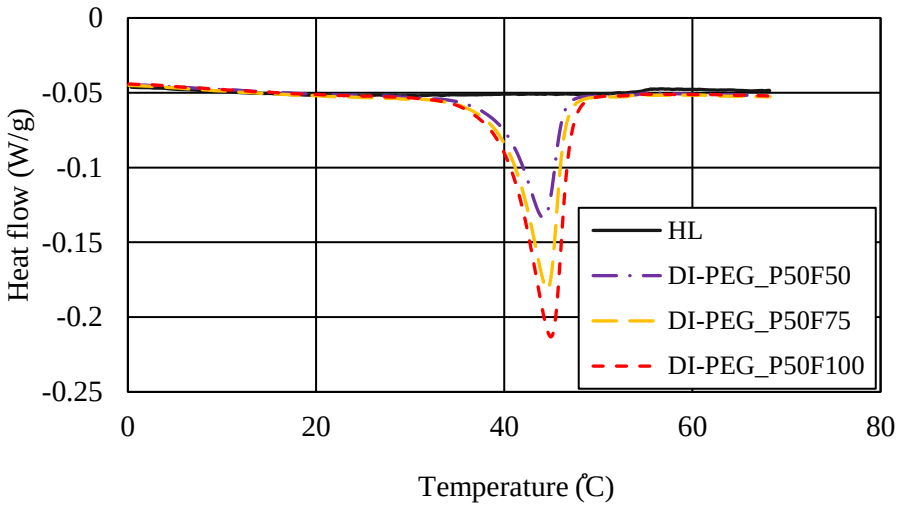

(b)

Fig. 42 DSC curves of materials: (a) PEG and (b) Mastics.

Table 18. The Measured DSC Data, Calculated Enthalpy, and PCM Efficiency

Materials	**T_m (°C)**	**ΔH_{tm} (J/g)**	**ΔH_{Tm} (J/g)**	**η (%)**
PEG	39.8	166.7	-	-
DI-PEG_P50F50	39.7	11	12.52	87.9
DI-PEG_P50F75	40.0	16.9	19.43	87.0
DI-PEG_P50F100	39.9	23.32	26.81	87.0

4.3.3. Thermal Conductivity and Volumetric Heat Capacity

Thermal conductivity and specific heat capacity are important thermal properties that directly related to the changes of pavement temperatures. Higher thermal conductivities accelerate the heat transfer within the asphalt layer. As presented in Table 19, lower thermal conductivity of modified mastics was observed compared to the control mastic as PEG had low thermal conductivity. Another thermal parameter was specific heat capacity which was measured at the melting point of mastics. Unlike the thermal conductivity, an increasing trend was manifested for the modified mastic. A greater specific heat capacity can decrease the temperature gradient of asphalt pavement and contribute to the thermal regulation of the pavement system.

Table 19. Thermal Conductivity and Volumetric Heat Capacity of Mastics

Sample	Thermal conductivity (W/mK)	Specific heat capacity (J/kg.K)
HL	0.345	930.2
DI-PEG_P50F50	0.241	1565.7
DI-PEG_P50F75	0.222	1745.6
DI-PEG_P50F100	0.207	2124.1

4.3.4. Real-Time Temperature Performance Test (Thermoregulation of Mastics)

The real -time temperature performance test was conducted to directly investigate the thermal regulation performance of CPCMs in asphalt mastic. The testing results are presented in Fig. 43 and Fig. 44. It can be observed that the modified mastics with CPCMs had consistently lower temperatures compared to the control mastic throughout the test. The increase of the mastic temperature was effectively delayed with addition of CPCMs. The observation validated the thermal regulation effect of CPCMs. The difference between the temperatures of the control sample and the modified mastics was greater as higher content of fillers were replaced by the CPCMs. The maximum temperature difference during the test was observed with the DI-PEG_P50F100 mastic, which was as high as 6.3 ℃. In addition, it can be observed in Fig. 43 that for the DI-PEG_P50F75 and F100, the temperature increasing rate decreased as temperature approached the melting point.

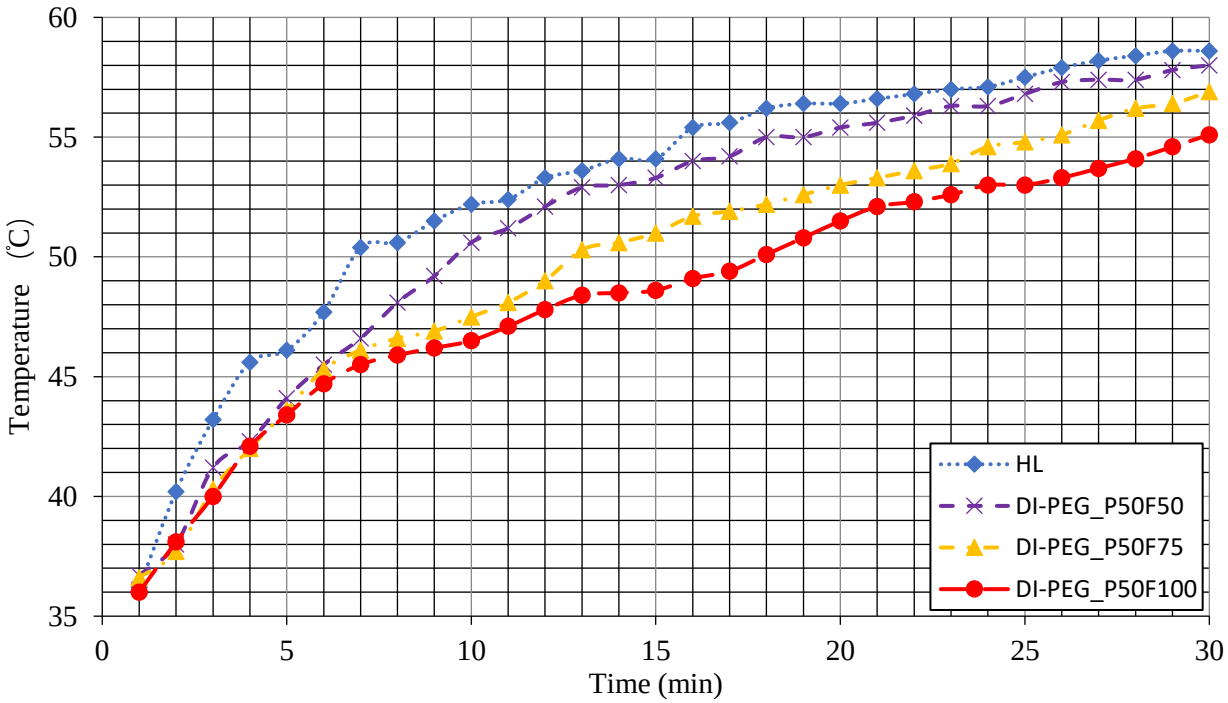

Fig. 43 Real-time temperature performance of mastics.

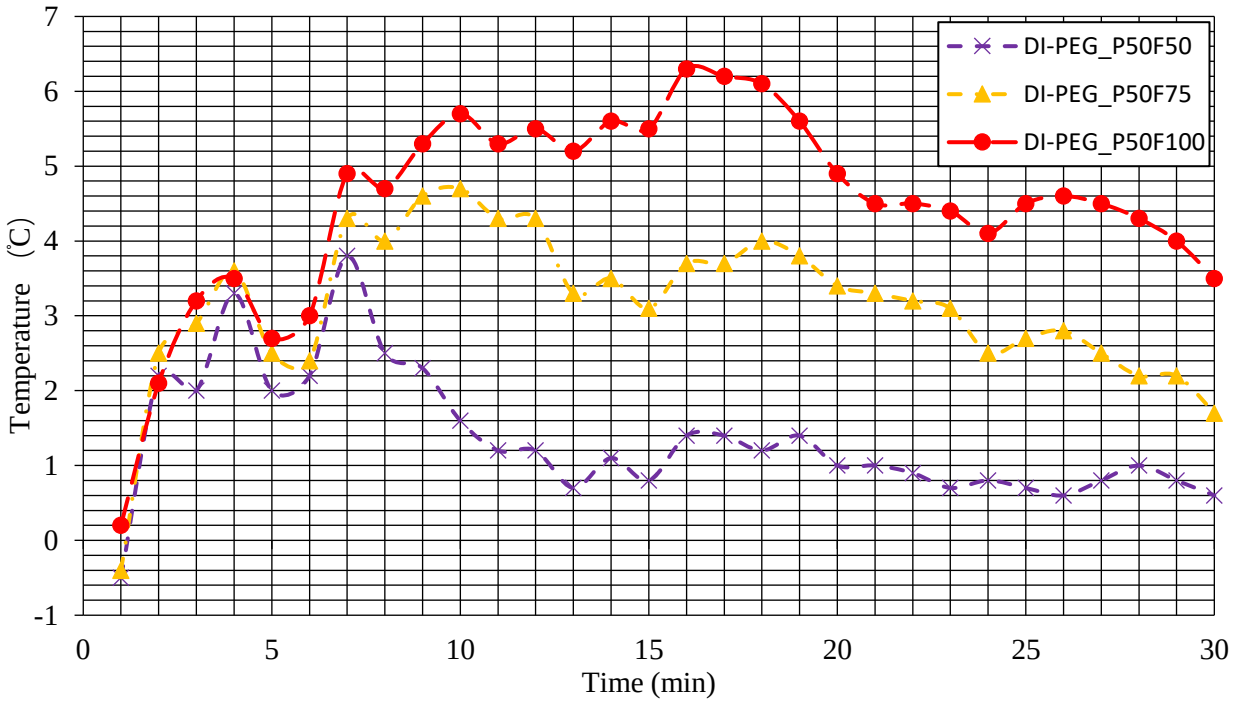

Fig. 44 Temperature difference of mastics.

4.3.5. Rutting Performance by Superpave Rutting Factor (G*/sinδ)

The Superpave rutting factor, $G^*/\sin\delta$, was used to evaluate the rutting resistance of the binder, where G* was the complex modulus and the δ was the phase angle. A higher $G^*/\sin\delta$ value indicated higher resistance to permanent deformation. Fig. 45 presents the calculated rutting factors of the control and modified mastic. It can be observed that below 58ºC, the mastic with CPCMs had lower rutting resistance; however, at temperatures higher than 64ºC, the difference between the modified mastics and the control binder was minor. As aggregate structure also plays an important role in rutting resistance in asphalt mixtures, the effects of the PCMs on permanent deformation resistance will be further evaluated on the mixture level in the future study.

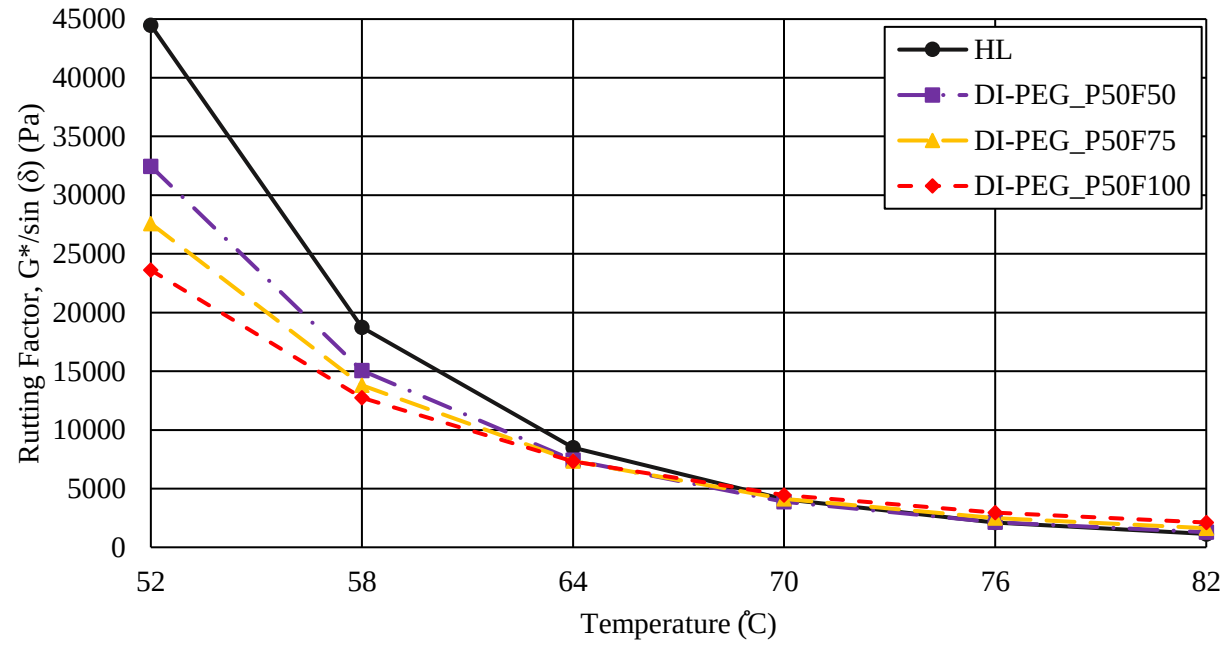

(a)

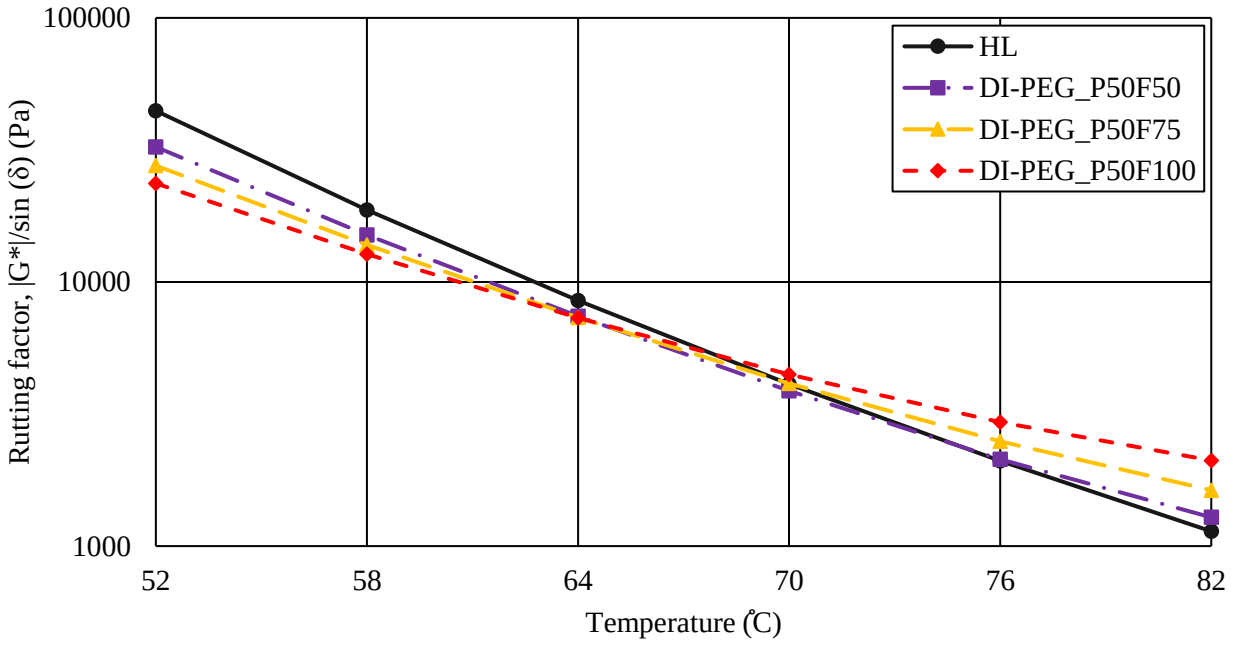

(b)

Fig. 45 Rutting factor at different temperatures: (a) Linear and (b) Semi-logarithmic.

4.3.6. BBR Low-Temperature Performance Test

The BBR test was conducted to evaluate the low-temperature rheological properties of mastics. Materials with high creep stiffness and low m-value lead to low low-temperature cracking resistance (Zhang 2015). Figs. 46 and 47 present the BBR results, including creep stiffness (S) and creep rate (m-value). It can be observed that mastics containing CPCMs had lower creep stiffness and higher m-values, which indicated that the addition of PEG could not only function as thermal regulators but was also able to improve the

low-temperature performance of the pavements.

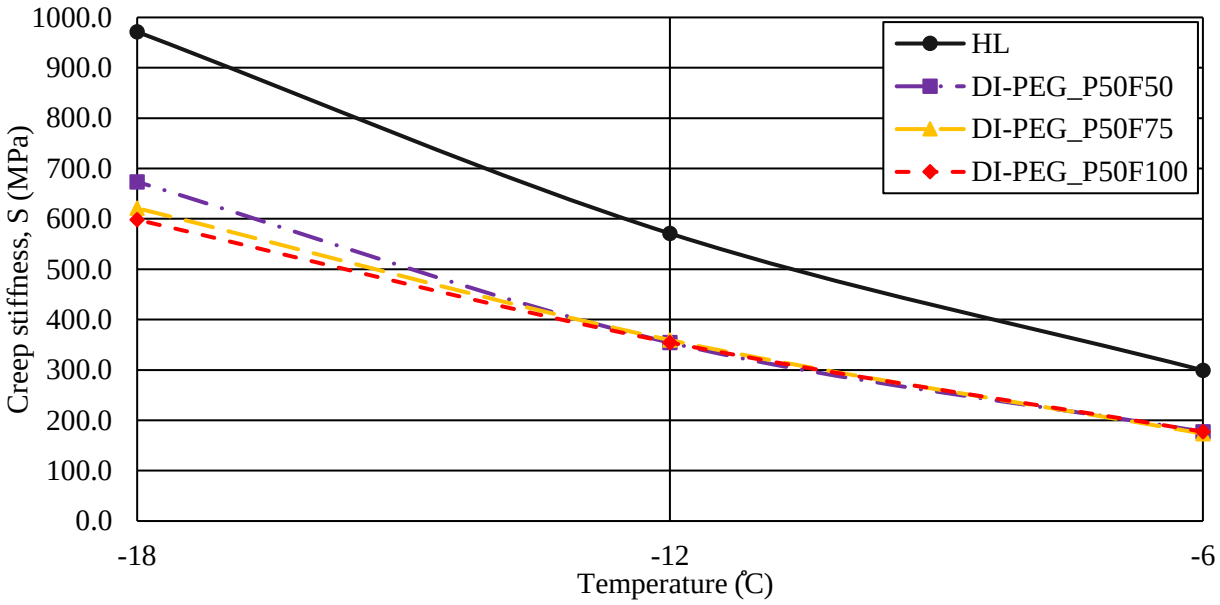

Fig. 46 Creep stiffness of mastics.

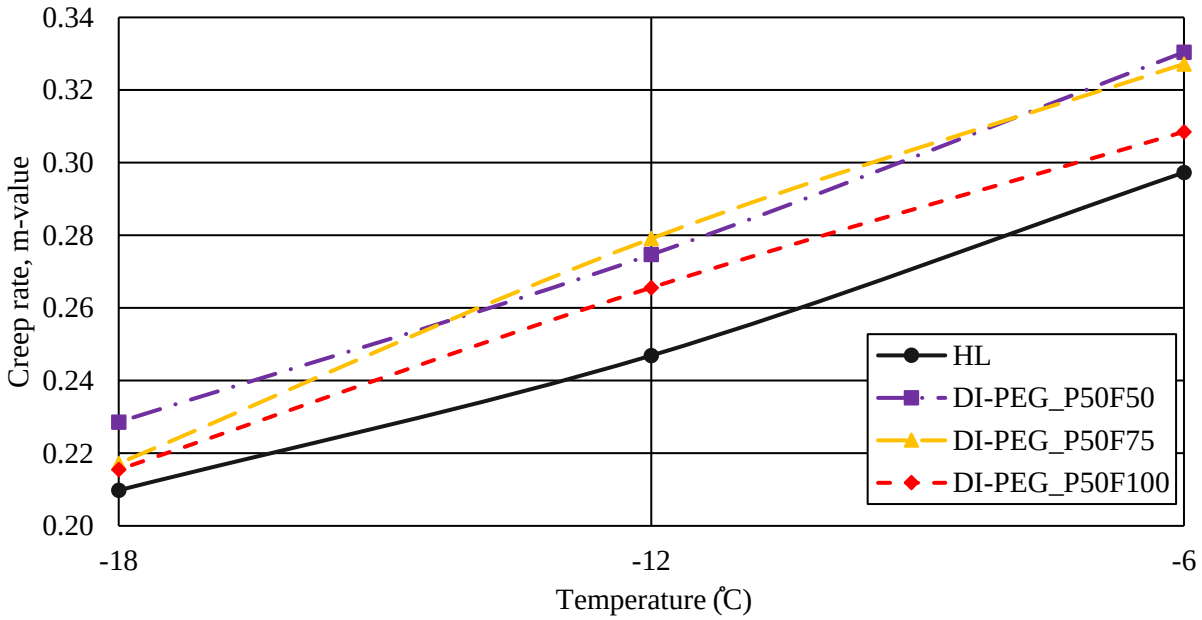

Fig. 47 Creep rate of mastics.

4.3.7. Fatigue Performance at Intermediate Temperature Using Linear Amplitude Sweep (LAS) Testing Results

The LAS test was conducted to evaluate the fatigue performance of the mastics at intermediate temperatures on the PAV-aged samples. Fig. 48 presents the fingerprint testing results which were measured under a frequency sweep test at 25°C with loading amplitude within the linear viscoelastic

range. The testing results suggested that the CPCM mastics had lower stiffness compared to the control mastic. The linear sweep amplitude tests were conducted directly following fingerprint test, and the test results were analyzed using the Simplified ViscoElastic Continuum (S-VECD) Model. For each material, a damage characteristic curve was obtained, which described the change of the material integrity (C) as a function of the damage intensity factor (S). Fig. 49 presents the obtained the damage characteristic curves of the mastics. The results showed that even though there were differences among the modulus of the mastics, the damage characteristic curves of different mastics almost overlapped on each other, which indicated the addition PCM did not have significant impact on the fatigue resistance of the mastics.

Fatigue lives of the mastics under different loading amplitudes were predicted using the S-VECD model. Fig. 50 presents the predicted number of cycles to failure (N_f) at a range of loading strain levels. Both the modulus values and the damage characteristic curves played important roles in the calculation. The results showed that at the same loading amplitude, the mastic with CPCMs generally exhibited slightly lower fatigue lives than the control mastic. However, in realistic situations, as the modulus of the materials were different, the strain levels applied on the material would be different as well. The full analyses on the effects of PCM on asphalt will be completed on the mixture level in the future study.

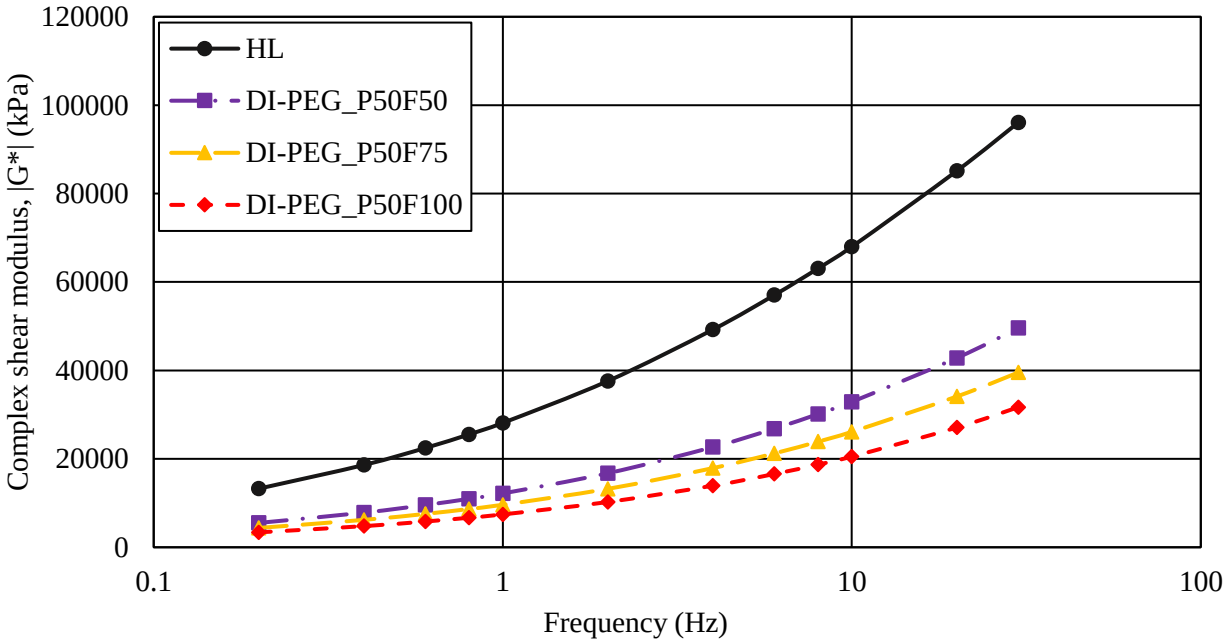

Fig. 48 Fingerprint test of mastics.

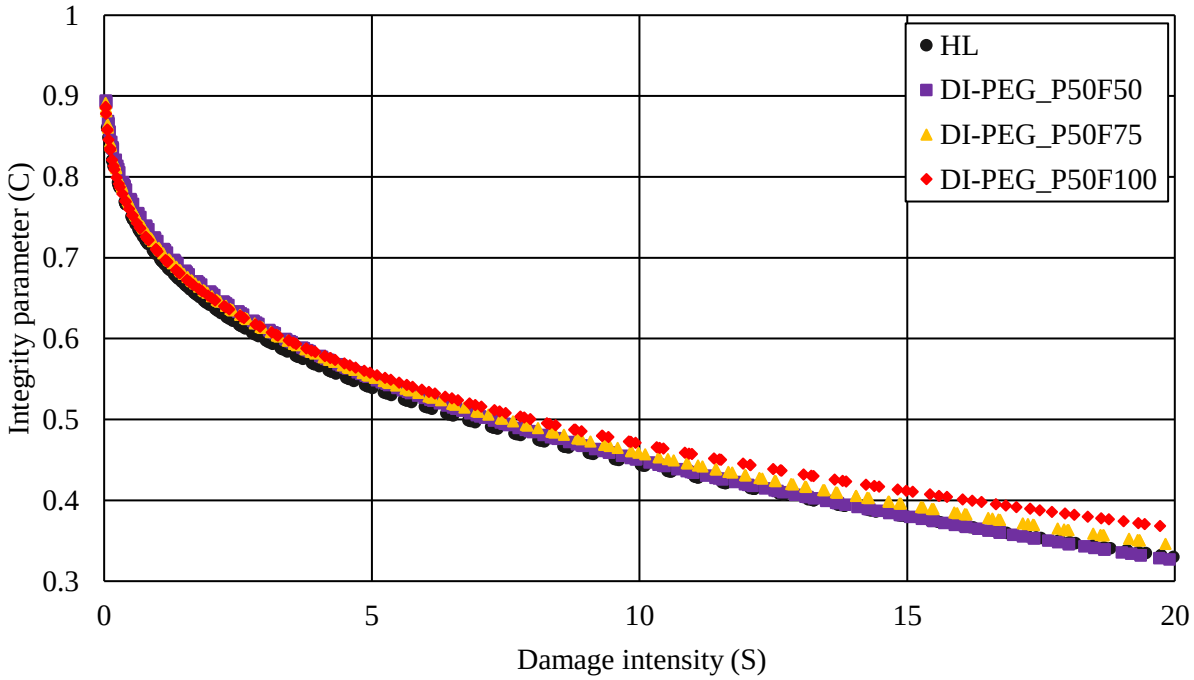

Fig. 49 Integrity parameter vs. damage intensity of binders.

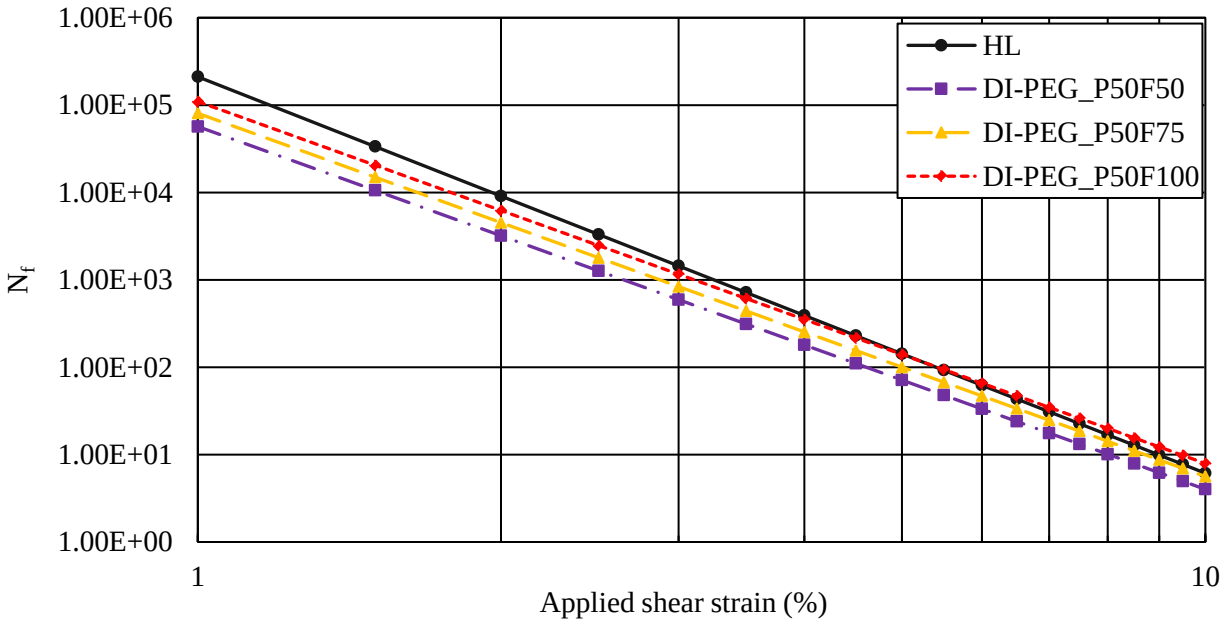

Fig. 50 Fatigue life of mastics.

4.4. Summary

In this study, porous fillers were used as carriers to incorporate PCMs into asphalt pavements. Thermal and Rheological tests were performed on the asphalt mastic to select the appropriate fillers, PCMs, and

the blending ratio. Two different carrier materials (diatomite and expanded perlite) and four types of phase change materials (PEG, LU, Pa-42, and Pa-58) were included in the research. Based on the results of the SEM image analysis, the filter paper test, and the temperature sweep test, the combination of diatomite and PEG with blending ratio of 50:50 was selected. The thermal and rheological behaviors of the mastics with CPCM were further evaluated with different filler replacement ratios. The following findings were made in the research:

- DSC results showed that modified mastics presented a peak in the DSC curve and enthalpy, which led to latent heat storage. The maximum latent heat storage was observed by DI-PEG_P50F100. The melting point of mastics were found very close to the melting point of PEG.
- Real-time temperature performance test confirmed the thermal regulation effect of CPCM on asphalt mastic; the highest temperature reduction was observed for mastic DI-PEG_P50F100 equals to 6.3 ˚C.
- The rutting factor obtained from the Superpave DSR test suggested that the rutting resistance of modified mastics was lower than the control mastic when the temperature was below 70°C; the mastics with CPCMs had higher permanent deformation resistance at high temperature.
- The low-temperature BBR tests confirmed that the modified mastics had higher low-temperature cracking resistance due to the addition of the PEG.
- The LAS fatigue performance tests at intermediate temperatures were conducted and analyzed by the S-VECD model. The predicted fatigue live of the modified mastics were slightly lower than the control mastic at the same strain level.

In summary, the study validated the concept of using porous fillers as carriers for the incorporation of PCM into asphalt pavements. The thermal analyses demonstrated the merits of the innovative material in terms of its thermal regulation effects. The rheological analyses confirmed that with the addition of PEG, while low-temperature performance of the asphalt mastics was improved, the performance at intermediate and high performance was not adversely affected by the PCM. For future research, the effects of the CPCM will be further evaluated at the mixture level. The pavement temperature profile and the pavement performance with the incorporation of CPCM will be predicted and simulated under different loading and climate conditions to complete the evaluation.

Chapter 5. Conclusions and Recommendations

In this research two different types of incorporation method were used to incorporate the phase change material (PCM) in asphalt.

PEG was first directly mixed with Gilsonite-modified binder to improve the low temperature performance and thermal properties of Gilsonite modified binder. The optimum mix proportions were found by analyzing low-temperature performance of modified binder with bending beam rheometer (BBR) test. The full Superpave performance grading tests were conducted on the binders with the recommended modifier dosages. The results indicate that the G3 and P5G6 binders managed to increase the high PG of the original binder by one grade without increasing the low PG. A series of performance tests were conducted after the PG were determined. A general trend in the testing results was that Gilsonite was able to improve the high-temperature performance of the binders but with compromises on performance at the low-temperatures and the utilization of PEG helped to balance the performance on both ends. The intermediate temperature tests suggested that all the tested binders passed the requirements for cracking resistance. The thermal tests indicated that the binders with Gilsonite have higher volumetric heat capacities than the neat binder, which meant the binders would absorb more energy as temperature changed. Given the testing results from the performance and thermal tests, the binder with 5% PEG and 6% Gilsonite is recommended for these particular material combinations for future application.

In the second approach, the impregnation method was used and two carrier materials and four types of PCMs were candidate to prepare composite phase change materials (CPCMs). To determine the appropriate CPCM for mastic production, testing methods including the SEM image analysis, filter paper test, and frequency sweep test were used. It was found that diatomite is a better candidate compared to expanded perlite regarding its high absorption and high dense pack porous structure which can function as an obstacle to prevent high leaking ratio. Also, among different PCM options, PEG was selected since it did not have great impact on the rheological properties of asphalt mastic. Different ratio of CPCM (composite of diatomite and PEG) were made and used as a replacement of hydrated lime at three levels of 50%, 75%, and 100%. A serious of thermal and rheological tests were performed to assess the performance of mastics. Thermal conductivity and volumetric heat capacity of mastics were measured. In addition, DSR test indicated that the Superpave rutting factor ($G^*/\sin\delta$) of modified mastics is decreased at temperatures lower than 70 ℃ and increased at higher temperatures (76 and 82 ℃). Modified mastics also have a low creep stiffness and high m-value in comparison to the control mastic which means a better low temperature performance. Finally, the fatigue performance was analyzed by two methods. The Superpave fatigue factor ($G^*.\sin\delta$) of modified mastics is lower than the control mastic, indicating the higher fatigue resistance of modified mastic relative to control mastic. The LAS was another test for evaluating the fatigue performance. The test was performed in the nonlinear viscoelastic range with real fatigue damage introduced. The test results indicated that although the integrity parameter of modified mastic is higher than control mastic, their fatigue life is slightly lower.

For future studies, it is recommended that base binders with different PGs be tested with the recommend dosages of PEG and Gilsonite to verify the findings from this study. Also, it is be recommended that using an asphalt job mix formula with higher filler percentage can result in incorporating more CPCM in mastic leading to a cooler pavement. Therefore, a higher volumetric concentration of 25%, using in this study, is recommended. It is also could be noticed that adding Gilsonite may improve the complex shear modulus of modified mastics to compensate the negative side effect of CPCM. Furthermore, it would be beneficial if performance and thermal behavior analyses can be performed on the corresponding asphalt mixtures in the future.

References

Aflaki, S., & Tabatabaee, N. (2009). Proposals for modification of Iranian bitumen to meet the climatic requirements of Iran. Construction and Building Materials, 23(6), 2141–2150. https://doi.org/10.1016/j.conbuildmat.2008.12.014

Alkan, C., Günther, E., Hiebler, S., Ensari, Ö. F., & Kahraman, D. (2012). Polyurethanes as solid-solid phase change materials for thermal energy storage. Solar Energy, 86(6), 1761–1769. https://doi.org/10.1016/j.solener.2012.03.012

Ameri, M., Mansourian, A., Ashani, S. S., & Yadollahi, G. (2011). Technical study on the Iranian Gilsonite as an additive for modification of asphalt binders used in pavement construction. Construction and Building Materials, 25(3), 1379–1387. https://doi.org/10.1016/j.conbuildmat.2010.09.005

Ameri, M., Mansourian, A., & Sheikhmotevali, A. H. (2012). Investigating effects of ethylene vinyl acetate and gilsonite modifiers upon performance of base bitumen using Superpave tests methodology. Construction and Building Materials, 36, 1001–1007. https://doi.org/10.1016/j.conbuildmat.2012.04.137

Ameri, M., Mirzaiyan, D., & Amini, A. (2018). Rutting Resistance and Fatigue Behavior of Gilsonite-Modified Asphalt Binders. Journal of Materials in Civil Engineering, 30(11), 04018292. https://doi.org/10.1061/(asce)mt.1943-5533.0002468

Anderson, D. A., Lapalu, L., Marasteanu, M. O., Le Hir, Y. M., Planche, J.-P., & Martin, D. (2001). Low-Temperature Thermal Cracking of Asphalt Binders as Ranked by Strength and Fracture Properties. Transportation Research Record: Journal of the Transportation Research Board, 1766(1), 1–6. https://doi.org/10.3141/1766-01

Baldino, N., Gabriele, D., Rossi, C. O., Seta, L., Lupi, F. R., & Caputo, P. (2012). Low temperature rheology of polyphosphoric acid (PPA) added bitumen. Construction and Building Materials, 36, 592–596. https://doi.org/10.1016/j.conbuildmat.2012.06.011

Bian, X., Tan, Y. Q., Lv, J. F., & Shan, L. Y. (2012). Preparation of Latent Heat Materials Used in Asphalt Pavement and Theirs' Controlling Temperature Performance. Advanced Engineering Forum, 5, 322–327. https://doi.org/10.4028/www.scientific.net/aef.5.322

Bo Guan, Biao Ma, & Fang Qin. (2011). Application of asphalt pavement with phase change materials to mitigate urban heat island effect. 2011 International Symposium on Water Resource and Environmental Protection, 3, 2389–2392. https://doi.org/10.1109/ISWREP.2011.5893749

Chen, M., Wan, L., & Lin, J. (2012). Effect of phase-change materials on thermal and mechanical properties of asphalt mixtures. Journal of Testing and Evaluation, 40(5), 1–8. https://doi.org/10.1520/JTE20120091

Chen, M. Z., Hong, J., Wu, S. P., Lu, W., & Xu, G. J. (2011). Optimization of phase change materials used in asphalt pavement to prevent rutting. Advanced Materials Research, 219–220, 1375–1378. https://doi.org/10.4028/www.scientific.net/AMR.219-220.1375

Chen, Z., Cao, L., Fang, G., & Shan, F. (2013). Synthesis and characterization of microencapsulated paraffin microcapsules as shape-stabilized thermal energy storage materials. Nanoscale and Microscale Thermophysical Engineering, 17(2), 112–123. https://doi.org/10.1080/15567265.2012.761305

Dissanayaka, T., & Senadheera, S. (2018). Assessing the Use of Phase Change Materials to Control Temperature in Asphalt Pavements. Transportation Research Board 97th Annual Meeting, 15p. https://trid.trb.org/view/1495715

Du, Y., Liu, P., Wang, J., Wang, H., Hu, S., Tian, J., & Li, Y. (2019). Laboratory investigation of phase change effect of polyethylene glycolon on asphalt binder and mixture performance. Construction and Building Materials, 212, 1–9. https://doi.org/10.1016/j.conbuildmat.2019.03.308

Fu, X., Liu, Z., Xiao, Y., Wang, J., & Lei, J. (2015). Preparation and properties of lauric acid/diatomite composites as novel form-stable phase change materials for thermal energy storage. Energy and Buildings, 104, 244–249. https://doi.org/10.1016/j.enbuild.2015.06.059

Gheni, A. (2020). Scholars' Mine Using Scrap Tires as an Aggregate in Chip Seal - Phase II Missouri Department of Natural Resources.

Hawes, D. W., Banu, D., & Feldman, D. (1992). The stability of phase change materials in concrete. Solar Energy

Materials and Solar Cells, 27(2), 103–118. https://doi.org/10.1016/0927-0248(92)90113-4
He, L. H., Li, J. R., & Zhu, H. Z. (2013). Analysis on application prospect of shape-stabilized phase change materials in asphalt pavement. Applied Mechanics and Materials, 357–360, 1277–1281. https://doi.org/10.4028/www.scientific.net/AMM.357-360.1277
He, L., Wang, H., Zhu, H., Gu, Y., Li, X., & Mao, X. (2018). Thermal properties of PEG/graphene nanoplatelets (GNPs) composite phase change materials with enhanced thermal conductivity and photo-thermal performance. Applied Sciences (Switzerland), 8(12). https://doi.org/10.3390/app8122613
Hung, C. H., Chen, W. T., Sehhat, M. H., & Leu, M. C. (2021). The effect of laser welding modes on mechanical properties and microstructure of 304L stainless steel parts fabricated by laser-foil-printing additive manufacturing. International Journal of Advanced Manufacturing Technology, 112(3–4), 867–877. https://doi.org/10.1007/s00170-020-06402-7
Jeong, S. G., Jeon, J., Lee, J. H., & Kim, S. (2013). Optimal preparation of PCM/diatomite composites for enhancing thermal properties. International Journal of Heat and Mass Transfer, 62(1), 711–717. https://doi.org/10.1016/j.ijheatmasstransfer.2013.03.043
Jin, J., Lin, F., Liu, R., Xiao, T., Zheng, J., Qian, G., Liu, H., & Wen, P. (2017). Preparation and thermal properties of mineral-supported polyethylene glycol as form-stable composite phase change materials (CPCMs) used in asphalt pavements. Scientific Reports, 7(1), 1–10. https://doi.org/10.1038/s41598-017-17224-1
Jin, J., Xiao, T., Zheng, J., Liu, R., Qian, G., Xie, J., Wei, H., Zhang, J., & Liu, H. (2018). Preparation and thermal properties of encapsulated ceramsite-supported phase change materials used in asphalt pavements. Construction and Building Materials, 190, 235–245. https://doi.org/10.1016/j.conbuildmat.2018.09.119
Liu, J,, and Li, P.. (2008). Experimental Study on Gilsonite-modified Asphalt.
Kakar, M. R., Refaa, Z., Worlitschek, J., Stamatiou, A., Partl, M. N., & Bueno, M. (2019). Thermal and rheological characterization of bitumen modified with microencapsulated phase change materials. Construction and Building Materials, 215, 171–179. https://doi.org/10.1016/j.conbuildmat.2019.04.171
Kakar, M. R., Refaa, Z., Worlitschek, J., Stamatiou, A., Partl, M. N., & Bueno, M. (2020). Impregnation of Lightweight Aggregate Particles with Phase Change Material for Its Use in Asphalt Mixtures. In M. Pasetto, M. N. Partl, & G. Tebaldi (Eds.), Proceedings of the 5th International Symposium on Asphalt Pavements & Environment (APE) (pp. 337–345). Springer International Publishing.
Karaman, S., Karaipekli, A., Sar, A., & Biçer, A. (2011). Polyethylene glycol (PEG)/diatomite composite as a novel form-stable phase change material for thermal energy storage. Solar Energy Materials and Solar Cells, 95(7), 1647–1653. https://doi.org/10.1016/j.solmat.2011.01.022
Kök, B. V., Yilmaz, M., & Guler, M. (2011). Evaluation of high temperature performance of SBS + Gilsonite modified binder. Fuel, 90(10), 3093–3099. https://doi.org/10.1016/j.fuel.2011.05.021
Kong, W., Liu, Z., Yang, Y., Zhou, C., & Lei, J. (2017). Preparation and characterizations of asphalt/lauric acid blends phase change materials for potential building materials. Construction and Building Materials, 152, 568–575. https://doi.org/10.1016/j.conbuildmat.2017.05.039
Lei, Z., Bahia, H., & Yi-Qiu, T. (2015). Effect of bio-based and refined waste oil modifiers on low temperature performance of asphalt binders. Construction and Building Materials, 86, 95–100. https://doi.org/10.1016/j.conbuildmat.2015.03.106
Li, F., Zhou, S., Chen, S., Yang, Z., Yang, J., Zhu, X., Du, Y., Zhou, P., & Cheng, Z. (2018). Preparation of low-temperature phase change materials microcapsules and its application to asphalt pavement. Journal of Materials in Civil Engineering, 30(11), 1–10. https://doi.org/10.1061/(ASCE)MT.1943-5533.0002514
Li, M., Wu, Z., & Tan, J. (2012). Properties of form-stable paraffin/silicon dioxide/expanded graphite phase change composites prepared by sol-gel method. Applied Energy, 92, 456–461. https://doi.org/10.1016/j.apenergy.2011.11.018
Liang, M., Xin, X., Fan, W., Wang, H., Jiang, H., Zhang, J., & Yao, Z. (2019). Phase behavior and hot storage characteristics of asphalt modified with various polyethylene: Experimental and numerical characterizations. Construction and Building Materials, 203, 608–620. https://doi.org/10.1016/j.conbuildmat.2019.01.095
Ma, B., Adhikari, S., Chang, Y., Ren, J., Liu, J., & You, Z. (2013). Preparation of composite shape-stabilized phase change materials for highway pavements. Construction and Building Materials, 42, 114–121.

https://doi.org/10.1016/j.conbuildmat.2012.12.027
Ma, B., Ma, J., Wang, D., & Peng, S. (2011). Preparation and properties of composite shape-stabilized phase change material for asphalt mixture. Applied Mechanics and Materials, 71–78, 118–121. https://doi.org/10.4028/www.scientific.net/AMM.71-78.118
Manning, B. J., Bender, P. R., Cote, S. A., Lewis, R. A., Sakulich, A. R., & Mallick, R. B. (2015). Assessing the feasibility of incorporating phase change material in hot mix asphalt. Sustainable Cities and Society, 19, 11–16. https://doi.org/10.1016/j.scs.2015.06.005
Mirzaiyan, D., Ameri, M., Amini, A., Sabouri, M., & Norouzi, A. (2019). Evaluation of the performance and temperature susceptibility of gilsonite- and SBS-modified asphalt binders. Construction and Building Materials, 207, 679–692. https://doi.org/10.1016/j.conbuildmat.2019.02.145
Moreno-Navarro, F., Sol-Sánchez, M., Gámiz, F., & Rubio-Gámez, M. C. (2018). Mechanical and thermal properties of graphene modified asphalt binders. Construction and Building Materials, 180, 265–274. https://doi.org/10.1016/j.conbuildmat.2018.05.259
Pan, P., Wu, S., Xiao, Y., Wang, P., & Liu, X. (2014). Influence of graphite on the thermal characteristics and anti-ageing properties of asphalt binder. Construction and Building Materials, 68, 220–226. https://doi.org/10.1016/j.conbuildmat.2014.06.069
Pourhassan, A., Gheni, A. A., & Elgawady, M. A. (2022). Water Film Depth Prediction Model for Highly Textured Pavement Surface Drainage. Transportation Research Record, 2676(2), 100–117. https://doi.org/10.1177/03611981211036349
Quintana, H. A. R., Noguera, J. A. H., & Bonells, C. F. U. (2016). Behavior of Gilsonite-Modified Hot Mix Asphalt by Wet and Dry Processes. Journal of Materials in Civil Engineering, 28(2), 04015114. https://doi.org/10.1061/(asce)mt.1943-5533.0001339
Ren, J., Ma, B., Si, W., Zhou, X., & Li, C. (2014). Preparation and analysis of composite phase change material used in asphalt mixture by sol-gel method. Construction and Building Materials, 71, 53–62. https://doi.org/10.1016/j.conbuildmat.2014.07.100
Ren, S., Liang, M., Fan, W., Zhang, Y., Qian, C., He, Y., & Shi, J. (2018). Investigating the effects of SBR on the properties of gilsonite modified asphalt. Construction and Building Materials, 190, 1103–1116. https://doi.org/10.1016/j.conbuildmat.2018.09.190
Roshan, A., & Shooshpasha, I. (2014). Numerical analysis of piled raft foundations in soft clay. EJGE, 19, 4541-4554.
Roshan, A., Ahmadi, M., & Ganji, D. D. (2022). Variational Iteration Method (VIM) and Parameter Perturbation Method (PPM) for the Solution of Nonlinear Differential Equation of Beam Elastic Deformation. Southeast Asian Bulletin of Mathematics, 46(1).
Rowe, G. M., King, G., & Anderson, M. (2014). The influence of binder rheology on the cracking of asphalt mixes in airport and highway projects. Journal of Testing and Evaluation, 42(5). https://doi.org/10.1520/JTE20130245
Ryms, M., Denda, H., & Jaskuła, P. (2017). Thermal stabilization and permanent deformation resistance of LWA/PCM-modified asphalt road surfaces. Construction and Building Materials, 142, 328–341. https://doi.org/10.1016/j.conbuildmat.2017.03.050
Saberi.K, F., Fakhri, M., & Azami, A. (2017). Evaluation of warm mix asphalt mixtures containing reclaimed asphalt pavement and crumb rubber. Journal of Cleaner Production, 165, 1125–1132. https://doi.org/10.1016/j.jclepro.2017.07.079
Sakulich, A. R., & Bentz, D. P. (2012). Incorporation of phase change materials in cementitious systems via fine lightweight aggregate. Construction and Building Materials, 35, 483–490. https://doi.org/10.1016/j.conbuildmat.2012.04.042
Santamouris, M. (2013). Using cool pavements as a mitigation strategy to fight urban heat island - A review of the actual developments. Renewable and Sustainable Energy Reviews, 26, 224–240. https://doi.org/10.1016/j.rser.2013.05.047
Sari, A., & Biçer, A. (2012). Thermal energy storage properties and thermal reliability of some fatty acid esters/building material composites as novel form-stable PCMs. Solar Energy Materials and Solar Cells, 101, 114–122. https://doi.org/10.1016/j.solmat.2012.02.026

Sari, A., Karaipekli, A., & Alkan, C. (2009). Preparation, characterization and thermal properties of lauric acid/expanded perlite as novel form-stable composite phase change material. Chemical Engineering Journal, 155(3), 899–904. https://doi.org/10.1016/j.cej.2009.09.005

Sari, A., & Kaygusuz, K. (2002). Thermal performance of palmitic acid as a phase change energy storage material. Energy Conversion and Management, 43(6), 863–876. https://doi.org/10.1016/S0196-8904(01)00071-1

Sarier, N., & Onder, E. (2007). The manufacture of microencapsulated phase change materials suitable for the design of thermally enhanced fabrics. Thermochimica Acta, 452(2), 149–160. https://doi.org/10.1016/j.tca.2006.08.002

Sarier, N., & Onder, E. (2012). Organic phase change materials and their textile applications: An overview. Thermochimica Acta, 540, 7–60. https://doi.org/10.1016/j.tca.2012.04.013

Sehhat, M. H., & Mahdianikhotbesara, A. (2021). Powder spreading in laser-powder bed fusion process. Granular Matter, 23(4), 1–18. https://doi.org/10.1007/s10035-021-01162-x

Sharma, S. D., & Sagara, K. (2005). Latent Heat Storage Materials and Systems: A Review. International Journal of Green Energy, 2(1), 1–56. https://doi.org/10.1081/GE-200051299

Sun, Z., Yi, J., Huang, Y., Feng, D., & Guo, C. (2016). Properties of asphalt binder modified by bio-oil derived from waste cooking oil. Construction and Building Materials, 102, 496–504. https://doi.org/10.1016/j.conbuildmat.2015.10.173

Tan, Y., Sun, Z., Gong, X., Xu, H., Zhang, L., & Bi, Y. (2017). Design parameter of low-temperature performance for asphalt mixtures in cold regions. Construction and Building Materials, 155, 1179–1187. https://doi.org/10.1016/j.conbuildmat.2017.09.094

Tang, W., Wang, Z., Mohseni, E., & Wang, S. (2018). A practical ranking system for evaluation of industry viable phase change materials for use in concrete. Construction and Building Materials, 177, 272–286. https://doi.org/10.1016/j.conbuildmat.2018.05.112

Wang, T., Xiao, F., Amirkhanian, S., Huang, W., & Zheng, M. (2017). A review on low temperature performances of rubberized asphalt materials. Construction and Building Materials, 145, 483–505. https://doi.org/10.1016/j.conbuildmat.2017.04.031

Wang, Y. D., Underwood, B. S., & Kim, Y. R. (2020). Development of a fatigue index parameter, Sapp, for asphalt mixes using viscoelastic continuum damage theory. International Journal of Pavement Engineering, 8436. https://doi.org/10.1080/10298436.2020.1751844

Wang, Y., & Richard Kim, Y. (2019). Development of a pseudo strain energy-based fatigue failure criterion for asphalt mixtures. International Journal of Pavement Engineering, 20(10), 1182–1192. https://doi.org/10.1080/10298436.2017.1394100

Wei, K., Ma, B., & Duan, S. Y. (2019). Preparation and Properties of Bitumen-Modified Polyurethane Solid-Solid Phase Change Materials. Journal of Materials in Civil Engineering, 31(8), 1–8. https://doi.org/10.1061/(ASCE)MT.1943-5533.0002795

Wei, Kun, Wang, X., Ma, B., Shi, W., Duan, S., & Liu, F. (2019). Study on rheological properties and phase-change temperature control of asphalt modified by polyurethane solid–solid phase change material. Solar Energy, 194(November), 893–902. https://doi.org/10.1016/j.solener.2019.11.007

Wei, T., Zheng, B., Liu, J., Gao, Y., & Guo, W. (2014). Structures and thermal properties of fatty acid/expanded perlite composites as form-stable phase change materials. Energy and Buildings, 68(PARTA), 587–592. https://doi.org/10.1016/j.enbuild.2013.09.050

Xu, B., Ma, H., Lu, Z., & Li, Z. (2015). Paraffin/expanded vermiculite composite phase change material as aggregate for developing lightweight thermal energy storage cement-based composites. Applied Energy, 160, 358–367. https://doi.org/10.1016/j.apenergy.2015.09.069

Yang, T., Ma, X., & Zhang, B. (2016). Preliminary Studies into Methods for Microstructural Improvements of Hydrated Lime Putty. Journal of Materials in Civil Engineering, 28(12), 04016160. https://doi.org/10.1061/(asce)mt.1943-5533.0001674

Yinfei, D., Pusheng, L., Jiacheng, W., Hancheng, D., Hao, W., & Yingtao, L. (2020). Effect of lightweight aggregate gradation on latent heat storage capacity of asphalt mixture for cooling asphalt pavement. Construction and Building Materials, 250, 118849. https://doi.org/10.1016/j.conbuildmat.2020.118849

Zhang, D., Chen, M., Wu, S., Riara, M., Wan, J., & Li, Y. (2019). Thermal and rheological performance of asphalt binders modified with expanded graphite/polyethylene glycol composite phase change material (EP-CPCM). Construction and Building Materials, 194, 83–91. https://doi.org/10.1016/j.conbuildmat.2018.11.011

Zhang, D., Li, Z., Zhou, J., & Wu, K. (2004). Development of thermal energy storage concrete. Cement and Concrete Research, 34(6), 927–934. https://doi.org/10.1016/j.cemconres.2003.10.022

Zhang, H., Wang, X., & Wu, D. (2010). Silica encapsulation of n-octadecane via sol-gel process: A novel microencapsulated phase-change material with enhanced thermal conductivity and performance. Journal of Colloid and Interface Science, 343(1), 246–255. https://doi.org/10.1016/j.jcis.2009.11.036

Zhang, W. (2015). Evaluation of Field Transverse Cracking of. August.

Zhang, Y., Lin, K., Zhang, Q., & Di, H. (2006). Ideal thermophysical properties for free-cooling (or heating) buildings with constant thermal physical property material. Energy and Buildings, 38(10), 1164–1170. https://doi.org/10.1016/j.enbuild.2006.01.008

Zhang, Y., Zhou, G., Lin, K., Zhang, Q., & Di, H. (2007). Application of latent heat thermal energy storage in buildings: State-of-the-art and outlook. Building and Environment, 42(6), 2197–2209. https://doi.org/10.1016/j.buildenv.2006.07.023

Zhang, Z., Shi, G., Wang, S., Fang, X., & Liu, X. (2013). Thermal energy storage cement mortar containing n-octadecane/expanded graphite composite phase change material. Renewable Energy, 50, 670–675. https://doi.org/10.1016/j.renene.2012.08.024

Zhou, X., Kastiukas, G., Lantieri, C., Tataranni, P., Vaiana, R., & Sangiorgi, C. (2018). Mechanical and thermal performance of macro-encapsulated phase change materials for pavement application. Materials, 11(8), 1–18. https://doi.org/10.3390/ma11081398